Electrochemical determination of extractives in wood pulp

Åbo Akademi University

Faculty of Science and Engineering

Ju-Yeon Seo

Master's programme in Excellence in Analytical Chemistry

Degree project in Analytical chemistry, 30 credits

Supervisor: Docent Dr. Tomasz Sokalski (Åbo Akademi Univeristy)

Co-supervisors: Docent Dr. Zekra Mousavi (Åbo Akademi University)

Prof. Ivo Leito (University of Tartu)

Examiner: Docent Dr. Adriana Ferancova (University of Oulu)

August 2023

Table of Contents

Abstract

The objective of this thesis is to establish electrochemical techniques for the qualitative and quantitative determination of pentacyclic triterpenes in wood extractives. These triterpenes, found in wood extractives, possess beneficial biological effects. However, in the context of paper production, their presence can be problematic due to their lipophilic nature, which can reduce paper strength and hinder subsequent processing steps such as the adhesion of coatings and inks. Among the pentacyclic triterpenes, betulin is the most abundant molecule present up to 30 % of the dry weight in a Scandinavian species (B. verrucosa) [1, 2]. To address the challenges associated with handling such compounds in paper mills, betulin and stearic acid were chosen as model compounds. This thesis introduces two distinct characterization techniques: potentiometric sensors in combination with principal component analysis, and voltammetric methods including square wave voltammetry and differential pulse voltammetry. Using ion-selective electrodes and principal component analysis the classification between samples containing KCl, KCl and ethanol and KCl, ethanol and betulin was possible. For voltammetric methods, a glassy carbon electrode with an in situ lead film was used. Both the aqueous and organic solvents were used as media.

The solvent used for preparing the standard solution significantly influenced the square wave voltammograms recorded in alkaline media. Therefore, Tris-HCl buffer (pH 7.4) was used as the medium, and dimethyl sulfoxide served as the solvent for the standard solution. The oxidation signal at 1.6 V for betulinic acid, oleanolic acid, and betulin was found to be proportional to the concentration when 5 mM of the stock solution was added. Additionally, differential pulse voltammograms were recorded using 0.1 M tetrabutylammonium hexafluorophosphate in acetonitrile considering the benefits such as a wider electrochemical window and compatibility with organic molecules. The preconcentration step enables the detection of analytes with higher signals compared to the DMSO blank. The imperfect proportionality between peak current and analyte concentration, indicated by the similarity in current signals obtained from 0.5 mM working solution and 5 mM stock solution, remained unresolved. Nonetheless, the obtained results demonstrated that higher concentrations of the stock solution yielded higher current signals when compared to the most diluted standard solution and solvent blank. Furthermore, the extracted birch and conifer samples were analysed affirming the method's capability to detect compounds of interest. The outcomes of this study highlight the validity of employing ISEs in combination with chemometric data treatment for the qualitative determination of betulin, and the potential of the voltammetric methods to detect pentacyclic triterpenes in various electrolytes. However, to validate the reliability of the voltammetric methods, it is imperative to undertake further investigations by repeating experiments in non-aqueous electrolytes aiming to discover the underlying causes of the imperfect proportionality. Notably, it is crucial to determine the concentration of analytes by an independent method after chromatographic separation in natural sample analysis.

Keywords: Potentiometric sensors, Stearic acid, Pentacyclic triterpenes, Betulin, Betulinic acid, Oleanolic acid, Lead film electrode, Adsorptive stripping voltammetry, Square wave voltammetry, Differential pulse voltammetry, Principal component analysis

Preface

This MSc thesis work was performed in the Laboratory of Molecular Science and Engineering at Åbo Akademi University as the final part of the Excellence in Analytical Chemistry Erasmus Mundus joint master's degree program.

I would like to express my earnest gratitude to my supervisor, Docent Tomasz Sokalski for his persistent supervision and encouragement when the direction of the experiments was at a loss. I was able to take my cast of mind as well as my knowledge to the next level thanks to your warm-hearted and experienced guidance. I could not have gotten through these times without you. Also, I would like to thank Docent Zekra Mousavi for her precious advice about the manuscript and for motivating me. To Professor Johan Bobacka, thank you for suggesting me this topic and encouraging me throughout the journey.

To Professor Ivo Leito, thank you for giving me the opportunity to be a part of the Excellence in Analytical Chemistry program, and for guiding me with my thesis manuscript. I am truly fortunate to encounter this opportunity to join the EACH program that comes once in my life. To Dr. Anu Teearu-Ojakäär, thank you for your administrative support from the beginning of the studies.

I am grateful to my EACH friends for spending pleasant and difficult times all along with me. Without you, I would have lacked one of the delights in my life.

To my dearest mom, dad, sisters, and brother, thank you for always supporting and trusting me. Again, I realized your existence is my fence and base forever. I love you.

Åbo June, 2023

Juyeon Seo

List of Symbols

A	Area of the electrode surface
a_i	Activity of species i
a_{Kjel}	Hydrated ion radius
C_i	Concentration of ion i
t_{int}	Interval time
t_{Pulse}	Pulse time
$t_{Modulation}$	Modulation time
E	Measured potential
E°	Standard potential
E_{pulse}	Pulse potential
E_{step}	Step potential
E_{base}	Base potential
$E_{Initial}$	Initial potential
$E_{Modulation}$	Modulation potential
I	Current
J	Ionic strength
j	Current density
γ_i	Activity coefficient of species i
R^+	Organic cations
R^-	Organic anions
S_d	Standard deviation
z_i	Charge of the ion i

List of Abbreviations

ACN	Acetonitrile
BA	Betulinic acid
CE	Counter electrode
CV	Cyclic voltammetry
DPV	Differential Pulse Voltammetry
DMSO	Dimethyl sulfoxide
DNPV	Differential Normal Pulse Voltammetry
DOS	Bis(2-ethylhexyl) sebacate
DA	n-Decyl alcohol
ETH-500	Tetradodecylammonium tetrakis (4-chlorophenyl) borate
EDOT	3,4-ethylenedioxythiophene
GC	Glassy carbon
ISM	Ion selective membrane
ISE	Ion selective electrode
KTFPB	Potassium tetrakis[3,5-bis(trifluoromethyl)phenyl] borate
oNPOE	2-Nitrophenyl octyl ether
OA	Oleanolic acid
PANI	Polyaniline
PCA	Principal component analysis
PEDOT	Poly(3,4-ethylenedioxythiophene)
PPy	Polypyrrole
PVC	Poly (vinyl chloride)
RE	Reference electrode
SPE	Screen-printed electrode
SWV	Square wave voltammetry
$TBAPF_6$	Tetrabutylammonium hexafluorophosphate
TDMACl	Tridodecylmethylammonium chloride
Tris-HCl	Tris(hydroxymethyl)aminomethane hydrochloride
WE	Working electrode

1. Introduction

Wood extractives can be described as lipophilic compounds comprising stearyl esters, fatty acids, waxes, etc. and these hydrophobic substances are called pitch or wood resins, causing pitch problems. Accumulation of pitch deposits in paper production facilities can cause spots, holes, and breaks in paper sheets, ultimately leading to a shutdown of paper mills [3, 4]. Given the difficulties of handling lipophilic compounds in wood extractives for paper material production sites, this thesis aims to establish electrochemical analytical methods which are low-cost, selective, and reversible, which aim towards online process control in the future. Potentiometric sensors were utilized to qualitatively analyze betulin and stearic acid, while voltammetric methods were employed for quantitative analysis of betulin, oleanolic acid(OA), ursolic acid (UA, an isomer of oleanolic acid), and betulinic acid (Figure1).

Woods contain up to 75 mg of lipophilic compounds per 100 g of wood. Hydrolysis of sterol esters (ca 38 % of total wood lipids) occurs during fungal decay. Fungi produce a variety of lipids including fatty acids which can cause lipid peroxidation reactions, a part of the lignin degradation process [5]. Lignin is much more sensitive to oxidation than cellulose, so in the initial degradation stage, lignin may serve as a shield for cellulose. However, free radicals, active forms of oxygen, and carboxyl groups that are produced during the lignin oxidation process will reduce the pH of papers and boost the entire cellulose degradation process, influencing the lifetime of the paper material [6]. Pentacyclic triterpenes are easily found in plants, particularly abundant in birch barks and licorice roots, which are common in the Finnish forests. Betulin (Betulinol) is the most stable and abundant pentacyclic triterpene in birch trees. Betulinic acid, one of the oxidized derivatives of betulin, is found in smaller amounts in plants in comparison to betulin. They are widely known for their beneficial biological effects such as anti-inflammatory, antitumor, anti-cancer, anti-HIV, and antibacterial activities [7–9]. However, it is not advisable to preserve them in paper materials since they downgrade the quality of paper materials. Thus, the separation and determination of betulin and betulinic acids are crucial for quality control. The necessity of the separation step before the voltammetric determination is to be investigated in this thesis considering the resolution in selectivity for pentacyclic triterpenes.

There is no data in the literature concerning using ISEs for the analysis of betulin, and very limited data addressing voltammetric method for pentacyclic triterpenes. This thesis introduces two distinct electrochemical analysis approaches: potentiometric sensors, serving as a qualitative method, and voltammetric methods, enabling quantitative analysis. An important application of these methods

involves employing potentiometric sensors to confirm the presence of betulin in wood extractives, followed by the quantitative determination of betulin using the voltammetric method. Typically, the selectivity of ion-selective electrodes relies on the presence of ionophores specific to the analytes. In this thesis, the target molecules are organic molecules, accordingly, the corresponding ionophores do not exist since ionophores bind to inorganic ions. Thus, the responses of prepared anionic, cationic, and neutral ion sensor arrays to the analytes in combination with chemometric data treatment were investigated. The investigation of potentiometric sensors focused on betulin due to the formation of a precipitate resulting from the addition of stearic acid. However, the product resulting from the addition of betulin to a mixture of potassium chloride and ethanol was not identified. Consequently, chemometric data analysis can provide clear correlations in this regard. Furthermore, the analytes are hydrophobic, thus selecting a suitable organic solvent that does not interfere with the determination of betulin and stearic acid is another challenge for voltammetric methods. To select a suitable organic solvent, the following aspects were considered: (1) Electrochemical window that does not overlap with analyte oxidation potential (2) Miscibility with an aqueous solution (3) Solubility of analytes, and non-toxicity.

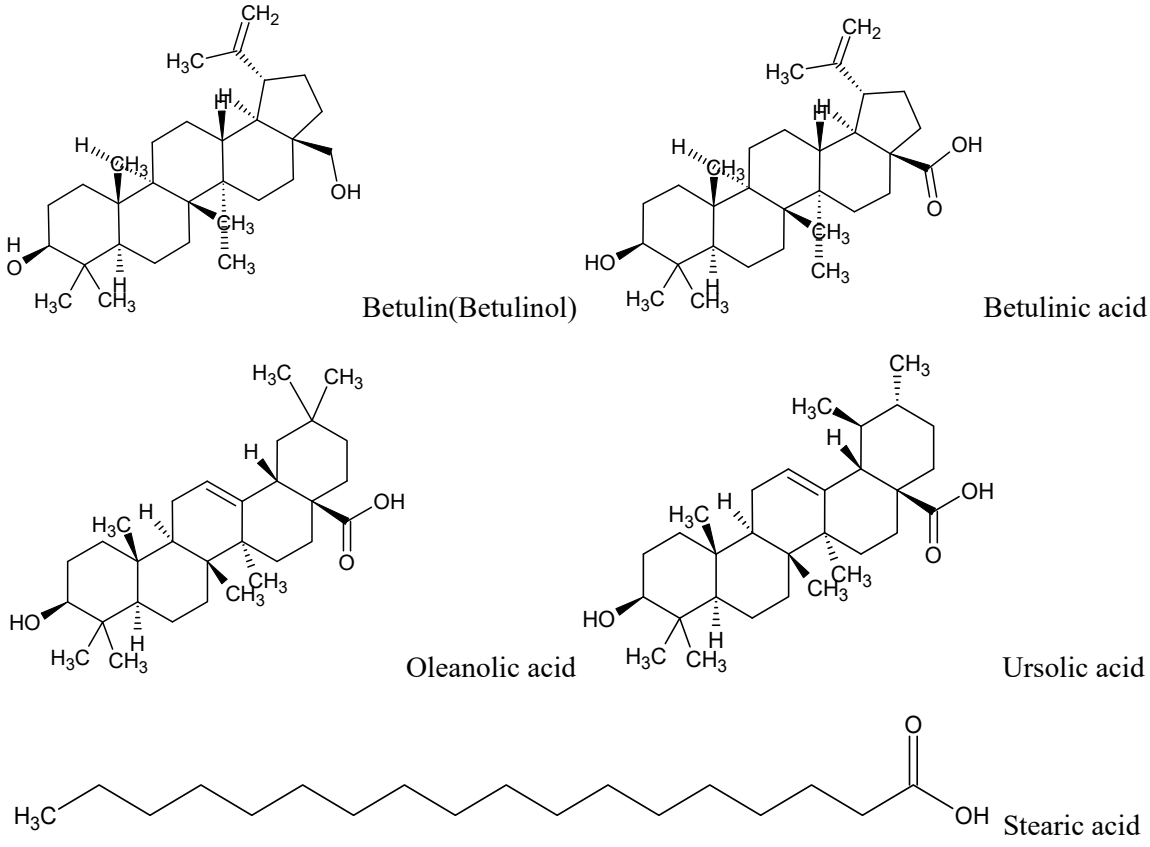

Figure 1. Chemical structures of the target molecules

2. Potentiometric ion sensors

Chemical sensors recognize the chemical information i.e., concentration, activity, and partial pressure of analytes, which can be transduced as mass, temperature, optical, and electrochemical changes. Ion-selective electrodes are considered potentiometric chemical sensors. At the sensor surface, chemical recognition is attained via a chemical equilibrium reaction [10].

Conventional ISEs consist of a membrane as an ionic conductor, an inner filling solution, and an Ag wire as an electronic conductor that is covered with AgCl as the internal reference electrode as shown in Figure 2 top. Due to the difficulty of fabricating small size conventional ISEs containing internal solution and internal electrode, solid contact ISEs were developed. Solid contact ISEs consisting of electronic conductor(substrate), transducer layer (conducting polymer), and membrane.

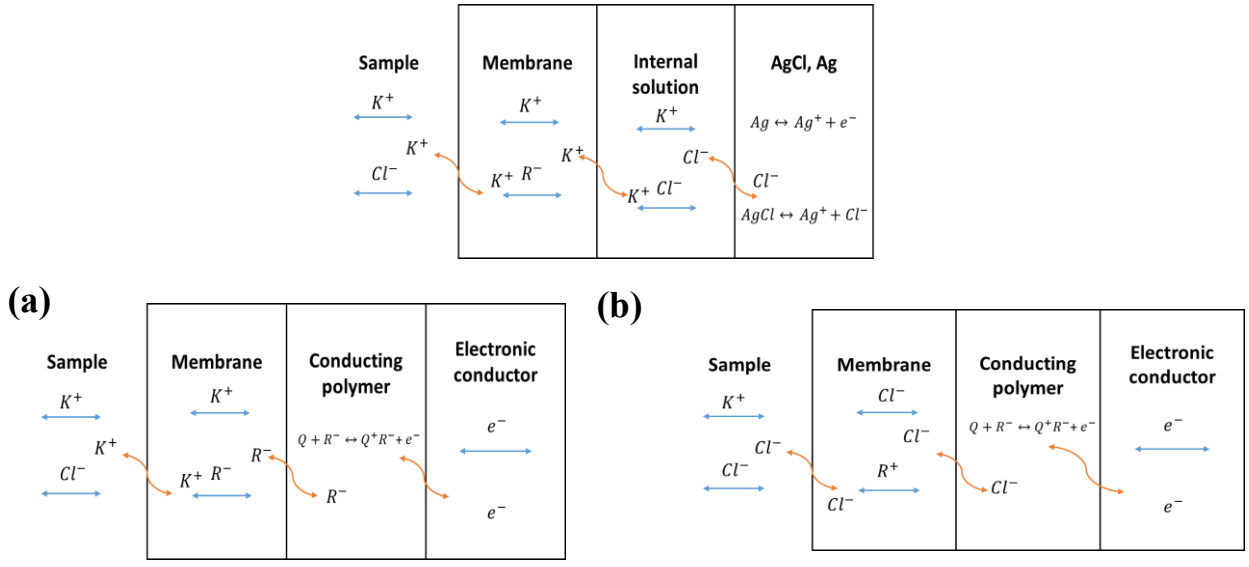

Figure 2. A conventional K^+ ISE (top), (a) K^+ selective solid contact electrode with a p-type conducting polymer (bottom), and (b) Cl^- selective solid contact electrode with a p-type conducting polymer (bottom) adopted from [11]

The internal solution of a conventional electrode must contain the ions for which the membrane is selective, by which the stability, as well as the reproducibility of potential, are obtained. Also, depending on the concentration of the sample solution, the concentration of the internal solution can be high or low. For instance, the internal solutions in K^+ ISEs for clinical and agricultural samples and NO_3^- ISEs for the analysis in fertilized soils contain high concentrations of target ions. On the other hand, Pb^{2+} ISEs are measured for trace-level analysis in the environment, thus the ISEs contain a low concentration of target ions in the internal solution.

In comparison to conventional ISEs, solid-contact ISEs of coated wire type have trouble maintaining long-term stability and reproducibility. The slope of the calibration curve *(S)* is typically stable

regardless of the ISE construction, but the standard potential(E°) changes often unpredictably. The interface between the ion-selective membrane and the electronic conductor(substrate) should record the stable and reproducible potential via a redox reaction. Therefore, the redox reaction must be fast to maintain equilibrium against the external species. The interface could be blocked if the ions are limited to the membrane and the electrons cannot travel to the substrate. To resolve these issues, conducting polymers are deposited and can stabilize the potentials of the solid-contact ISEs. Electrochemical transduction can be achievable by the deposition of conducting polymers serving as ion-to-electron transducers. By combining conducting polymer with an ion-selective membrane, selective and durable chemical sensors are obtained [11].

2.1. Ion selective membrane

The ion-selective membrane (ISM) is usually composed of polymeric matrix, plasticizers, ionophore, and ionic additives. Polymers must meet the subsequent requirements: processability, stability against temperature, hydrolysis, inertness, and insolubility in water. Poly (vinyl chloride) (PVC) based membranes meet these requirements by adding plasticizers. In most cases, PVC-based ISE membranes comprise a 1:2 mass ratio of PVC to Plasticizer, which is 30-33% of PVC and 60-66 % of plasticizer. The concentration of lipophilic ion exchangers in PVC-based membranes is approximately 0.01 M. As shown in Figure 3, the chemical structure of DOS is non-polar, and it is suitable for monovalent ion sensors, whereas oNPOE is a polar molecule and selective for divalent ions. They serve as solvents for ionophores and give the membrane elasticity [11].

Ionophores are the components determining the selectivity towards analytes and the type of potentiometric responses (cationic or anionic). Specifically, ionophores are organic neutral or charged molecules that bind to analytes and are the basis for determining potentiometric selectivity. The component in the membrane which gives permselectivity, a measurable ability to distinguish between cations and anions, is the lipophilic ion exchanger (Potassium tetrakis[3,5-bis(trifluoromethyl)phenyl] borate (KTFPB) or tridodecylmethylammonium chloride (TDMACl)) in this thesis (Figure 3). Tetradodecylammonium tetrakis (4-chlorophenyl) borate (ETH 500) consisting of a cation and an anion was combined into the membrane to decrease the resistance and enhance the limit of detection [12].

The selectivity of ISMs only containing lipophilic salts is dependent on the free energy of ion hydration. The interaction between the membrane and ions is an electrostatic character based on the Hofmeister

series, which makes the ion-site association constants low. The order of this series starts with low free hydration energy to high free hydration energy.

The Hofmeister series for anions is as follows:

$$R^- > ClO_4{}^- > SCN^- > NO_3^- > Br^- > Cl^- \approx HCO_3^- > H_2PO_4^- > SO_4^{2-}$$

The Hofmeister series for cations is as follows:

$$R^+ > Cs^+ > Cs^+ > K^+ > Na^+ > Li^+ > Ca^{2+} > Mg^{2+} > Al^{3+}$$

According to the Hofmeister series above, ion-exchanger based membranes are more selective to organic ions over hydrophilic ions [11].

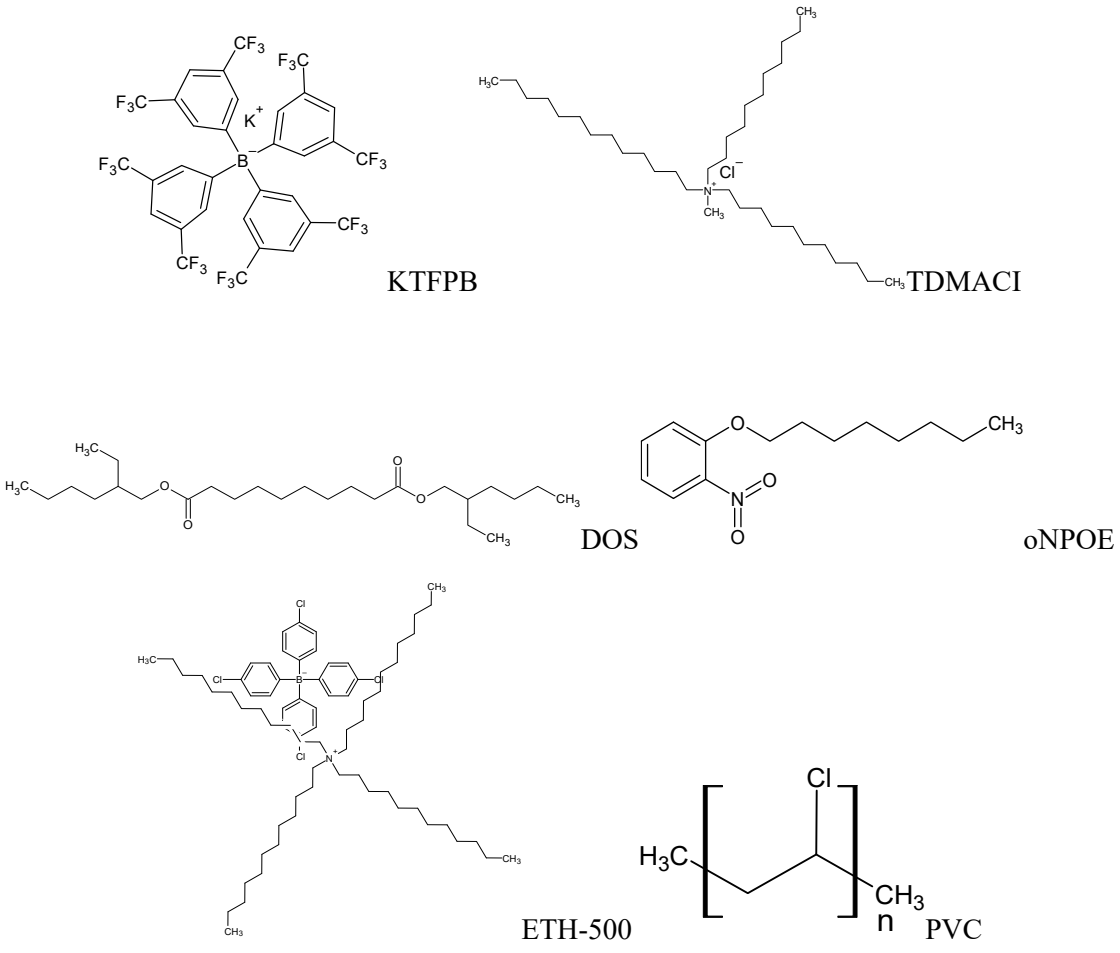

Figure 3. Chemical structures of the cocktail components

2.2 Conducting polymers as an electrochemical transducer layer

Conducting polymers are employed as ion-to-electron electrochemical transducer layer in the solid contact ISEs. As for solid contact ISEs, conducting polymer is doped/de-doped by applying a certain

potential or current to cause oxidation/reduction (electrochemical doping). Electrochemical polymerization is performed by three methods: the galvanostatic method by applying constant current, the potentiostatic method by applying constant potential, and the potentiodynamic method by applying constant sweep rate (e.g. mv/s). When undergoing oxidation, p-type conducting polymers are predominantly formed, and the doping process involving anions is employed to ensure macroscopic electroneutrality. Typically used p-type conducting polymers are poly (3,4-ethylene dioxythiophene) (PEDOT), polyaniline (PANI), poly(3-octylthiophenes) (POT), and polypyrrole (PPy). There are a couple of factors that influence the stability of CPs: pH, light, interaction with water, and temperature. In this thesis, the conducting polymer PEDOT (Figure 4) was deposited on the screen-printed carbon electrodes due to its stability in p-doped form, barely reacting with external reducing and oxidizing agents [11]. PEDOT has a high electronic conductivity that stabilizes the potential and has a high redox capacitance. PEDOT is not likely to be influenced by CO_2 and pH compared to PPy and PANI. However, it is sensitive to redox interference due to the ion flux related to the side reactions caused by its high capacitance, which results in a potential drift eventually [14].

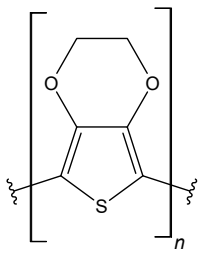

Figure 4. Chemical structure of PEDOT

3. Characterization Techniques

3.1. Potentiometry

Potentiometry is an electrochemical analytical technique to measure the potential difference between the constant potential of a reference electrode with constant potential and an indicator electrode under a negligible current. The potential of an individual electrode is not measurable, but the difference between two electrodes immersed in a solution can be measured. The indicator electrode responds to

the activity of analyte ions and follows the Nernst equation. The activity of the species i is expressed as

$$a_i = \gamma_i C_i \qquad \text{(Eq. 1)}$$

where γ_i is the activity coefficient of species i and C_i is the concentration of species i. The activity coefficient depends on ionic strength (Eq.2) and ion size and can be calculated using Debye-Hückel equation (Eq.3).

$$J = \frac{1}{2}\sum_{k=1}^{n} C_k z_k^2 \qquad \text{(Eq. 2)}$$

where J is the ionic strength of the solution, C_k is the concentration of ion k and z_k is the charge of ion k.

$$\text{Log}\,\gamma_i = -\frac{Az_i^2\sqrt{J}}{1+a_{Kjel}B\sqrt{J}} \qquad \text{(Eq. 3)}$$

a_{Kjel} is the hydrated(solvated) ion radius, A=0.512, and B=0.328 in aqueous solutions at 25℃.

On the other hand, the reference electrode preserves a constant potential [15]. In this thesis, a double junction electrode Ag/AgCl/3 M KCl/1 M LiOAc was employed since 1 M lithium acetate(LiOAc) prevents direct contact with the solution containing KCl and has similar mobility with potassium chloride (KCl). In two electrodes set up that consists of an indicator electrode and a reference electrode, the electromotive force (EMF) follows the equation where E is the measured EMF, E° is the standard EMF value at $a_1 = 1$.

$$E = E^0 + Sloga_1 \qquad \text{(Eq. 4)}$$

Hence, the practical experimental slope is $\text{S} = \frac{dE}{dloga_1}$ [11].

3.2. Chemometric data treatment - Principal component analysis (PCA)

Chemometric data treatment allows us to extract information from massive quantities of experimental data by advanced statistical calculations. The principal component analysis is one of the multivariate analysis techniques. In terms of multivariate analysis with an extreme volume of data, it is difficult to comprehend the correlations. Principal component analysis helps to reduce the data in case the data has certain relationships and patterns.

The purpose of PCA is to discover the principal components $Z_1, Z_2, \cdots, Z_n$ that are proportional to the combinations of the original variables relating to each specimen, $X_1, X_2, \cdots, X_n$. The coefficients, a_{11}, a_{12}, a_{13}, etc., should be set in order for new variables not to be associated with each other. Thus, the coefficients, $a_{11}, a_{12}, a_{13}, etc$, exclusively belong to the principal component, Z_1.

$$Z_1 = a_{11}X_1 + a_{12}X_2 + a_{13}X_3 + \cdots a_{1n}X_n \qquad \text{(Eq. 5)}$$

$$Z_2 = a_{21}X_1 + a_{22}X_2 + a_{23}X_3 + \cdots a_{2n}X_n \qquad \text{(Eq. 6)}$$

⋯etc

The first principal component, Z_1, has the largest variation, and the second principal component, Z_2, has the second largest variation. Orthogonality is one of the characteristics of principal component analysis wherein every principal component is positioned perpendicularly to one another in multi-dimensional space. Constructing a new set of variables does not mean it would increase the number of useless data, but we could acquire a much smaller number of useful principal components than the original variables if there are significant correlations. Thus, the amount of data can be reduced [16].

3.3. Cyclic Voltammetry

Cyclic voltammetry is a voltammetric technique in which a triangular-shaped potential is applied as shown in Figure 5 and both oxidation and reduction occur at the working electrode. Cyclic voltammetry is used to investigate the redox behavior of analytes and the kinetics of electrode reactions. During cathodic and anodic scans, the diffusion rate is too low to exceed the reaction rate of reduced (R) or oxidized (O) product near the electrode (Figure 5). Thus, the current reaches a peak and then decreases as the product is depleted. In a reversible process, anodic and cathodic peak currents have equivalent magnitude. Also, the reactant and product remain in equilibrium concentration at the electrode surface and the peak current is proportional to the square root of the sweep rate ($v^{1/2}$). On the other hand, the peak current of an irreversible redox reaction, such as the electroactive species accumulated on the electrode, is proportional to the sweep rate (v) [15].

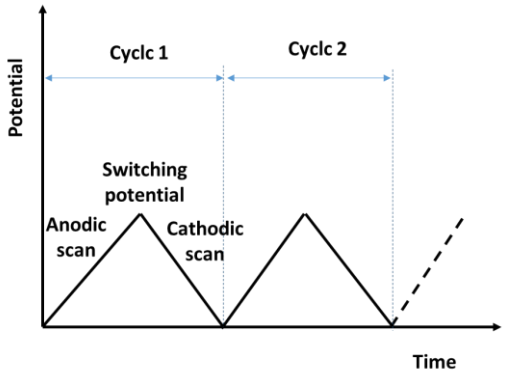

Figure 5. Cyclic voltammetry(CV) potential-time triangular waveform

3.4. Square Wave Voltammetry (SWV)

Square wave voltammetry(SWV) is one of the most advanced pulse voltammetric techniques and has advantages in terms of electrode mechanism comprehension and improved analytical sensitivity. The SWV technique is quite fast, which can be recorded up to 1 V/s scan rate. It is suitable for the analysis of reversible and quasi-reversible electrode reactions. There are a couple of advantages to using SWV. It consumes a lower analyte than differential pulse voltammetry (DPV) since DPV has its drawback with the adsorption of analyte and it can cause the electrode surface to be blocked eventually [17].

$$I_{dl} = C_{dl} \frac{dv}{dt} \qquad \text{(Eq. 7)}$$

$$I_{total} = I_{faradaic} + I_{dl} \quad \text{(Eq. 8)}$$

In Eq. 7, I_{dl} is capacitive current, C_{dl} is capacitance, and $\frac{dv}{dt}$ is the derivative of the voltage with respect to time. In Eq.8, the total current is equal to the sum of the faradaic current and the capacitive current. Capacitive current is a background current that is associated with double-layer charging. Faradaic current results from redox reactions of analyte at the working electrode. Capacitive current(I_{dl}) is preferably eliminated by replacing continuous potential with the staircase potential, which significantly enhances the sensitivity of the analysis.

A three-electrode cell is employed in voltammetry where the current is measured between the working electrode and the counter electrode as a function of potential between working electrode and reference electrode. The analyte is reduced at the electrode during the cathodic pulse and reoxidized during the anodic pulse (Figure 6a). The current is measured at the end of each current potential, which diminishes the influence of the capacitive current [15].

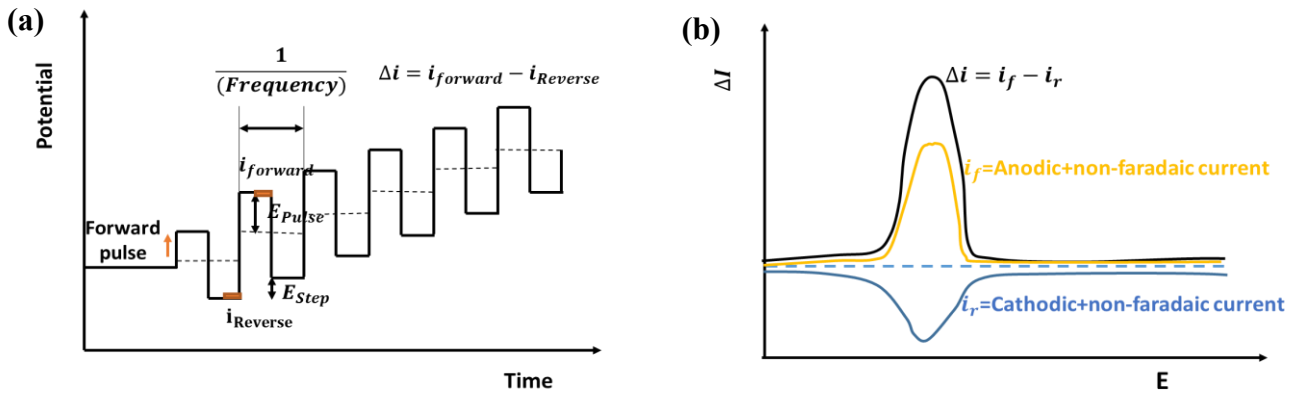

Figure 6. Square wave voltammetry (SWV)(a) potential-time waveform and (b)current-potential response

Redox peak can be confirmed by the current subtraction of two opposite pulses at once. Subtraction of forward current and reverse current is quite useful since the current difference is zero in the range of limiting current, thereby influence of reduction current by dissolved oxygen can be negligible (Figure 6b) [17].

3.5. Anodic stripping voltammetry

Anodic stripping voltammetry is the most sensitive voltammetric technique since the pre-concentration step precedes the scan in order to lower the detection limit of the analyte. The analyte of interest is deposited on a thin film of mercury or other electrodes by reduction reaction under the stirring condition and it is oxidized back into the electrolyte without stirring (non-convective condition) [18]. Typically, it is a suitable technique for trace metal analysis, but a derivation of this technique, lead film electrode was reported to show that it is feasible to detect betulinic acid and oleanolic acid [19–22]. The lead film electrode (PbFE) has its advantages in terms of less volatility and lower toxicity compared to the mercury electrodes. It can be measured in a broader potential window, a wide range of pH media, and simple operation regarding the renewal of surface area and preparation. Additionally, the measurements can be carried out without deaeration of the sample [21]. The electroactive species is accumulated on the electrode at the negative value of standard reduction potential [18].
In neutral media electrolyte, the following in situ lead film is formed [20].

$$Pb^{2+} + 2H_2O \rightarrow Pb(OH)_2 + 2H^+$$

However, in highly alkaline media, the following complex is formed instead of hydrolyzing.

$$Pb^{2+} + 4OH^- \rightarrow Pb(OH)_4{}^{2-}$$

In this thesis, lead film formation in neutral, alkaline aqueous media and non-aqueous media was investigated with the accumulation of analytes prepared in either Ethanol or DMSO.

The deposition time must be measured carefully, and reproducible stirring should be applied. Deposition time for 30 seconds significantly decreases the limit of detection down to 10^{-7} M and the limit of detection of the deposition time for 20 minutes reaches down to 10^{-10}~ 10^{-11} M [18]. In this thesis, 30 seconds and -1.0V were used as a deposition time and absorption potential, correspondingly, since it reached a maximal peak current in this condition as demonstrated in the cited article [19]. Anodic stripping voltammetry and adsorptive stripping voltammetry are analogous electroanalytical techniques. Anodic stripping voltammetry involves electrocatalysis during the preconcentration step,

while the preconcentration step in adsorptive stripping voltammetry is based on adsorption on the WE surface [23].

3.6. Differential pulse voltammetry (DPV)

Differential pulse voltammetry (DPV) is a pulse voltammetry technique that is intended to minimize the charging current. The pulse potential is placed on each other as a linear gradient and the base potential is increased between pulses by the equivalent magnitude (Figure7). The pulse potential(E_{pulse})and step potential(E_{Step}) are kept constant, and the pulse time(t_{pulse}) is much shorter than that of between pulses ($t_1=t_{int}-t_{Pulse}$). The background current is significantly reduced by measuring the current before the next pulse and the current difference($\Delta t = t_2 - t_1$) is calculated at the end of each pulse. The main advantage of this technique is high sensitivity with low capacitive current. On the other hand, the analysis time is longer than other pulse techniques [24]. In terms of analysis for organic compounds using mercury-drop electrodes, DPV gives a better response than normal pulse voltammetry (NPV) because the remaining capacitive current is subtracted in the differential waveform. Moreover, the differential pulse waveform mitigates the current signal influence caused by adsorption on solid electrodes by treating differently the application of the constant pulses before and after [17].

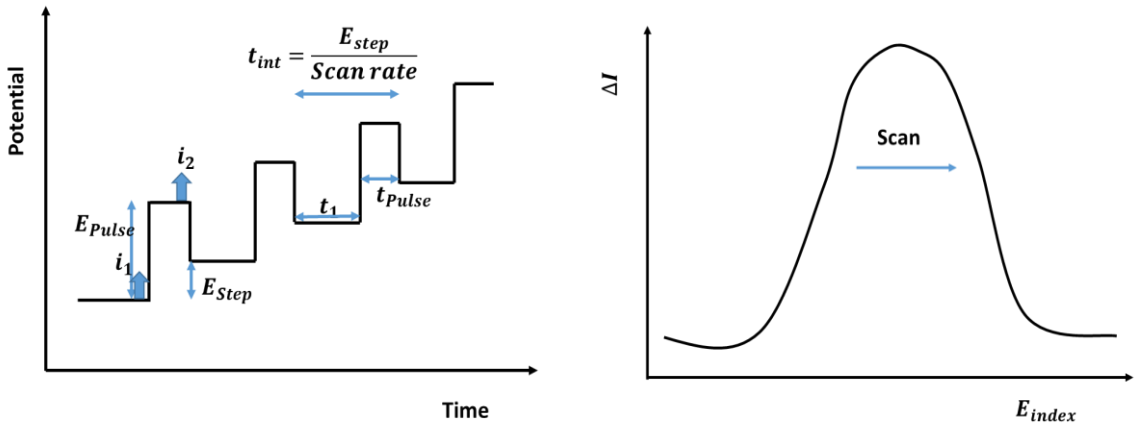

Figure 7. Differential pulse voltammetry(DPV) (a)Potential-time waveform and (b)current-potential response

3.7. Normal pulse voltammetry (NPV)

Normal pulse voltammetry (NPV) is a pulse voltammetric technique that a certain step potential added on top of the preceding pulse potential forms rectangular potential pulses(E_p) based on the initial

potential (Figure 8). Each pulse potential is applied for a constant pulse time (t_{Pulse}) and in between each pulse, the potential returns to the constant baseline potential, and the next pulse potential as high as the step potential added to the prior potential is applied. The baseline potential (E_{Base}) is smaller than the potential that oxidation or reduction reaction of analytes can occur. The baseline potential is mainly attributed to the DC offset located in the limiting current region of a prior oxidation/reduction reaction, by which the preceding wave is negligible in the pulse current [25].

As a common advantage for pulse voltammetric techniques, a higher faradaic current is detectable in comparison to potential sweep voltammetric techniques (CV and LSV) since the current signal is measured at the end of each applied potential pulse.

In this thesis, normal pulse voltammetry was not employed. However, differential normal pulse voltammetric measurements, a derivative technique from normal pulse voltammetry, were performed to compare the shapes of voltammograms and the clear proportionality to the addition of standard solution.

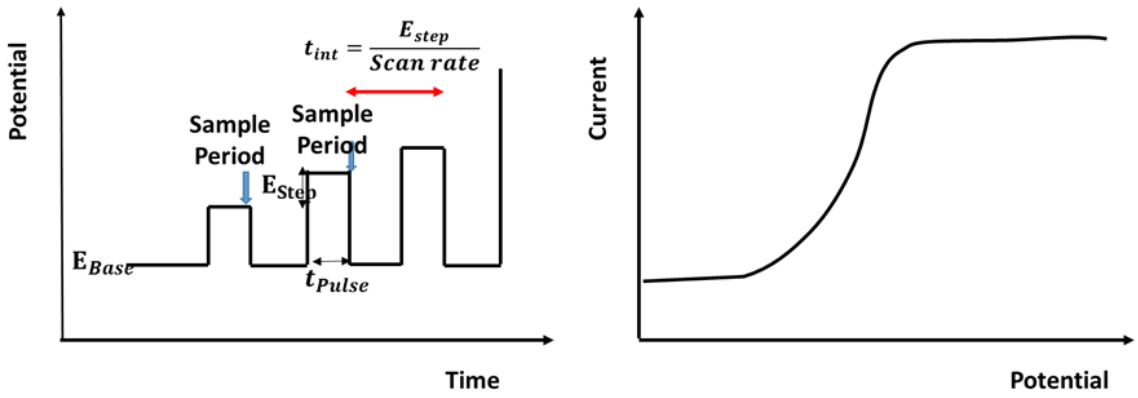

Figure 8. Normal pulse voltammetry (NPV) (a)Potential-time waveform and (b)current-potential response

3.8. Differential normal pulse voltammetry (DNPV)

Differential normal pulse voltammetry (DNPV) is a hybridization of normal pulse and differential pulse voltammetry combining the advantages of the two techniques (Figure 9). The current difference is plotted as a function of potential and the current difference is measured before the pulse and at the end of the pulse. The background current can be subtracted to consider the faradaic current entirely for analysis since background capacitive currents are constant. The essential pulse waveform shape of DNPV is equal to the normal pulse voltammetry (NPV) waveform where there is a double potential step is applied in each wave pulse and turns back to the constant base potential at the end of each pulse

[26]. It is advantageous in terms of adsorption problems compared to differential pulse voltammetry [17].

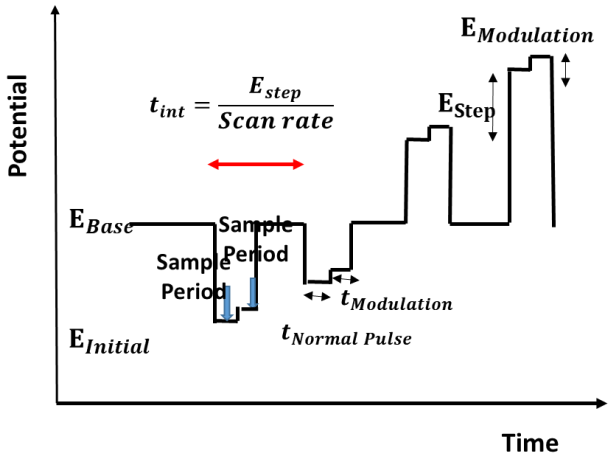

Figure 9. Differential normal pulse voltammetry (DNPV) Potential-time waveform

4. Experimental procedure

4.1. Chemicals

Dimethyl sulfoxide (DMSO, ≥ 99.9 %) was purchased from Honeywell (Charlotte, North Carolina, USA). Betulinic acid (≥ 97.0 %) and oleanolic acid (≥ 97 %), tetrahydrofuran (THF, > 99.5 %), and anhydrous acetonitrile (ACN, 99.8 %) were obtained from Sigma Aldrich (St Louis, MO, USA). Betulin (≥ 97 %) and stearic acid (≥ 97 %) model compounds were provided by UPM. Bis(2-ethylhexyl) sebacate, tetradodecylammonium tetrakis (4-chlorophenyl) borate, 2-nitrophenyl octyl ether, tridodecylmethylammonium chloride was acquired from Honeywell (Charlotte, North Carolina, USA). Potassium tetrakis [3,5-bis(trifluoromethyl)phenyl] borate was obtained from Sigma Aldrich (St Louis, MO, USA). Ethanol (Etax 94.0 %, Altia Oyj, Rajamäki, Finland) was used as a solvent to prepare the standard solution for principal component analysis of potentiometric measurements. Another ethanol (Ethanol≥ 96 %, TechniSolv®, pure) was obtained from VWR chemicals (Radnor, Pennsylvania, USA). The ethanol was used for the preparation of electrolytes and standard solution for preliminary qualitative potentiometric measurements. Sodium hydroxide (≥ 97.0 %), tris(hydroxymethyl)aminomethane (≥ 99.8 %), tetrabutylammonium hexafluorophosphate (98 %), and potassium chloride (KCl, ≥ 99 %) were obtained from Sigma-Aldrich (St Louis, MO, USA). Hydrochloric acid 0.1 M standard solution was obtained from Thermo Fisher Scientific (Waltham, Massachusetts, USA). 0.01 M Pb $(NO_3)_2$ solution was prepared by dissolving lead (II) nitrate

($Pb(NO_3)_2$, ≥ 99.5 %) obtained from Sigma Aldrich (St Louis, MO, USA). Distilled and deionized water (ELGA Purelab Ultra; resistivity 18.2 MΩ cm) was used to prepare the aqueous electrolyte solutions and 0.01 M Pb $(NO_3)_2$ solution.

4.2. Galvanostatic polymerization of PEDOT(Cl) and PEDOT(PSS)

As for electropolymerization, the galvanostatic method was employed to deposit the conducting polymer PEDOT on the screen-printed electrodes. A constant current was applied between WE and CE for a certain time to acquire the desired polymerization charge (C). A polymerization solution, containing 0.01 M 3,4-Ethylenedioxythiophene (EDOT) and 0.1 M Sodium polystyrene sulfonate (NaPSS) dissolved in deionized water, was prepared for the cationic ion selective electrodes. Another 25 mL volume polymerization solution containing 0.01 M 3,4-Ethylenedioxythiophene (EDOT) as a monomer with 0.1 M KCl as a supporting electrolyte was prepared for the preparation of anionic ion selective electrodes. The polymerization solutions wrapped with aluminum foil were stirred overnight since the solubility of EDOT in water is low. The polymerization solution was purged with N_2 gas for 15 minutes and the gas outlet kept above the surface of the solution throughout the experimentation. A constant current of 0.0000251 A (0.0251 mA) was applied for 710 seconds (C = 17.8 mC). As for glassy carbon (3 mm diameter) electrodes, typically 0.0141 mA was applied for 710 seconds (10 mC) was applied. However, a different value of current should be applied considering the area of the working electrode (diameter) in order to polymerize the conducting polymers (CPs) on screen-printed electrodes (SPEs).

$$\text{Current density}(j) = I/A \qquad \text{(Eq. 7)}$$

$$\frac{A_{SPE}}{A_{GCE}} = \frac{\pi(2mm)^2}{\pi(1.5mm)^2} = 1.78 \qquad \text{(Eq. 8)}$$

$$I_{SPE} = 1.78 \times 0.0141\text{mA} = 0.0251\text{mA} \qquad \text{(Eq. 9)}$$

The potentiostat Autolab general-purpose electrochemical system (AUTO30.FRA2-Autolab Eco Chemie, B.V., The Netherlands) was used with a two-electrode electrochemical cell in which an SPE was connected as the WE, and a GC rod as the CE to avoid contamination by the supporting electrolytes in the reference electrodes. After the polymerization was completed, the SPEs were rinsed with water and the formation of a conducting polymer layer was confirmed by cyclic voltammetry. Subsequently, the electrodes were kept in 0.01 M KCl conditioning solution for at least 24 hours.

4.3. Cyclic voltammetric measurements

Cyclic voltammograms were recorded to confirm the cleanliness of polished GC electrodes and the deposition of conducting polymer layer on screen-printed carbon electrodes. The measurements were performed in a three-electrochemical cell by the Autolab general-purpose electrochemical system. A Metrohm single junction electrode Ag/AgCl/3 M KCl was used as RE and a GC rod was connected as CE. A PVC-mounted glassy carbon electrode was connected to WE in 0.1 M KCl electrolyte. The open circuit potential was set as the start potential and the potential range was −0.5 V to 0.5 V with the scan rate of 0.1 V/s (3 cycles). The 0.1 M KCl solution was purged with N_2 for 15 minutes, and the gas outlet was kept above the electrolyte throughout the measurements.

4.4. Fabrication of cationic, anionic, and neutral solid-contact ISEs

As shown in Figure 10, screen-printed carbon electrodes were used to fabricate the cationic, anionic, and neutral ion-selective electrodes due to their simplicity of preparation without polishing step, being low-cost, and disposable. These properties are important for preparing numerous ISEs without ionophores since the ionic selective membrane based on lipophilic salts loses its selectivity within a short period compared to ion-selective membranes based on ionophores. The ion-selective membrane without an ionophore is more likely to be leached into an aqueous phase because the ionophore is complexed with counter ions, which results in less concentration of them in the solution and gives more hydrophobicity [13].

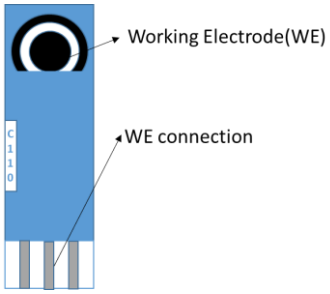

Figure 10. Screen-printed Carbon Electrodes ref. C110, Metrohm DropSens, Oviedo, Spain, Ceramic substrate: L33 x W10 x H0.5 mm/ Working electrode: Carbon (4 mm diameter) [9]

When betulin is dissolved in ethanol and introduced into a 0.01 M potassium chloride (KCl) solution with varying ethanol content, it is anticipated to maintain its dissolved state. Ethanol, being a polar solvent, can effectively solvate betulin by interacting with its polar functional groups. However, in the presence of KCl, the interaction between ethanol and betulin can be affected as ethanol molecules

surrounding betulin undergo ionization or dissociation. The polar nature of the KCl solution can disrupt the ethanol-betulin interactions, potentially leading to the formation of betulin ions. However, the specific form of betulin in the KCl solution is unidentified and it is influenced by various factors such as pH, concentration, and temperature. Ionized betulin or a neutral form of betulin can generate potential responses by a set of anionic, cationic, and neutral ISEs.

Five SPEs with Carbon/PEDOT: PSS and five SPEs with Carbon/PEDOT: Cl were rinsed with water and they were dried for at least 24 hours before drop-casting the ion-selective membranes. The ISM with the composition shown in Table 1-5 was drop-casted on the corresponding screen-printed electrodes. A total 50µL ISM cocktail was drop-casted with reference to the ideal working volume [27]. A 25 µL of ISM cocktail was drop-casted first and dried for approximately 15 minutes. An additional 25 µL of ISM cocktail was drop-casted and dried for 48 hours while being covered with a glass container to protect them from contaminants. The fully dried electrodes were kept in 0.01 M KCl conditioning solution for at least 24 hours before further measurements.

Solid contact ISEs with cationic ion-selective membranes were prepared by drop-casting the ISM cocktails on PEDOT(PSS) solid contact. The cationic ISM cocktails (dry mass 14.9 %) were prepared by dissolving the compounds in 1.5 mL THF (Table 1 and 2).

Table 1. Dry mass composition of PVC-based cationic ISM cocktails using DOS as plasticizer

Dry membrane components	Model 1a		Model 1b	
	wt. (%)	mass (g)	wt. (%)	mass (g)
Valinomycin	0.00%	0.0000	0.0000	0.0000
KTFPB	0.52%	0.0012	0.52%	0.0012
ETH-500	1.03%	0.0024	0.00%	0.0000
DOS	65.62%	0.1527	66.30%	0.1527
PVC	32.83%	0.0764	33.17%	0.0764
Total	100.00%	0.2327	100.00%	0.2303

Table 2. Dry mass composition of PVC-based cationic ISM cocktails using oNPOE as plasticizer

Dry membrane components	Model 2a		Model 2b	
	wt. (%)	mass (g)	wt. (%)	mass (g)
Valinomycin	0.00%	0.0000	0.00%	0.0000
KTFPB	0.52%	0.0012	0.52%	0.0012
ETH-500	1.03%	0.0024	0.00%	0.0000
oNPOE	65.62%	0.1527	66.30%	0.1527
PVC	32.83%	0.0764	33.17%	0.0764
Total	100.00%	0.2327	100.00%	0.2303

Solid contact ISEs with anionic ion-selective membranes were prepared by drop-casting the ISM on PEDOT(Cl) layer. The anionic ISM cocktails (dry mass 15.2 %) were prepared by dissolving the compounds in 2.0 mL THF (Table 3 and 4).

Table 3. Dry mass composition of PVC-based anionic ISM cocktails using DOS plasticizer

Dry membrane components	Model 3a		Model 3b	
	wt. (%)	mass (g)	wt. (%)	mass (g)
TDMACl	1.16%	0.0037	1.20%	0.0037
ETH-500	3.14%	0.0100	0.00%	0.0000
DOS	62.75%	0.2000	64.79%	0.2000
PVC	32.95%	0.1050	34.01%	0.1050
Total	100.00%	0.3187	100.00%	0.3087

Table 4. Dry mass composition of PVC-based anionic ISM cocktails using oNPOE plasticizer

Dry membrane components	Model 4a		Model 4b	
	wt. (%)	mass (g)	wt. (%)	mass (g)
TDMACl	1.16%	0.0037	1.20%	0.0037
ETH-500	3.14%	0.0100	0.00%	0.0000
oNPOE	62.75%	0.2000	64.79%	0.2000
PVC	32.95%	0.1050	34.01%	0.1050
Total	100.00%	0.3187	100.00%	0.3087

Solid contact ISEs with neutral ion-selective membranes were prepared by drop-casting the ISM on PEDOT(Cl) and PEDOT(PSS). The neutral ISM cocktails (dry mass 15.1 %) were prepared by dissolving the compounds in 2.0 mL THF (Table 5). In this thesis, the term “neutral ISEs” means that they contain neither KTFPB nor TDMACl that makes them non-permselective to cations or anions.

Table 5. Dry mass composition of PVC-based neutral ISM cocktails using DOS or oNPOE as plasticizer

Dry membrane components	Model 5a		Model 5b	
	wt. (%)	mass (g)	wt. (%)	mass (g)
ETH-500	3.17%	0.010	3.17%	0.010
DOS for 5a/ oNPOE for 5b	63.49%	0.200	63.49%	0.200
PVC	33.33%	0.105	33.33%	0.105
Total	100.00%	0.315	100.00%	0.315

4.5. Potentiometric measurements

Potentiometric measurements were performed using a 16 channel multi-voltmeter (Lawson Labs. Inc., Malvern, PA, USA). The prepared four cationic, four anionic, and two neutral ion selective electrodes were calibrated with a sequential dilution by using a Metrohm Dosino 700 pump. Two electrode set-up was employed where Ag/AgCl/3 M KCl/1 M LiOAc was used as RE and ten ISEs (four cationic, four anionic, and two neutral ISEs) were connected to the WE channel. A 50 mL 0.1 M KCl solution was diluted down to 10^{-7} M KCl by sucking 45 mL from the previous solution and filling up with the same volume of DI water during each dilution step. The potential was stabilized for 5 minutes between every dilution step. The activity coefficients of K^+ (r_{K+}) and Cl^- (r_{cl-}) measured in the concentration of 10^{-1} to 10^{-6} M were computed by using the Debye-Hückel equation to calculate the activity of potassium(a_{K+}) and chloride ions(a_{cl-}). The logarithm value of activity formed the x-axis of the calibration curve and the five last stable potential values before the dilution step were averaged to construct the y-axis of the calibration curve.

The stock solution of betulin and stearic acid was prepared considering the solubility of betulin and stearic acid in ethanol, 0.5 mg/mL and 10 mg/mL, respectively. 0.0125 g of betulin was dissolved in ethanol 25 mL and 0.2500 g of stearic acid was dissolved in ethanol 25 mL. They are ultra-sonicated until they are completely dissolved. 5 % (w/w) ethanol, 10 % (w/w) ethanol, 15 % (w/w) ethanol, and 20% (w/w) ethanol in 0.01 M KCl were prepared respectively as electrolytes. First, 50 mL of 5 % (w/w) ethanol in 0.01 M KCl solution was transferred to a measuring cell and the potential response was measured under two electrode set-ups, Ag/AgCl/3 M KCl/1 M LiOAc as RE and 10 ISEs (four cationic, four anionic, and two neutral ISEs) as WEs. Subsequently, the potential response was recorded by the standard addition method. 1 mL of the stock solution was added into 5 % (w/w) ethanol in 0.01 M KCl successively up to 5 mL. After each 1 mL addition of stock solution, the electrolyte was stirred for 1 min and the potential was left to be stabilized for 5 minutes. The five stable potential was averaged to construct the y-axis of the calibration curve and the final concentration of the standard was computed to form the x-axis of the calibration curve. The identical procedure was applied to 10 % (w/w) ethanol, 15 % (w/w) ethanol, and 20 % (w/w) ethanol in 0.01 M KCl electrolyte.

Based on the obtained results, a multi-dimensional calibration approach was employed to explore the correlation between the response of the prepared ion-selective electrodes (ISEs) and the analytes. Three distinct classes of electrolytes were prepared for this investigation. Class 1 consisted of 5 % (w/w) ethanol in 0.01 M KCl solution, class 2 comprised 0.01 M KCl solution, and class 3 consisted of 5 % (w/w) ethanol in 0.01 M KCl supplemented with 1 mL of betulin stock solution. A total of eight

potentiometric measurements were conducted for each class, with five measurements designated as training sets and three measurements treated as samples. This procedure was repeated for all three classes, resulting in a total of 24 measurements. To ensure measurement accuracy, a stabilization time of five minutes was allowed for each individual measurement.

4.6. Glassy carbon electrode preparation

Glassy carbon electrodes mounted by PVC cylinder were polished by sandpapers 1000, 2500, and 4000 using Grinder (Buehler Metaserv 3000 Grinder polisher, Buehler, USA). Successively, the GC electrodes were polished using the diamond paste (15 μm, 9 μm, 3 μm, and 1 μm) on a DP-Plan cloth, and then the diamond paste was wiped with ethanol wetted Kimtech wipes. Additionally, the electrodes were polished with 0.3 μm alumina slurry, followed by a water wetted DP-Nap cloth. As a last step, they were ultra-sonicated for 5 minutes in ethanol and water, respectively. To confirm the cleanliness of the GC electrodes, cyclic voltammograms were recorded as demonstrated in the section 4.3.

The glassy carbon electrode was polished before every square wave voltammetric measurements using 0.3 μm alumina slurry on a DP-Nap cloth to remove residual substances on the surface. Afterwards, the electrode was rinsed with ethanol and water thoroughly, and wiped with a Kimtech wipe.

4.7. Square Wave voltammetric measurements

Square wave voltammograms were recorded in the scan range from -1.0 V to 1.7 V in Tris-HCl buffer (pH 7.4) and NaOH 0.2 M both containing 7.5×10^{-5} M $Pb(NO_3)_2$. The supporting electrolyte was prepared in a manner that 75 μL of $Pb(NO_3)_2$ was transferred to a 10 mL volumetric flask and the rest was filled up to the mark. 10 mL of the supporting electrolyte was transferred to a three-electrochemical cell in which Ag/AgCl/3 M KCl/3 M KCl, a glassy carbon electrode mounted in PVC cylinder, and a glassy carbon rod were used as RE, WE, and CE, respectively. The experimental parameter for amplitude and frequency was 50 mV and 200 Hz, correspondingly. The step potential was set as 2 mV; accordingly, the scan rate was 0.4 V/s. As a pretreatment step, 0.5 V conditioning potential was applied for 30 seconds to remove the lead film remaining from the preceding measurement, and at -1.0V, the lead film was deposited on the electrode by reduction and the analyte was accumulated simultaneously for 30 seconds. The solution was stirred throughout the cleaning and pre-concentration step, and it was followed by an equilibrium step at -1.0 V for 5 seconds during

which the stirring was stopped. The scan was initiated from the deposition potential at -1.0 V towards the anodic direction. All measurements were carried out without deaeration. Experimental investigations were conducted on betulin and betulinic acid under both unpurged and purged with nitrogen in the electrochemical cells. The outcomes of these investigations are presented in Figures D-1 and D-2 (Appendix D). In addition, the GC electrodes were not polished between the measurements because this can affect the sensitivity of the determination [19].

For the square wave voltammetric measurements in 0.2 M NaOH as a supporting electrolyte, the stock solutions of betulin and betulinic acid (100 mg/L) were prepared by dissolving 0.0025 g of standard in 25 mL Ethanol solvent. The working solution (0.1 mg/L) was prepared by sequential dilution according to the cited articles [19, 22].

On the other hand, as for the measurements conducted in Tris-HCl buffer (pH 7.4) as a supporting electrolyte, DMSO was used as a solvent. The standard solutions of betulin, betulinic acid, and oleanolic acid (5 mM) were prepared by dissolving an appropriate amount in DMSO with reference to solubility to DMSO and detectable concentration of the analyte according to the article [9]. The stock solution and working solution containers were tightly closed and kept in the dark covered with tin foil at around 4 ℃. betulin, oleanolic acid stock solutions were prepared in a 2 mL volume, and betulinic acid in a 1 mL volume considering the stability and availability of the standard materials in the chemical storage. The prepared solutions were stored under inert gas to protect them from oxidation.

4.8. Differential pulse voltammetric (DPV) measurements

Differential pulse voltammograms were registered in the scan range from -1.0 V to 2.4 V in $TBAPF_6$ containing 7.5×10^{-5} M $Pb(NO_3)_2$. The non-aqueous supporting electrolyte was selected considering an advantage of a wider electrochemical potential window and the possible water electrolysis at a high potential when using an aqueous electrolyte. 75 µL volume of 0.01 M Pb $(NO_3)_2$ solution was placed in a 10 mL volumetric flask, and the rest was filled up with 0.1 M $TBAPF_6$ prepared in anhydrous acetonitrile. The supporting electrolyte was transferred to a three-electrochemical cell in which a Ag/AgCl wire electrode, a Pt wire, and a PVC-mounted GC electrode were connected as RE, CE, and WE, respectively. The step potential was set as 0.015 V and the interval time was 0.3 s, accordingly, the scan rate was 50 mV/s. The modulation amplitude was 50 mV and the modulation time was 0.05 s. The identical pretreatment step with the SWV measurements was applied to the DPV measurements. A 0.5 V conditioning potential was applied for 30 seconds to remove the lead film remaining from the

preceding measurements, and at −1.0 V, the lead film was deposited on the electrode by reduction and the analyte was accumulated simultaneously for 30 seconds. The solution was stirred throughout the cleaning and pre-concentration step, and it was followed by an equilibrium step at −1.0 V for 5 seconds during which the stirring was stopped. The scan was initiated from the deposition potential at -1.0V towards the anodic direction.

Differential pulse voltammograms without the pre-treatment step were also recorded to investigate the influence of adsorption on sensitivity and the formation of the lead film on the GC electrode surface in a non-aqueous solution. They are registered from −1.0 V to 2.4 V with identical experimental parameters but without the pre-treatment step. All measurements were carried out in undeaerated solutions under ambient conditions considering the redox potential of dissolved oxygen in air saturated ACN/H_2O mixture and the negligible diffusion coefficients of oxygen and superoxide radical anion in acetonitrile [28].

The standard stock solution (5mM) was prepared for the measurements. Additionally, considering the high signals of the peak current, 0.5 mM and 0.05 mM of the standard working solution was prepared by diluting the stock solution.

4.9. Differential normal pulse voltammetric measurements

To compare the sensitivity of the voltammetric methods under investigation, differential normal pulse voltammetric measurements were conducted. The differential normal pulse voltammograms were recorded using the same procedure as SWV and DPV. Specifically, a 75 µL volume of a 0.01 M Pb $(NO_3)_2$ solution was transferred into a 10mL volumetric flask, and the remaining volume was filled with either 0.1M $TBAPF_6$ or Tris-HCl buffer (pH 7.4). The scan range for Tris-HCl buffer at pH 7.4 was set from −1.2 V to 2.0 V, while for 0.1M $TBAPF_6$, it was set from −1.2 V to 2.4 V. The broad scan range was selected to observe the redox peaks effectively. The step potential and interval time were set to 0.015 V and 0.3 s, respectively, resulting in a scan rate of 50mV/s. The modulation amplitude was fixed at 25 mV, with both the normal pulse time and modulation time set to 0.025s. Prior to initiating the scan from −1.2 V, the GC electrode was cleaned at 0.5 V, followed by the deposition of the lead film and the analyte at −1.0 V. During the pre-treatment step, the solution was stirred, and the stirring was stopped while equilibrium was achieved at −1.2 V for 5 seconds. All measurements were carried out without deaeration. Following the same procedure as the SWV and DPV measurements, a standard stock solution with a concentration of 5 mM was prepared. Working

solutions with concentrations of 0.5 mM and 0.05 mM were obtained by diluting the stock solution. The results from the differential normal pulse voltammetry are not included in the thesis and can be found in Figures F-1 and F-2 (Appendix F).

4.10. DPV measurements for the wood pulp samples

Differential pulse voltammetry was employed to analyze the samples. Four sample solutions (Conifer 2, Conifer 4, Betula 3, and Betula 5) were prepared, and analyzed by adding them to the non-aqueous electrolyte. Conifer 2 and Conifer 4 samples do not contain betulin, while Betula 3 and Betula 5 samples contain approximately 0.05 mg of betulin in a 1g sample according to the gas chromatography results. A 1g of the pulp samples were weighed; Betula 3 (1.0149 g), Betula 5 (1.0356 g), Conifer 2 (1.0079 g), and Conifer 4 (1.0162 g). The samples were cut into small pieces and soaked in 10mL DMSO overnight. Afterwards, they were filtered in glass vessels and stored at 4℃ before the analysis. The total volume of added working solution was 2 µL, 10 µL, 20 µL, 30 µL, 40 µL, and 50 µL.

5. Results and Discussion

5.1. Potentiometric Ion Sensors

5.1.1. Calibration of SPEs

Calibration using a Metrohm Dosino 700 pump was performed to verify the potential responses of the prepared ISEs. The calibration curves of 10 ISEs (4 cationic ISEs, 4 anionic ISEs, and 2 neutral ISEs) were acquired in 10^{-1} to 10^{-6} M KCl solution as shown below (Figure 11, Table 6). Each type of SPEs could not reproduce the comparable slope and the standard potential two months after they were first prepared. The selectivity towards potassium deteriorated within a short period of time since tetraphenylborate derivatives, KTFPB is lost rapidly from the membrane compared to the membranes

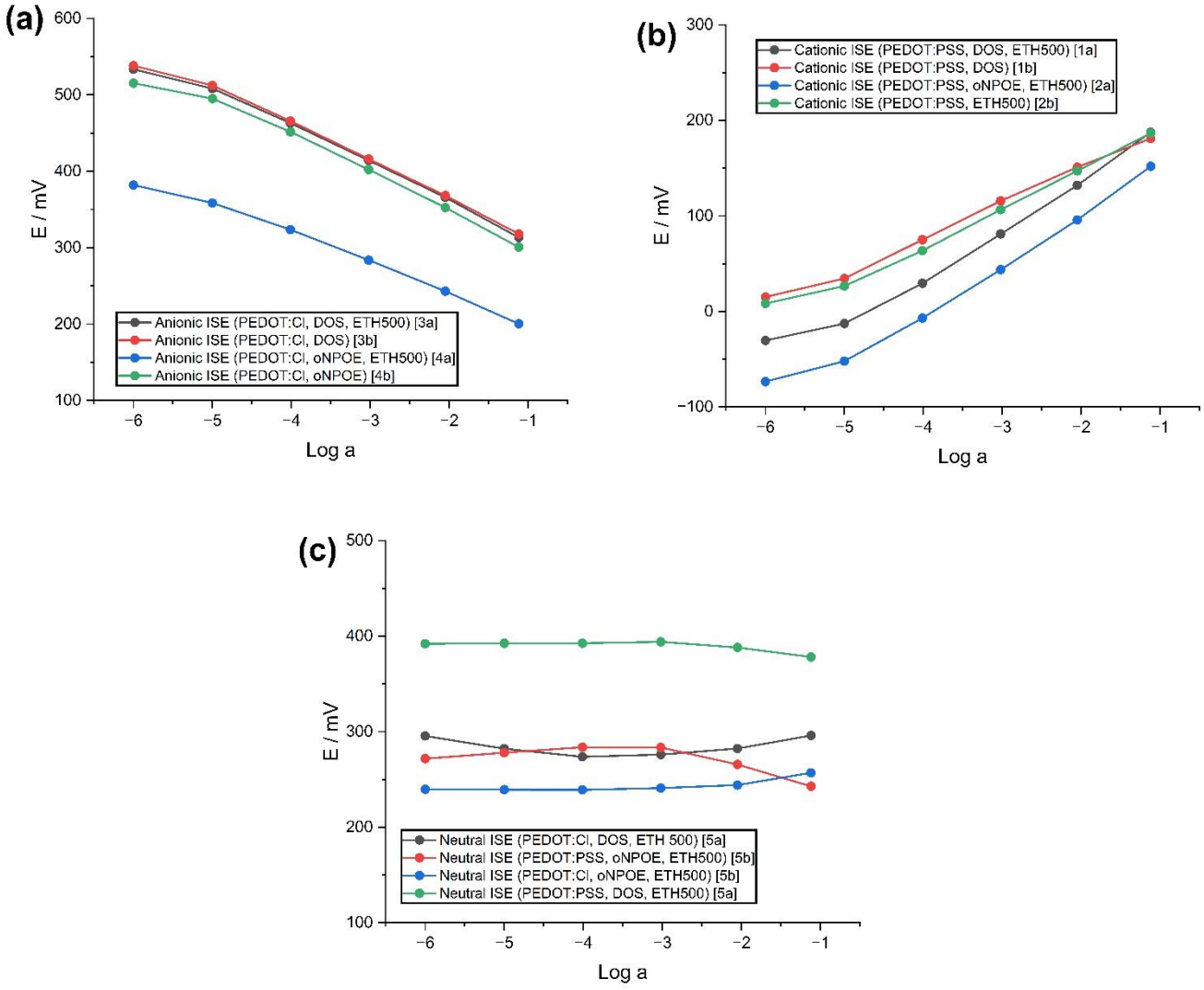

Figure 11. Calibration plot of a batch of prepared ISEs for principal component analysis (a) anionic ISEs (b) cationic ISEs, and (c) neutral ISEs

containing valinomycin ionophores. The complexation of the cationic counter ion with the ionophore prevents the lipophilic salt from leaching into the aqueous phase and helps keep it in the organic phase by lowering the concentration of free counter ions [13]. Thus, a total of three sets of ISEs were fabricated during this thesis work, and the calibration of each set was carried out before further investigations. In comparison to the value of the Nernstian slope, 59.2 mV decade^{-1} for monovalent cation and −59.2 mV decade^{-1} for monovalent anion, their absolute value of the slope was smaller than the theoretical value. As described in section 2.1, the selectivity towards potassium or chloride ions is lower than the case where ISMs containing ionophores since ISEs based on ion exchangers are more selective to hydrophobic ions than hydrophilic ions obeying the Hofmeister series. Also, the interaction between ISM and ions in a sample is electrostatic-based, thus it is weaker than the ionophore-based ISEs. It does not fully follow the Nernstian slope, but they were proved to be repeatable over three batches of ISEs. Thus, the ISEs were used in the succeeding measurements.

Table 6. Potentiometric calibration data for anionic, cationic, and neutral ISEs (S_d = standard deviation, n=3)

ISE type	**Anionic ISE (PEDOT:Cl, DOS, ETH500) [3a]**	**Anionic ISE (PEDOT:Cl, DOS) [3b]**	**Anionic ISE (PEDOT:Cl, oNPOE, ETH500) [4a]**	**Anionic ISE (PEDOT:Cl, oNPOE) [4b]**
Slope ± S_d / mV decade^{-1}	-45.4 ± 0.9	-45.1 ± 1.0	-42.9 ± 4.6	-44.8 ± 0.3
E ° ± S_d / mV	269.8 ± 1.5	271 ± 8.0	232.2 ± 58.3	257.7 ± 18.7
ISE type	**Cationic ISE (PEDOT:PSS, DOS, ETH500) [1a]**	**Cationic ISE (PEDOT:PSS, DOS) [1b]**	**Cationic ISE (PEDOT:PSS, oNPOE, ETH500) [2a]**	**Cationic ISE (PEDOT:PSS, oNPOE) [2b]**
Slope ± S_d / mV decade^{-1}	46.8 ± 1.6	42.0 ± 5.8	47.3 ± 1.8	45.9 ± 7.4
E ° ± S_d / mV	231.2 ± 5.1	237.2 ± 28.8	205.0 ± 9.9	243.1 ± 20.1

ISE type	**Neutral ISE (PEDOT:Cl, DOS, ETH 500) [5a]**	**Neutral ISE (PEDOT:PSS, oNPOE, ETH500) [5b]**
Slope ± S_d / mV decade^{-1}	0.1 ± 6.8	-1.4 ± 8.1
E ° ± S_d / mV	302.6 ± 76.5	214.8 ± 33.3

Also, two additional neutral ISEs were prepared for chemometric data treatment to observe if a different supporting electrolyte in conducting polymer layer influence on signals (Figure 11). However, significant correlations were not discovered as demonstrated in section 5.1.4. Thus, they were not included in the potentiometric measurements to which the standard stock solutions were added, but they were involved in the multi-dimensional calibration for principal component analysis.

5.1.2. Potentiometric response to the model compounds

The mechanism of response of ISE to betulin and stearic acid is unknown, due to the lack of literature data. The solubility of betulin and stearic acid in water is very low. For betulin, it is 0.00032 g/L(7.23×10^{-7} mol/L) [29] and for stearic acid, it is 0.00029 g/100 g (20 °C) [30], equivalent to 0.0029 g/L and 1.02×10^{-5} mol/L. Solubility in ethanol for betulin is 0.0195 mol/kg (298.2 K, 25.05 ℃) [31], equal to 6.81 g/L and 0.0154 mol/L . Solubility in ethanol for stearic acid is 2.25 g/100 g (20 °C) [30], which can be approximately equivalent to 17.76 g/L and 0.062 mol/L. These compounds are also very lipophilic, log P for betulin and stearic acid is 5.34 [29] and 8.02 [32], respectively.

Stearic acid exhibits an amphipathic nature due to the presence of a hydrophobic chain comprising 18 carbon atoms at one end and a hydrophilic carboxyl group at the other end. Stearic acid is a weak acid (pKa = 4.5), it can exist in the undissociated (neutral) or dissociated (anionic) form depending on the pH. Therefore, it can cause the cationic or anionic answer of ISEs. Betulin is a neutral compound, but it is an alcohol. Tsukatani and Toko [33] proposed a method for ethanol sensing using chloride polymeric ion-selective electrodes with different plasiticizers (oNPOE and n-decylalcohol (DA)). The chemometric approach was used in this thesis to study the possibility of differentiating samples with and without the presence of model compounds, without elucidating ISE response mechanism to these substances.

Betulin

Potentiometric measurements were conducted to investigate the responses of different ion-selective electrodes to the addition of betulin. Figure 12 presents the answers of ion-selective electrodes to the increasing concentration of betulin.

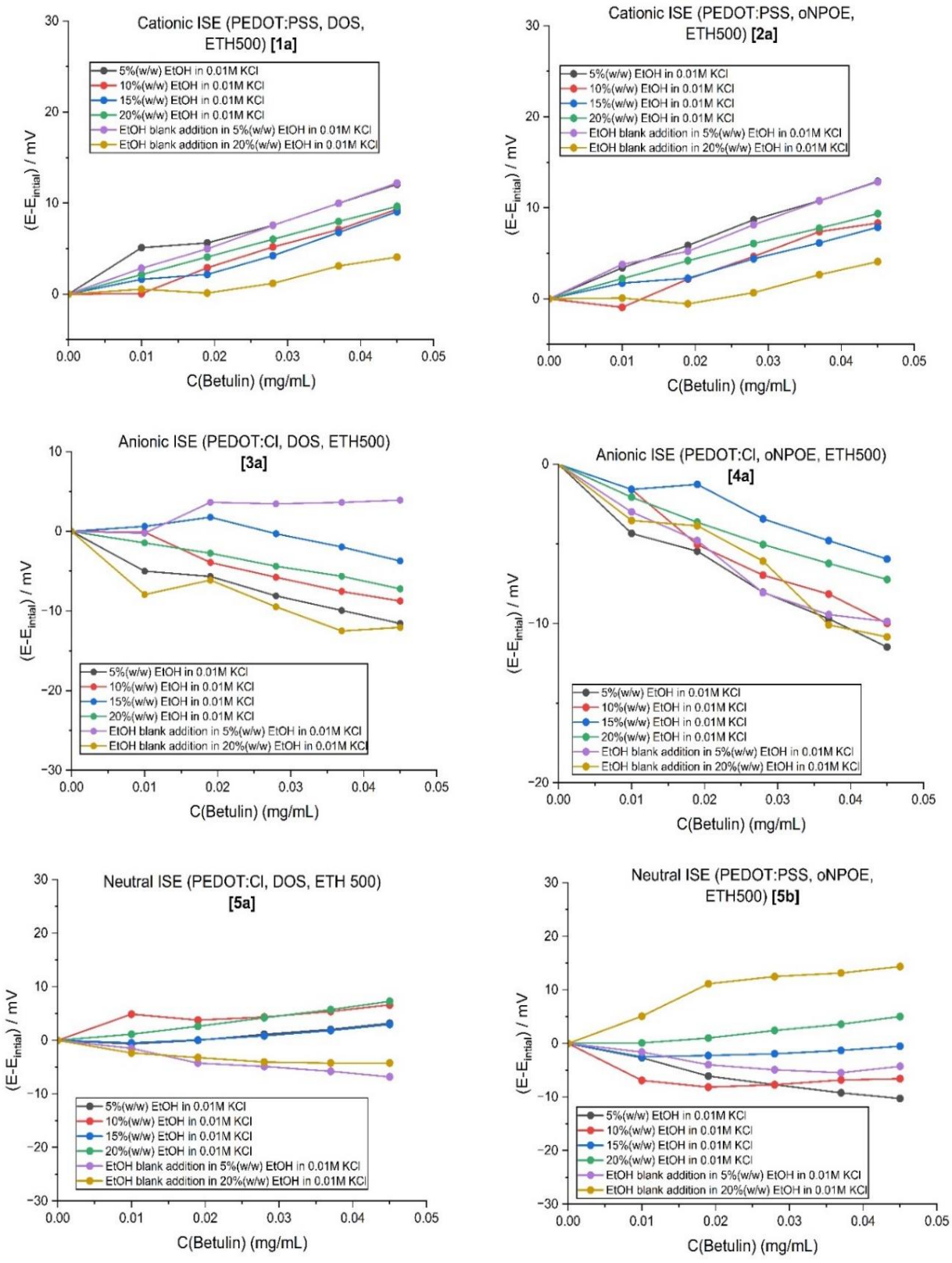

Figure 12. Potential responses of the cationic, anionic, and neutral ISEs to the increasing concentration of betulin

The effects of adding betulin stock solution to 0.01 M KCl solution with varying concentrations of ethanol have not been previously reported, making it challenging to infer potential reactions. Nevertheless, through careful analysis of the obtained results and subsequent multi-dimensional calibrations in section 5.1.4, correlations for the recognition of betulin on each type of ion-selective electrode were established. Therefore, these experimental results are the foundation for progressing multi-dimensional calibrations with chemometric data analysis techniques. A concentration of 5 % (w/w) ethanol was selected for subsequent measurements to allow multi-dimensional calibration, considering the observed slope of potential changes.

Stearic acid

The equivalent measurement by the addition of stearic acid was conducted to interpret the responses of ISEs with varying compositions of ISMs to the increasing concentration of stearic acid (Figure 13).

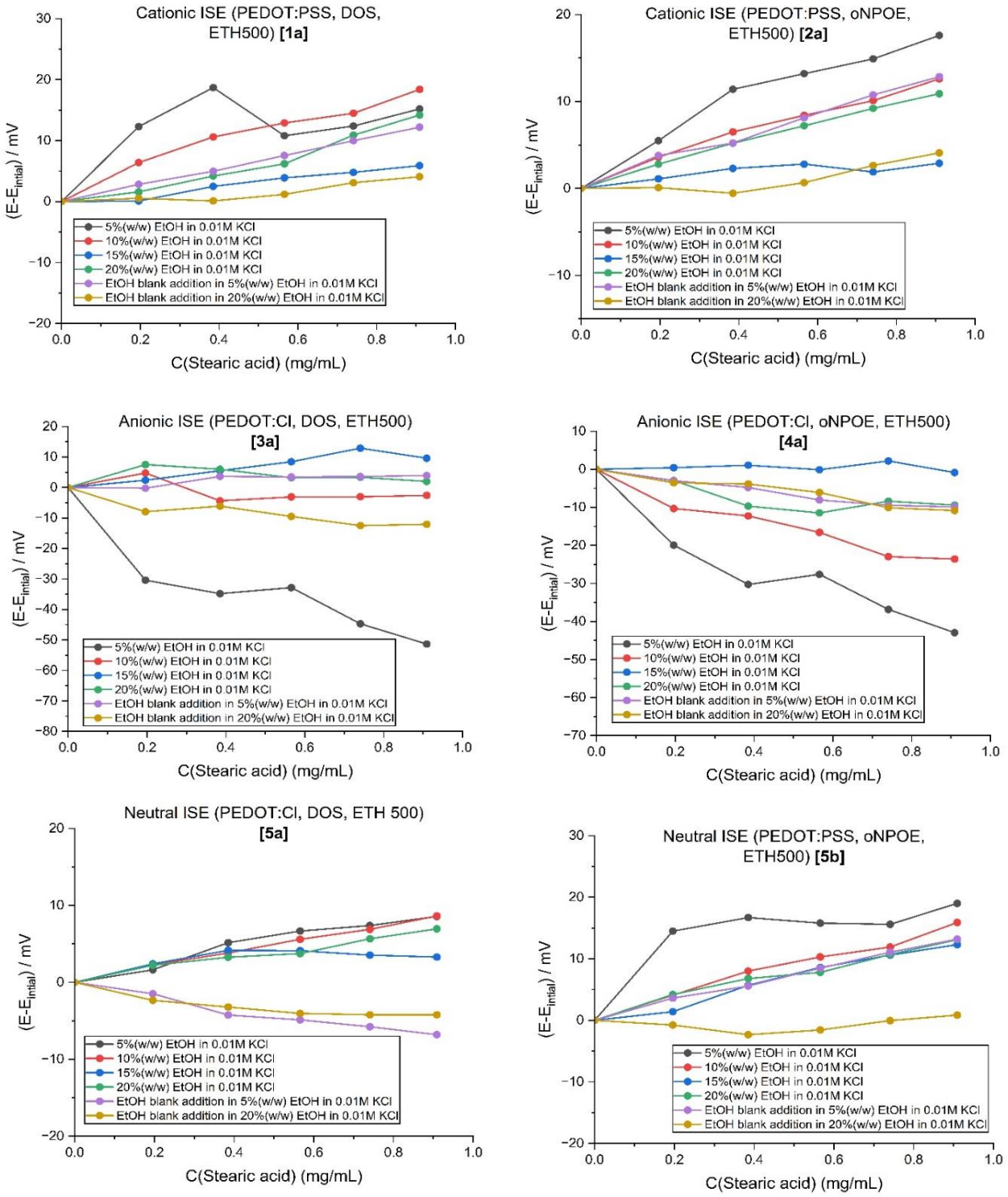

Figure13. Potential responses of the cationic, anionic, and neutral ISEs to the increasing concentration of stearic acid

Stearic acid is a weak acid with the acid dissociation constant of 4.50 [34]. Therefore, it will exist in the solution predominantly in the acidic form. On the other hand, if the pH of the solution is adjusted to pH 7.0 for example, then based on the Henderson-Hasselbalch Equation, $pH = pK_a + \log([A^-]/[HA])$, stearic acid is predominantly present in its anionic form. Unlike the addition of betulin, a precipitate

started to form after the stock solution was first added (1 mL). As demonstrated in Figure 14, the precipitate adhered to the membrane surface. As shown in Table 7,8 and Table 9,10 (Appendix B), the slope of the calibration curve became worse after the potentiometric measurement with stearic acid addition compared to the slope of cationic and neutral ISEs.

Table 7. Potentiometric calibration data for anionic ISEs before the Stearic acid stock solution addition

	Anionic ISE (PEDOT:Cl, DOS, ETH500) [3a]	Anionic ISE (PEDOT:Cl, DOS) [3b]	Anionic ISE (PEDOT:Cl, oNPOE, ETH500) [4a]	Anionic ISE (PEDOT:Cl, oNPOE) [4b]
Slope	-44.30	-44.19	-44.72	-44.58
Intercept	271.01	277.63	271.24	275.24
R^2	0.996	0.995	0.994	0.994

Table 8. Potentiometric calibration data for anionic ISEs after the Stearic acid stock solution addition

	Anionic ISE (PEDOT:Cl, DOS, ETH500) [3a]	Anionic ISE (PEDOT:Cl, DOS) [3b]	Anionic ISE (PEDOT:Cl, oNPOE, ETH500) [4a]	Anionic ISE (PEDOT:Cl, oNPOE) [4b]
Slope	-2.49	-6.66	-14.79	-24.88
Intercept	215.19	208.69	173.07	164.11
R^2	0.306	0.564	0.827	0.929

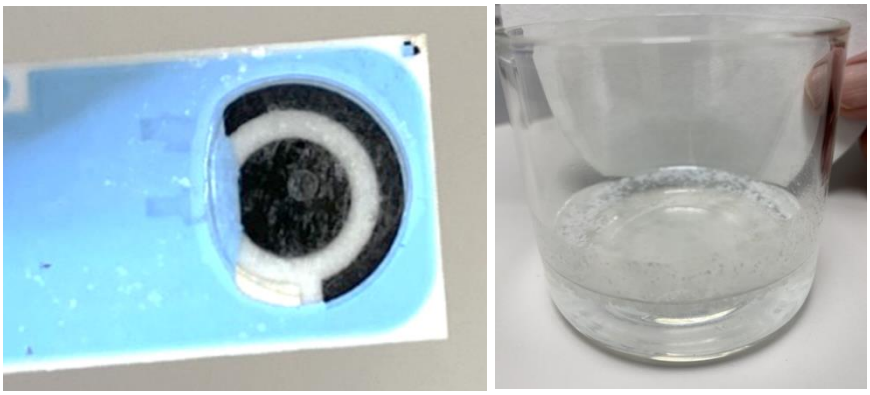

Figure 14. The precipitate by the introduction of stearic acid adhered to the membrane

Based on the partition coefficient, it can be comprehended that stearic acid adhered to the membrane, leading to a higher probability of hindering the sensitivity of potentiometric sensors. The partition coefficient, denoted as K, the equilibrium concentration ratio ($[C_{organic}]/[C_{water}]$) between an organic medium and an aqueous medium, serves as a quantitative measure of the organic compound's hydrophilicity or hydrophobicity [35]. Due to the structural differences between stearic acid and betulin, stearic acid is more hydrophobic than betulin, having a higher partition coefficient, thus it interacts more with lipophilic ion exchangers. In addition, stearic acid can be incorporated into the ion-selective membranes to assist the complexation of potassium ions in the mixture with valinomycin by

taking advantage of the stable formation of potassium stearate [36]. As a result, the examination of potentiometric sensors for the determination of stearic acid was excluded from the scope of this thesis. In future investigations concerning stearic acid determination, it is worth considering the utilization of cationic and neutral ion-selective electrodes (ISEs) instead of anionic ISEs to mitigate issues related to irreversibility caused by stearate adherence to anionic ion-selective membranes. However, the formation of precipitates presents challenges in terms of attaining accurate analysis. Consequently, the exploration of alternative electrolytes devoid of salts could be recommended.

5.1.4. Principal component analysis

The principal component analysis is intended to reduce the data dimensions, and its acceptable level depends on the application. In this thesis, the principal component analysis is applied for the simulation aimed at qualitative analysis for betulin. Three classes of electrolytes in three discrete glass vessels were prepared: class 1 holding 5% w/w ethanol in 0.01 M KCl, class 2 containing 0.01 M KCl, and class 3 containing 0.01 g/L betulin in 5% w/w ethanol in 0.01 M KCl. 12 ISEs (4 Anionic ISEs, 4 Cationic ISEs, and 4 neutral ISEs) were connected to 16 channel multi-voltmeter (Lawson Labs. Inc., Malvern, PA, USA). The potential was measured in random order. Each class was measured 8 times among which 5 times determination was considered as training, and 3 times were treated as simulation for sample analysis. As a general overview to identify the potential differences by each class, Figure 15 presents the averaged potentials and standard deviations.

ISE type	Anionic ISE (PEDOT:Cl, DOS, ETH500) [3a]	Anionic ISE (PEDOT:Cl, DOS) [3b]	Anionic ISE (PEDOT:Cl, oNPOE, ETH500) [4a]	Anionic ISE (PEDOT:Cl, oNPOE) [4b]	Cationic ISE (PEDOT:PSS, DOS, ETH500) [1a]	Cationic ISE (PEDOT:PSS, DOS) [1b]	Cationic ISE (PEDOT:PSS, oNPOE, ETH500) [2a]	Cationic ISE (PEDOT:PSS, oNPOE) [2b]	Neutral ISE (PEDOT:Cl, DOS, ETH 500) [5a]	Neutral ISE (PEDOT:PSS, oNPOE, ETH500) [5b]	Neutral ISE (PEDOT:Cl, oNPOE, ETH500) [5b]	Neutral ISE (PEDOT:PSS, DOS, ETH500) [5a]
E(Class 1) ± S_d / mV	215.09 ± 2.43	309.28 ± 2.01	221.62 ± 1.98	292.67 ± 1.38	139.60 ± 1.19	195.97 ± 0.71	113.79 ± 0.79	176.56 ± 1.11	275.45 ± 16.12	233.77 ± 8.75	245.09 ± 4.79	270.77 ± 40.00
E(Class 2) ± S_d / mV	229.30 ± 9.84	315.38 ± 3.98	232.74 ± 2.04	305.71 ± 1.84	130.53 ± 0.72	186.45 ± 0.41	102.86 ± 0.79	165.46 ± 0.79	276.90 ± 12.83	241.66 ± 7.70	249.60 ± 3.35	297.99 ± 16.81
E(Class 3) ± S_d / mV	210.05 ± 1.82	306.30 ± 1.90	218.10 ± 1.04	288.51 ± 1.19	143.04 ± 0.74	199.54 ± 1.00	117.69 ± 0.89	180.37 ± 0.99	267.56 ± 2.72	233.06 ± 4.84	246.22 ± 1.57	282.46 ± 11.06

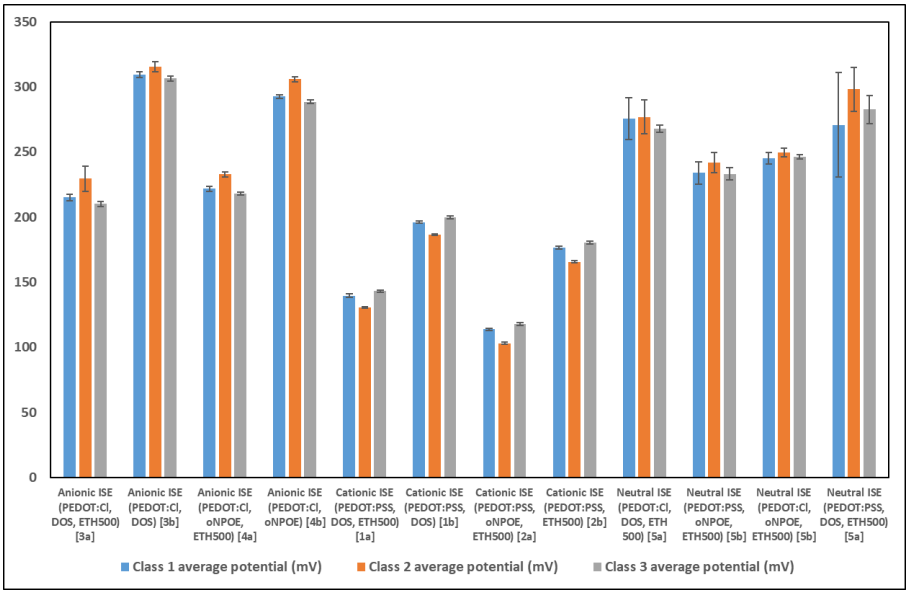

Class 1 = 5%w/w EtOH in 0.01M KCl (50mL)

Class 2 = 0.01M KCl (50mL)

Class 3 = 5% w/w EtOH in 0.01M KCl (50mL) + Betulin stock solution (1mL)

C(Betulin stock) (g/L) = 0.52 g/L

C(Betulin in class 3) (g/L) = 0.01 g/L

Figure 15. The measured potentials and their standard deviation (s_d) n=8

The principal components are denoted in descending order in which PC1 demonstrates the most deviation in data and PC2 is the second variation in the data. For instance, by looking at the first two components, the extent of variation in most of the data can be understood. The column shows the eigenvalue, and the plotted line represents cumulative variation of percentage [37]. As shown in Figure 16, the first two principal components explain 81.17 % of the variation in the data, which means 18.83 % of the data is missing if the data is characterized in a dimensional chart. Likewise, three-dimensional charts can describe 93.24 % variance of the data. The multi-dimensional charts (Figure 17 and Figure C-1, Fugure C-2 in Appendix C) proved that the samples could recognize the corresponding classes correctly and the two-dimensional charts are sufficient for qualitative analysis purposes.

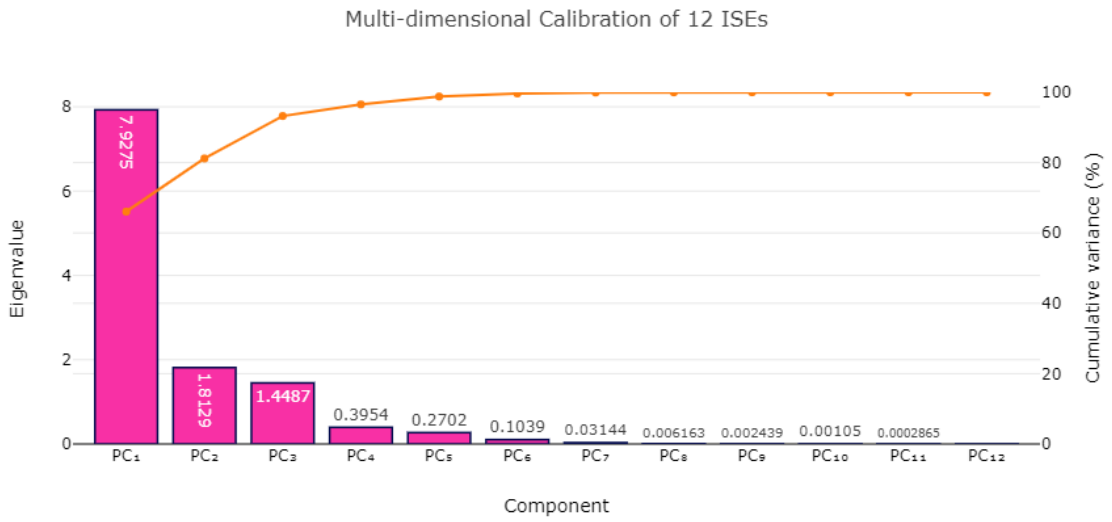

Parameter	PC₁	PC₂	PC₃	PC₄	PC₅	PC₆	PC₇	PC₈	PC₉	PC₁₀	PC₁₁	PC₁₂
Eigenvalue	7.93	1.81	1.45	0.4	0.27	0.1	0.031	0.0062	0.0024	0.0011	0.00029	0.00013
% of Variance	66.06	15.11	12.07	3.29	2.25	0.87	0.26	0.051	0.02	0.0088	0.0024	0.0011
Cumulative (%)	66.06	81.17	93.24	96.54	98.79	99.65	99.92	99.97	99.99	100	100	100

Figure 16. Scree plot, eigenvalues of the principal components by 12 ISEs

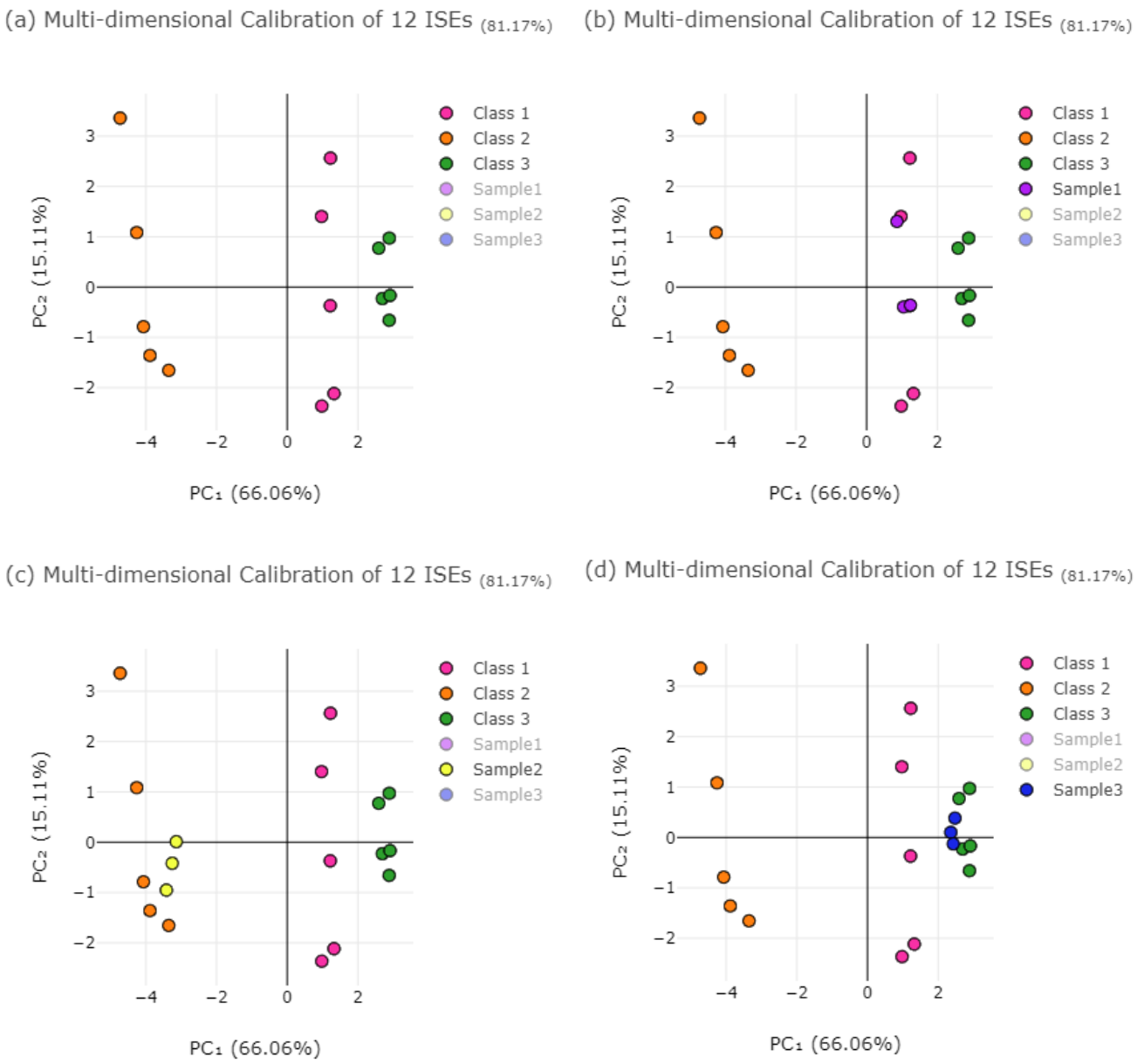

Figure 17. Two-dimensional PCA charts (a) Three classes without samples, (b) Sample 1 recognition to the 1st class, (c) Sample 2 recognition to the 2nd class, and (d) Sample 3 recognition to the 3rd class

Exclusion of the potentiometric responses of the neutral ISEs resulted in two first principal components reaching 95.89 % as shown in Figure 18 and more accurate sample classification as described in Figure 19 for the two-dimensional PCA chart, Figure C-3, Figure C-4 in Appendix C for the three-dimensional PCA chart. The cationic and anionic ISE responses to the class 3 containing betulin show a better correlation than those with neutral ISEs based on the potentiometric measurements shown in Figure 12 and Appendix A. Consequently, it is suitable to use the data of all 12 ISEs for qualitative analysis and description of the data with two-dimensional charts, and 8 ISEs (cationic and anionic ISEs) can be used for further studies.

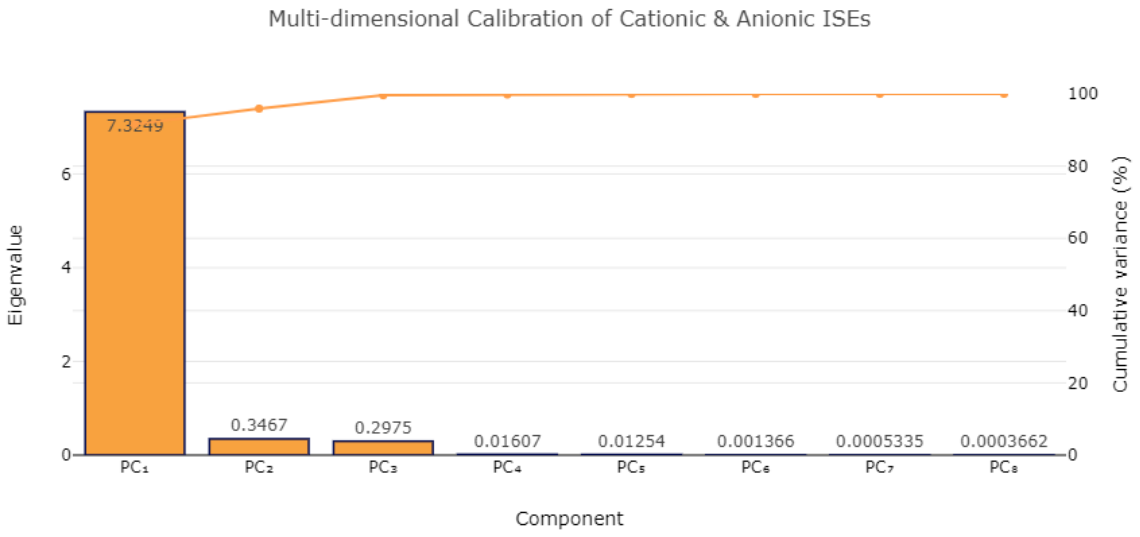

Parameter	PC₁	PC₂	PC₃	PC₄	PC₅	PC₆	PC₇	PC₈
Eigenvalue	7.32	0.35	0.30	0.02	0.01	0.00	0.00	0.00
% of Variance	91.56	4.33	3.72	0.20	0.16	0.02	0.01	0.00
Cumulative (%)	91.56	95.89	99.61	99.82	99.97	99.99	100.00	100.00

Figure 18. Scree plot, eigenvalues of the principal components by cationic and anionic ISEs

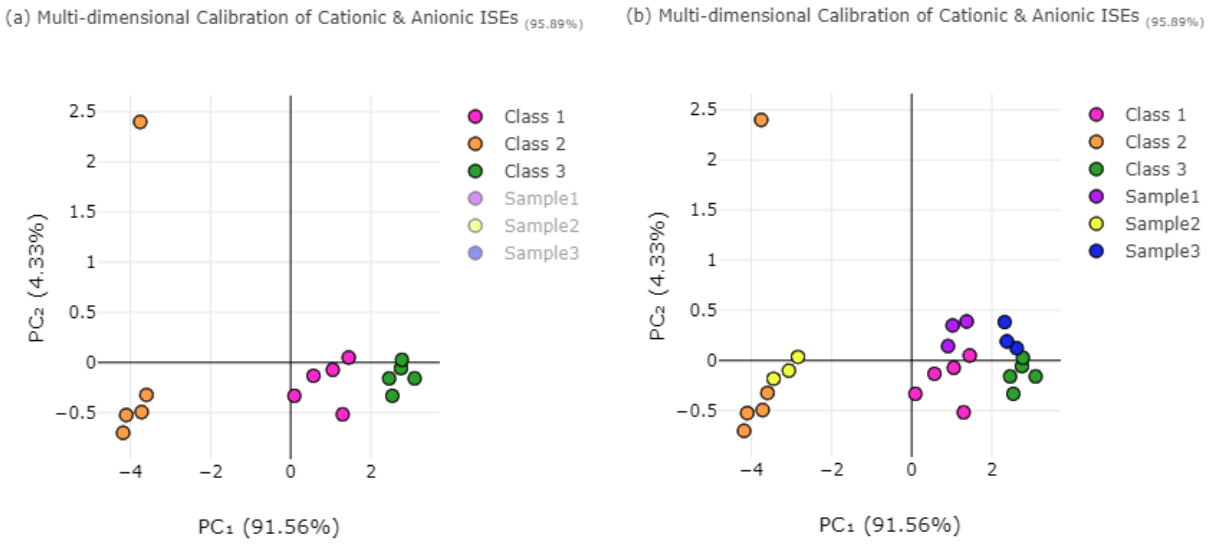

Figure 19. Two-dimensional PCA charts

(a) Three classes without samples, (b) Sample recognition simulation to the corresponding classes

5.2. Voltammetric measurements

5.2.1. SWV measurements in aqueous media

Alkaline media

Regarding the electrochemical determination of pentacyclic triterpenes in wood extractives, there is a scarcity of data in the existing literature. However, in earlier studies by Tyszczuk-Rotko et al. [19, 22], betulinic acid and oleanolic acid were determined by voltammetric method at lead film electrode in a solution of sodium hydroxide as a supporting electrolyte. The linearity range determined in the earlier work [19] was from 0.02 µg/L to 0.5 µg/L with a limit of detection equal to 0.009 µg/L. Notably, the oxidation signal of oleanolic acid displayed proportionality to its concentration, ranging from 0.02 ng/L to 3.0 ng/L, with detection and quantification limits of 0.0075 ng/L and 0.025 ng/L, respectively [22]. These promising outcomes from the aforementioned studies served as the foundation for the investigation in this thesis.

The square wave voltammetric (SWV) measurements were carried out in 0.02 M and 0.2 M NaOH electrolytes. The proposed concentration for NaOH supporting electrolyte used in the SWV determination of betulinic acid is 0.02 M NaOH [19]. However, 0.2 M NaOH solution was used as a supporting electrolyte for further experiments due to lack of responses by addition of the working solution and unstable current signals acquired in 0.02 M NaOH. Furthermore, a higher current signal was observed in 0.2 M NaOH as reported in the cited article [22].

The total volume of added working solution was 2 µL, 10 µL, 20 µL, 30 µL, 40 µL, and 50 µL. The data were processed in a way that the background current signals were subtracted from the succeeding current signals, and the starting point was fixed to 0 µA by deducting the initial current value from the rest. The background capacitive current signal was subtracted during data treatment. The current responses were proportional to the addition of the betulinic acid and betulin working solution (0.1 mg/L). However, the current responses were also in proportion to the addition of blank Ethanol solvent that was used in earlier works [19, 22]. The results showed that the current signals were not due to the analytes, but mostly attributed to the solvent itself (Figure 20).

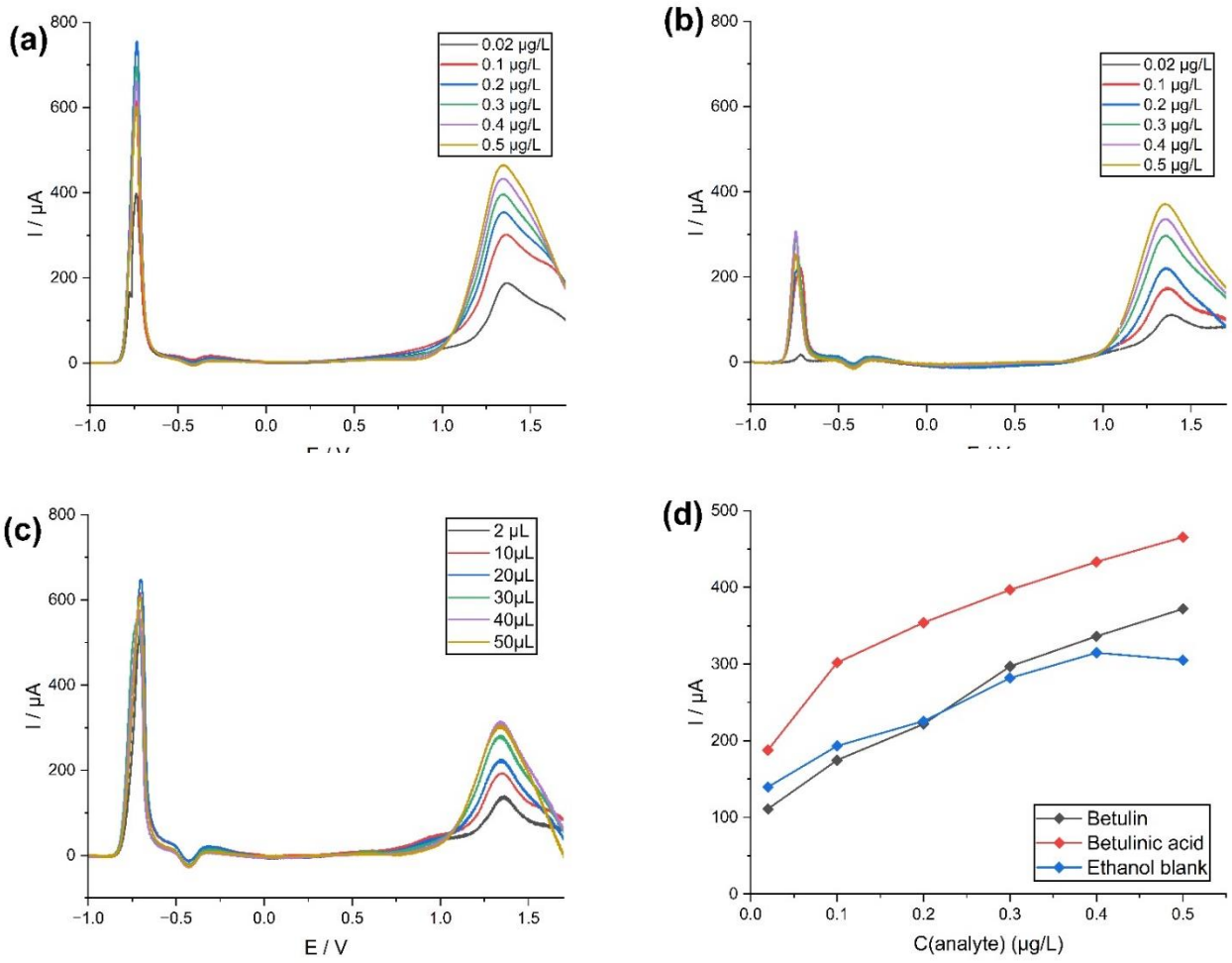

Figure 20. Square wave voltammograms obtained at the lead film electrode in 0.2 M NaOH solution containing 7.5×10^{-5} M $Pb(NO_3)^2$ with the working solution addition, (a) Betulinic acid, (b) Betulin, (c) Ethanol blank, and (d) Calibration curve of peak current signals

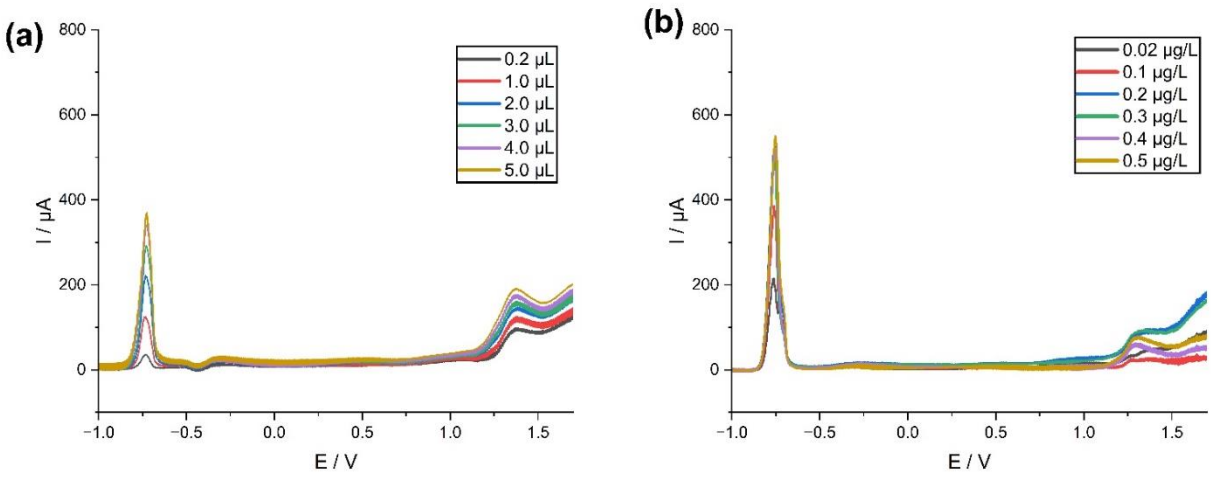

Figure 21. Square wave voltammograms obtained at the lead film electrode in 0.2 M NaOH solution containing 7.5×10^{-5}M $Pb(NO_3)^2$ with adjusted added volume of the working solution(1 mg/L), (a) Ethanol, and (b) Betulinic acid

To mitigate the influence from solvents and enhance the responses to the analytes, 10 times more concentrated working solution was prepared. The final concentration of the analytes remained unchanged, but the added volume of working solution was adjusted. A 1 mg/L working solution was prepared by 100 times dilution of 100 mg/L stock solution. The total volume of added 1 mg/L working solution was 0.2 µL, 1.0 µL, 2.0 µL, 3.0 µL, 4.0 µL, and 5.0 µL. The experimental results showed that the peak current of ethanol blank was more significant than that of betulinic acid (Figure 21). Also, the current signals increased depending upon the added volume of ethanol, whereas the peak current of betulinic acid was not completely proportional to the added volume.

The initial stock solution was prepared with a concentration of 100 mg/L, maintaining a molar ratio of ethanol to betulinic acid at 1.26×10^5. Subsequently, the working solution was prepared through sequential dilution. The first working solution was obtained by diluting the stock solution 100 times, resulting in a concentration of 1.0 mg/L. The second working solution, derived from the first working solution, was further diluted 10 times, yielding a concentration of 0.1 mg/L. Consequently, the molar ratios of ethanol to betulinic acid in the first and the second working solution were calculated to be 1.26×10^7 and 1.26×10^8, respectively. Considering the recommended stock solution concentrations mentioned in the articles [19, 22], ethanol was found to inevitably influence the current signals. This is problematic since the concentration of betulinic acid and betulin in wood pulp is certainly low (0.03 mg/g up to 0.13 mg/g). For the purpose of quantitative analysis of betulinic acid and betulin in samples, the concentration of the working solution should be as low as possible. As a result, a major influence from the solvent is unavoidable in this experimental setup. Therefore, the stock solutions were not prepared in ethanol as a solvent for further measurements. Based on the experimental results above,

other organic solvents for the preparation of standard solution were selected considering the solubility of pentacyclic triterpenes, water miscibility, and the redox potential of the organic solvent [38]. The selected candidates were methanol, acetone, DMF, and DMSO. However, these solvents also turned out to be oxidized at 1.35V in 0.2 M NaOH supporting electrolytes (Figure D-3 in Appendix D).

Neutral media

Square wave voltammograms (SWV) were registered in Tris-HCl buffer (pH 7.4) as a supporting electrolyte. The stock solutions were prepared in DMSO as a solvent due to non-toxicity, wider electrochemical redox potential window, and high solubility of pentacyclic triterpenes. The measurements in 0.2 M NaOH as a supporting electrolyte with Ag/AgCl as a RE have a drawback since there is a possibility of forming silver oxide (Ag_2O) ultimately. Thus, a double junction Ag/AgCl/ 3 M KCl / 3 M KCl was utilized as the RE in alkaline media to avoid direct contact between the AgCl and alkaline electrolyte. In that sense, Tris-HCl buffer (pH 7.4) has an advantage over alkaline media. As a derivative method of the cyclic voltammetry with Ct-(ds) DNA reported in the cited article [9], square wave voltammograms with the lead film in Tris-HCl (pH 7.4) buffer were recorded (Figure 22).

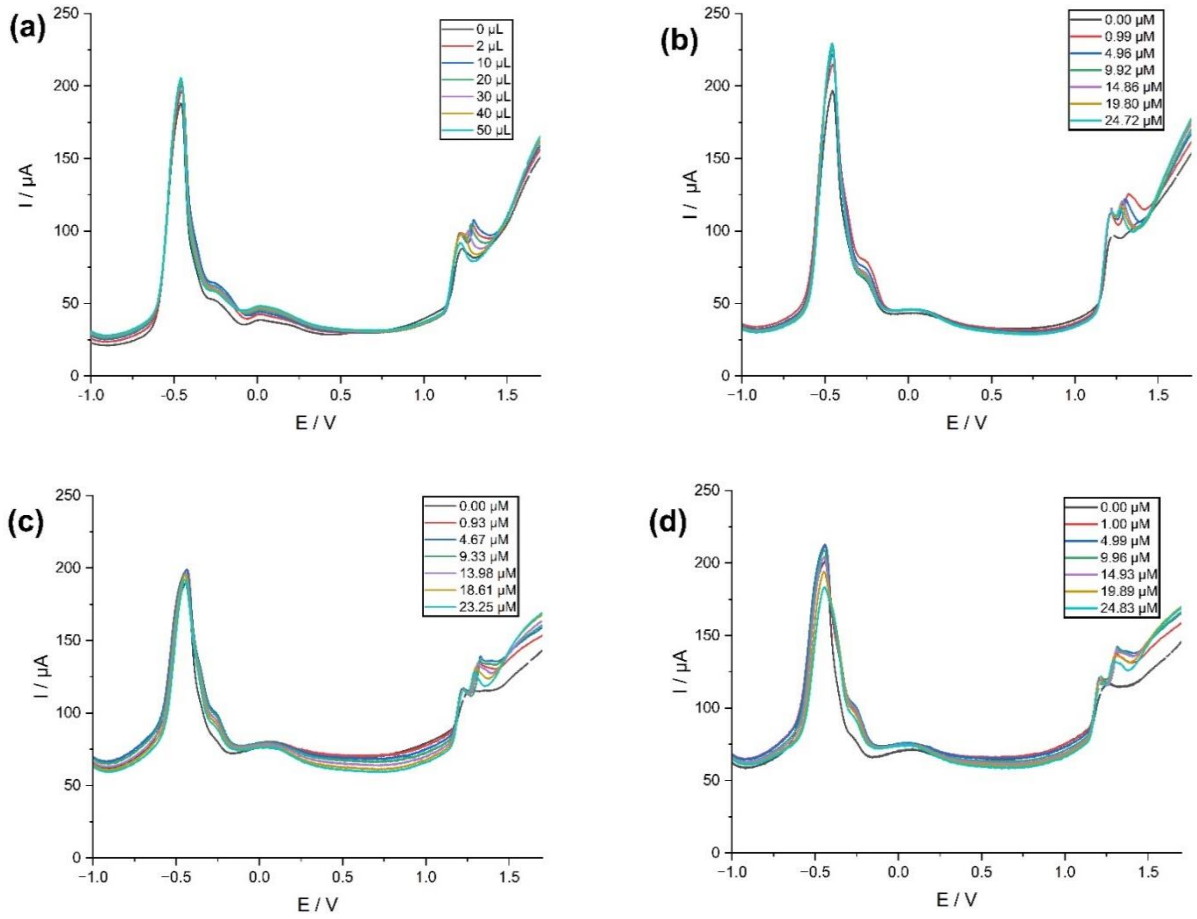

Figure 22. Square wave voltammograms (a) DMSO addition in Tris-HCl buffer (pH 7.4)

(b) Betulin stock solution (5 mM) addition in Tris-HCl buffer (pH 7.4)

(c) BA stock solution (5 mM) addition in Tris-HCl buffer (pH 7.4)

(d) OA stock solution (5 mM) addition in Tris-HCl buffer (pH 7.4)

The background response (0 uL or 0.00 uM in the voltammograms) was subtracted to isolate the faradaic processes by the analytes from the rest (Figure 23).

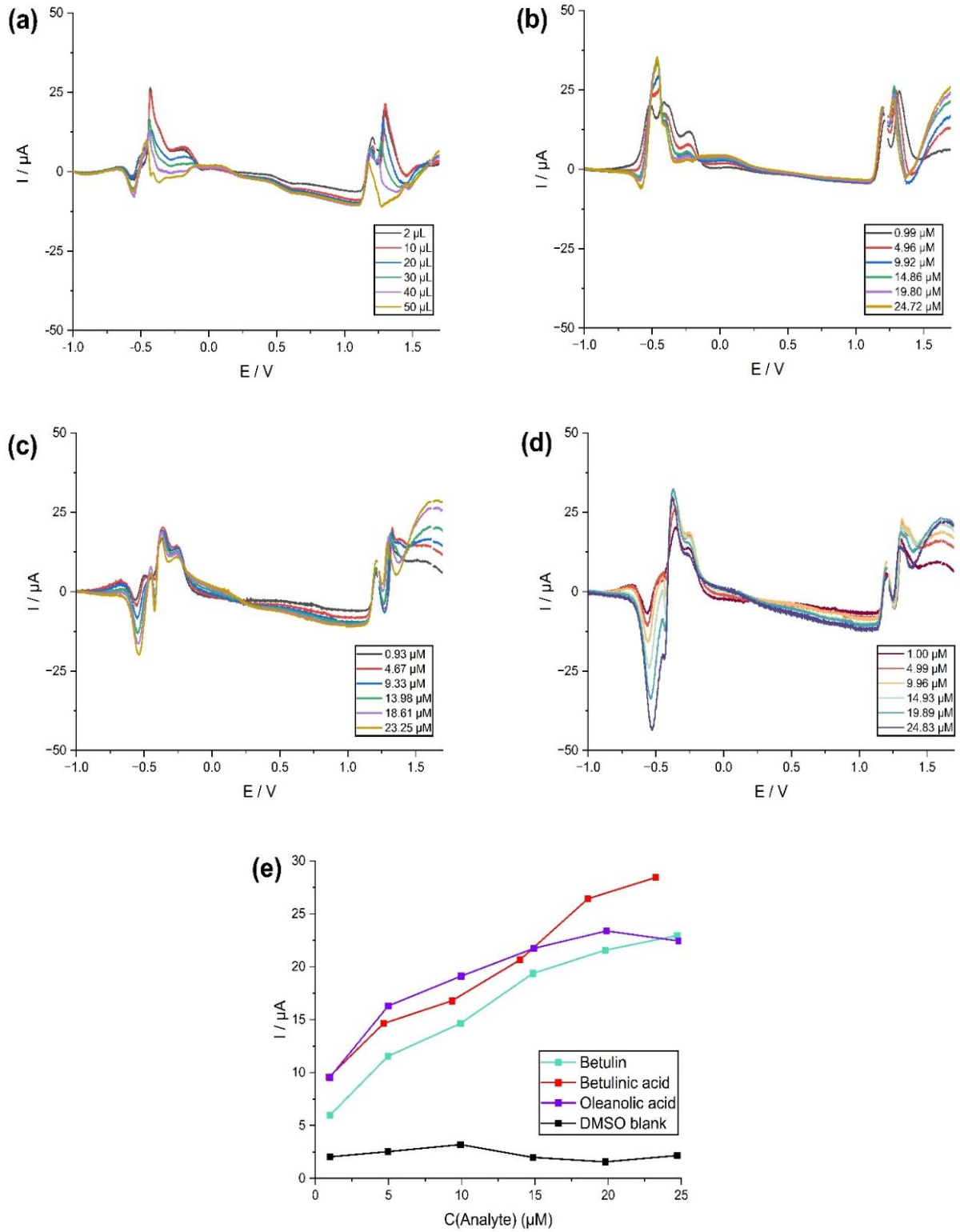

Figure 23. The background current subtracted from square wave voltammograms

(a) DMSO addition in Tris-HCl buffer (pH 7.4)

(b) Betulin stock solution (5 mM) addition in Tris-HCl buffer (pH 7.4)

(c) BA stock solution (5 mM) addition in Tris-HCl buffer (pH 7.4)

(d) OA stock solution (5 mM) addition in Tris-HCl buffer (pH 7.4)

(e) Calibration curves by the peak current of (a), (b), (c), (d) in Tris-buffer (pH 7.4)

As the stock solution was added consecutively, the current signals increased proportionally at approximately 1.6 V. To reach down to the concentration of pentacyclic triterpenes in wood pulp extractives, 10 times lower concentration of the working solution was prepared, and the identical procedure of addition was carried out.

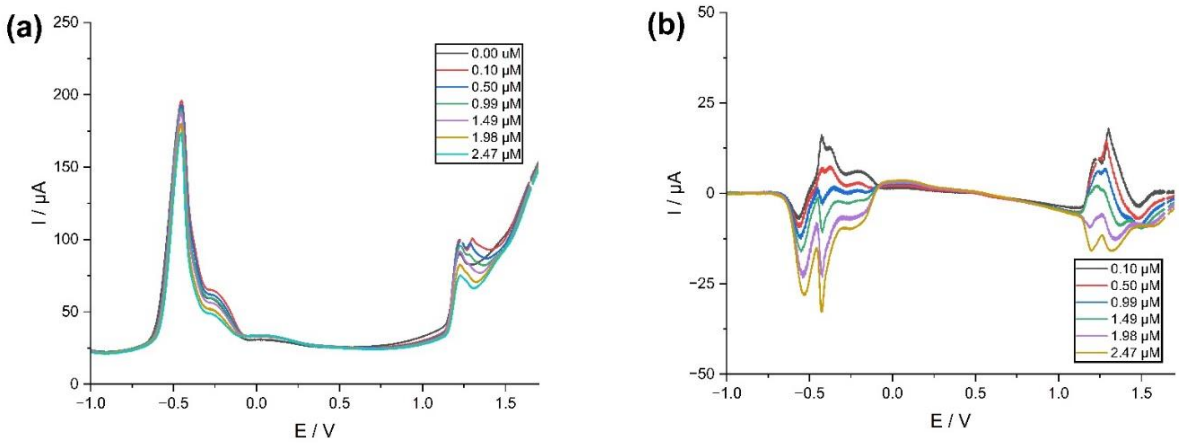

Figure 24. Square wave voltammograms by betulin working solution (0.5 mM) addition in Tris-HCl buffer (pH 7.4) (a) without the background current subtraction, (b) with the background current subtraction

As demonstrated in Figure 24, the oxidation peaks were attributed to the lead film and DMSO when the betulin working solution (0.5 mM) was added. The peaks at 1.6 V were not detectable compared to the results in Figure 23. Thus, the square wave voltammetric measurements were not proceeded with much lower concentrations of pentacyclic triterpenes.

5.2.2. DPV measurements in non-aqueous media

Without pretreatment step

Differential pulse voltammograms were recorded in $TBAPF_6$ 0.1 M prepared in anhydrous acetonitrile (Figure 25). Non-aqueous electrolyte is beneficial in terms of a wider electrochemical range. Acetonitrile barely undergoes solvent decomposition as well as side reactions compared to aqueous media due to its higher breakdown voltage, and organic molecules are easily soluble in acetonitrile. DPV measurements without pretreatment step were carried out first to confirm the necessity of the lead film deposition as well as the adsorption of analytes since the cited article [19, 22] claimed that the lead film deposition is achievable in an aqueous condition. Considering the availability of the standard materials, oleanolic acid was used for measurements since betulin, oleanolic acid, and betulinic acid are oxidized at the equivalent potential.

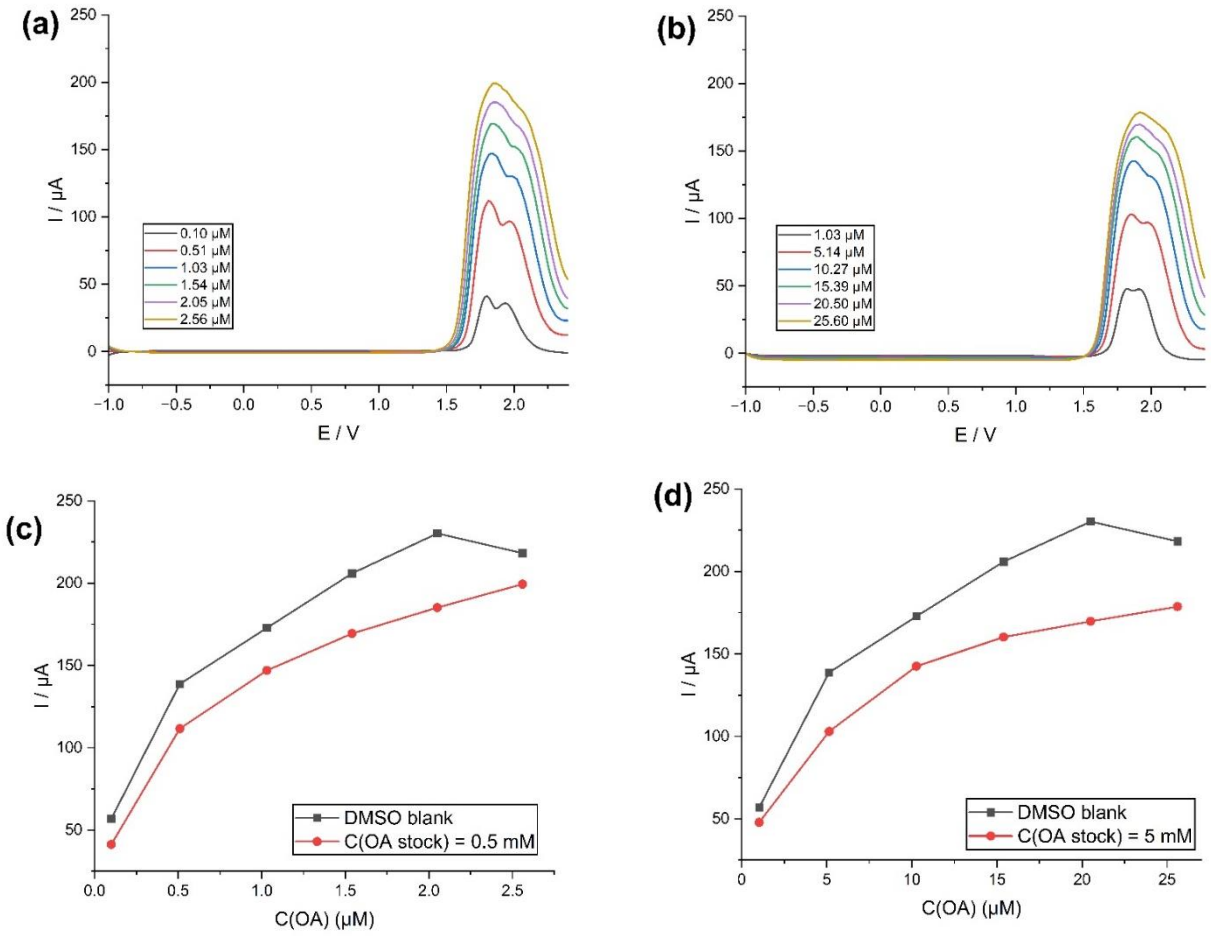

Figure 25. Differential pulse voltammograms (a) OA working solution (0.5 mM) addition in $TBAPF_6$ 0.1M (Acetonitrile)

(b) OA stock solution (5 mM) addition in $TBAPF_6$ 0.1M (Acetonitrile)

(c) Calibration curve of OA working solution (0.5 mM) addition in $TBAPF_6$ 0.1M (Acetonitrile) and the DMSO blank

(d) Calibration curve of OA stock solution (5 mM) addition in $TBAPF_6$ 0.1M (Acetonitrile) and the DMSO blank

The added stock solution volume into a measuring cell was 2 µL, 8 µL, 10 µL,10 µL, 10 µL, and 10 µL. After each addition, the stock solution volume contained in the measuring cell was 2 µL, 10 µL, 20 µL, 30 µL, 40 µL, and 50 µL. As presented in Figure 26, the DPV voltammograms were processed in a manner that the voltammogram of the background (reagent blank) was subtracted from the rest so that only the redox behavior of the analyte can be quantified accurately.

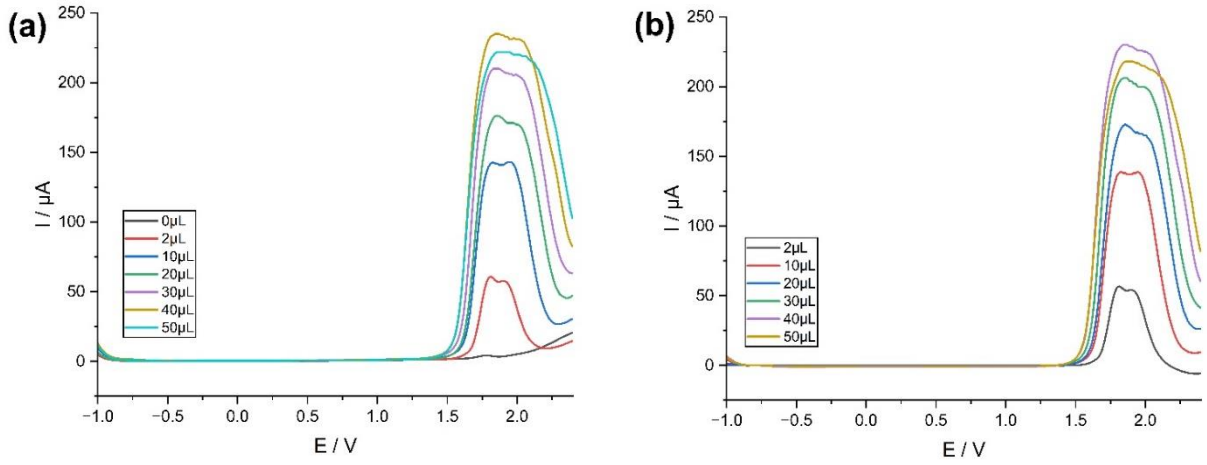

Figure 26. Differential pulse voltammograms (a)Blank DMSO addition in $TBAPF_6$ 0.1 M (Acetonitrile) (b) Data treatment of (a), Subtraction of the first background current signal (0.00 µM, black) from the rest

The calibration curves showed that the signals of the solvent blank reached higher intensity than the oleanolic acid. The experimental results demonstrated that solvent blank contributed to the current signal more in lower oleanolic acid concentrations and a higher OA concentration resulted in a lower current signal. Therefore, the pre-concentration step before the scan was deemed essential due to the considerable influence of the solvent blank. Also, the analytes could be accumulated on the surface during the scan, and it could affect the sensitivity of the GC electrode, so the cleaning step was necessary following the procedure described in section 4.6.

With pretreatment step

The pretreatment step was performed to resolve the issues that the current peak signals of the pentacyclic triterpenes are lower than the blank DMSO. Although the oxidation peak of the lead film was not visible, it was obvious that the analytes contribute more to the current signals at approximately 1.82 V (Appendix E). The peak current signals in the voltammograms were plotted to build the calibration curves (Figure 27).

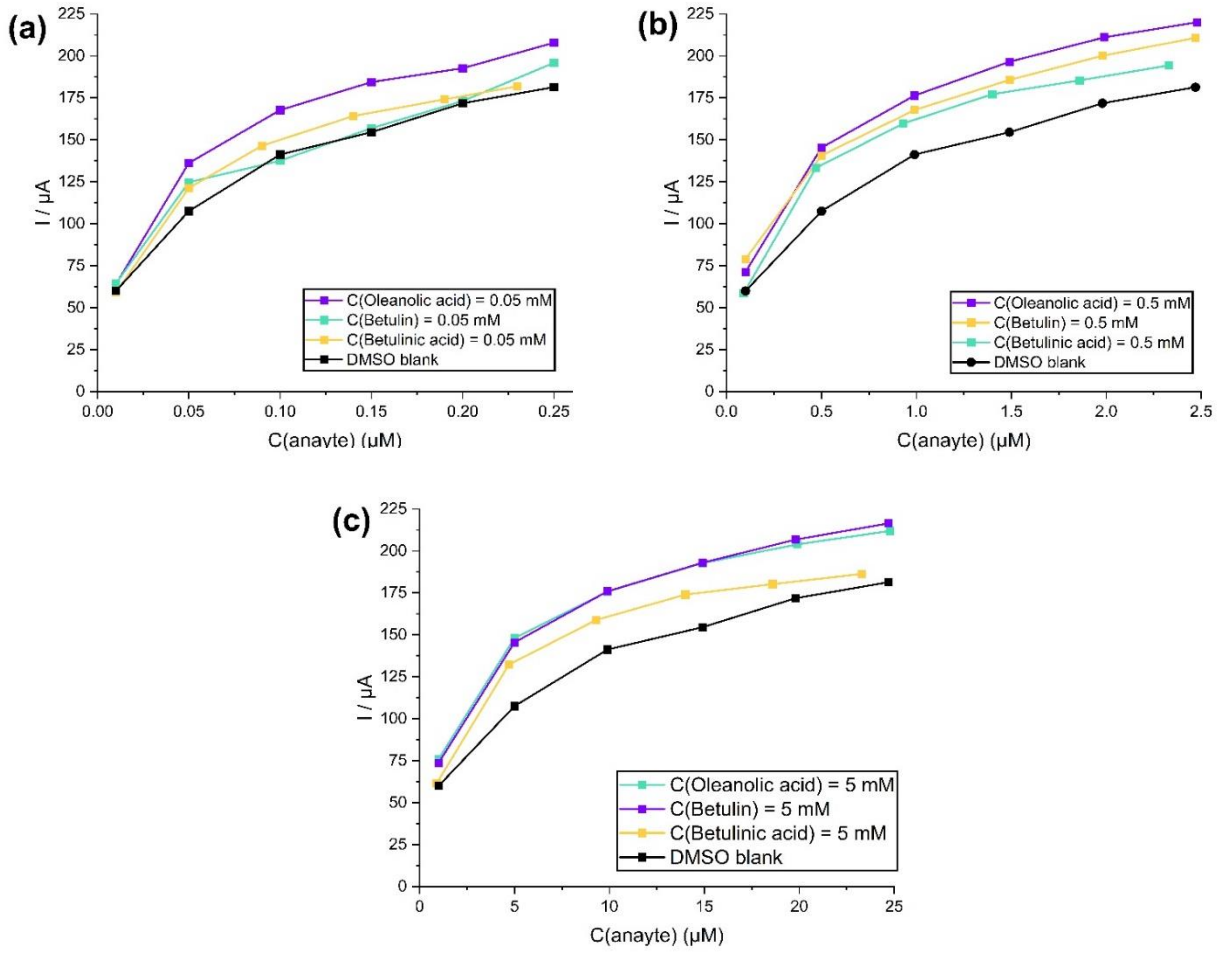

Figure 27. Calibration curves of differential pulse voltammograms by the concentration of added working solution (a) 0.05 mM, (b) 0.5 mM, and (c) 5 mM standard solution

The measurements were conducted by the addition of 5 mM betulin stock solution, 10 times diluted working solution (0.5 mM), and 100 times diluted working solution (0.05 mM). However, the current peak signals were not entirely proportional to the analyte concentration. The current peak signals resulting from the addition of the 5 mM solution and 0.5 mM working solution were similar depending on the added volume of the solution. However, the peak current signals by the addition of 0.05 mM

working solution were slightly lower than the addition of the higher concentration working solutions 0.5 mM and 5 mM (Figure 28). As shown in Figures 28a and b, when adding 0.05 mM betulin and betulinic acid solution, the peak current signals were comparable to those of DMSO blank addition. On the other hand, as presented in Figure 28c, the current signals by the addition of 0.05 mM OA working solution showed lower signals than 0.5mM and 5mM, but higher than those of the blank DMSO.

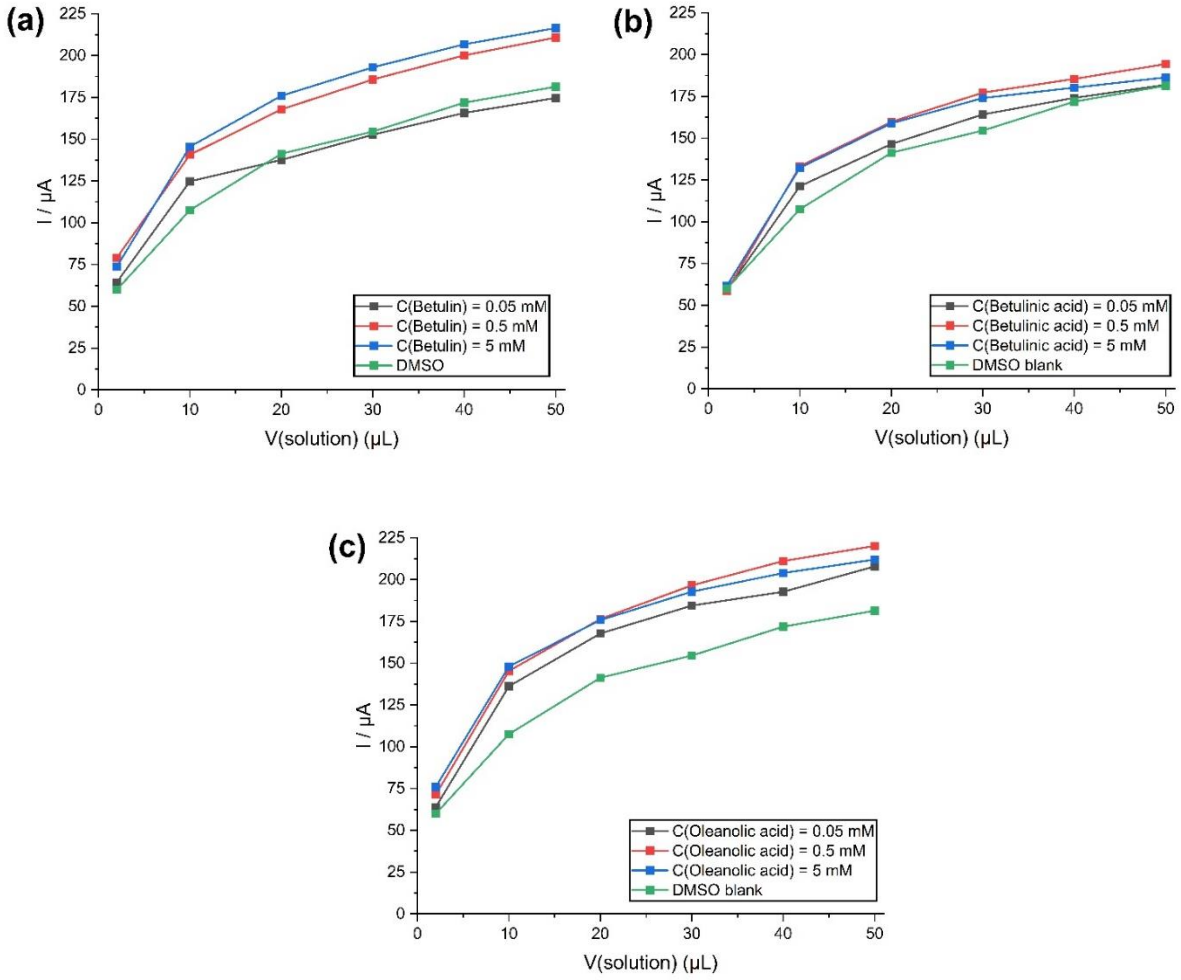

Figure 28. Calibration curves vs added volume of the working and stock solution (a)Betulin, (b)Betulinic acid, and (c) Oleanolic acid

This problem might be caused by diffusion limitations, and the analyte molecules had trouble reaching the GC electrode due to repetitive pretreatment on the GCE in combination with the lead film. One of the disadvantages of employing differential pulse voltammetry is to block the electrode surface, which diminishes the sensitivity of the electrodes [17]. The remaining lead film was not able to be fully removed during the pretreatment step at 0.5 V for 30 seconds. In a non-aqueous electrolyte, the lead film oxidation peak was not visible, which means the lead film and the analyte accumulated gradually on the surface, but the GC surface could not be regenerated properly. Also, incomplete adsorption might be a cause. The preconcentration time was insufficient to accumulate the analyte on the GC

electrode or the extent of stirring was not optimal to achieve complete adsorption. Two approaches were used to examine the causes of non-proportionality to the analyte concentration: (1) applying longer deposition time, and (2) polishing of the GC electrode between measurements before each standard addition.

With 30 seconds deposition time, the results showed that the peak current signals of betulin in lower concentrations (0.05 mM) reached as high as the peak current signals of DMSO. On the other hand, with 10 times higher concentrations of betulin (0.5 mM), the peak current signals by betulin solution addition are higher than that of DMSO. This means that betulin is electrochemically oxidized, but the influence of DMSO is still significant (Figure 29). A longer deposition time (1min) was applied to see how the peak current changed depending on the deposition time, but it did not affect the peak current signals much. Much longer pre-concentration time is not favorable in terms of practicality, thus the experiments with even longer pre-concentration were not performed.

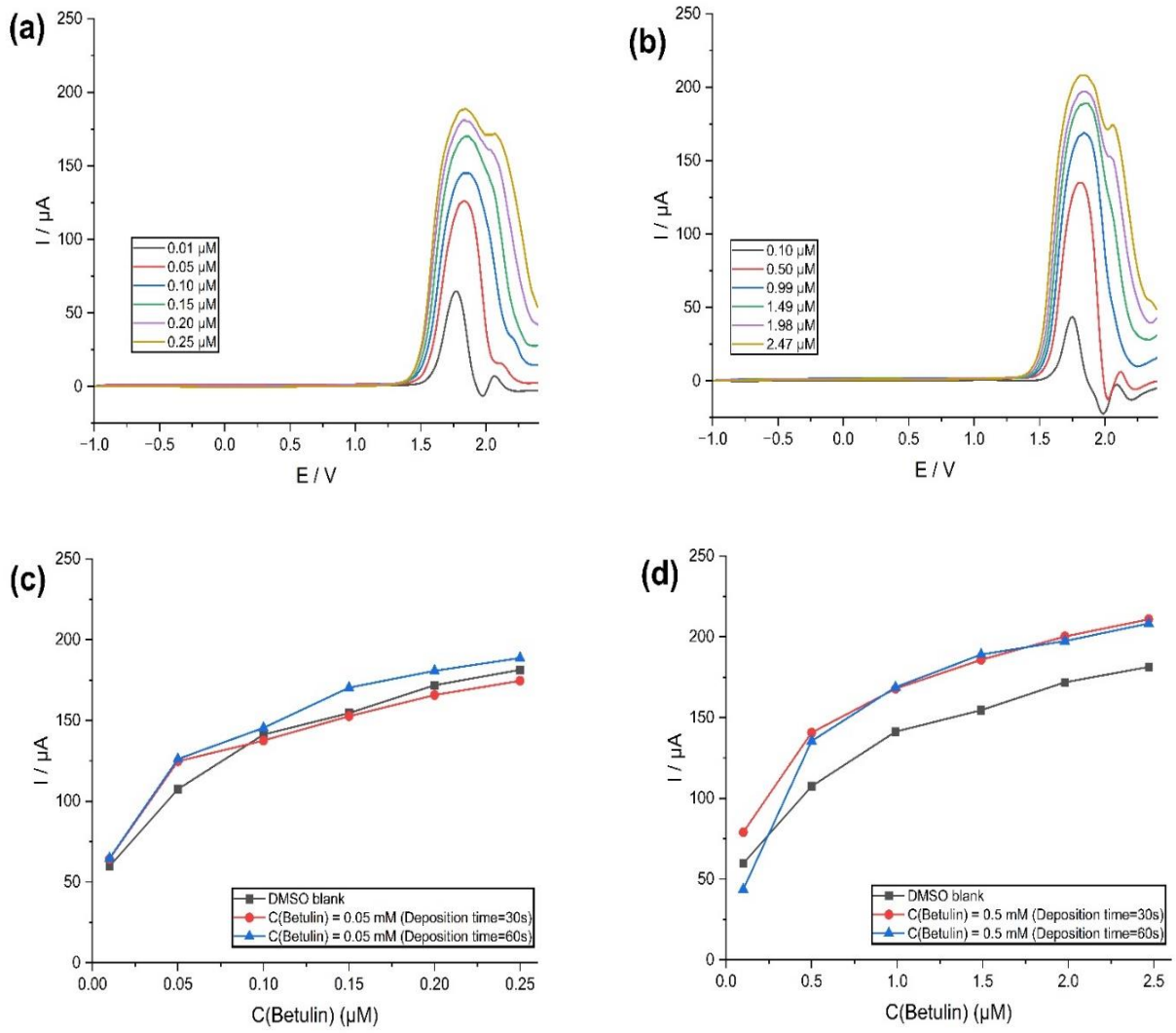

Figure 29. (a) Betulin working solution (0.05 mM) addition in $TBAPF_6$ 0.1 M (Acetonitrile), deposition time for 60s

(b) Betulin working solution (0.5 mM) addition in $TBAPF_6$ 0.1 M (Acetonitrile), deposition time for 60s

(c) Calibration curve comparison of Betulin working solution (0.05 mM) addition in $TBAPF_6$ 0.1 M (Acetonitrile)

(d) Calibration curve comparison of Betulin working solution (0.5mM) addition in $TBAPF_6$ 0.1M (Acetonitrile)

As previously specified, unlike the voltammograms recorded in the aqueous electrolyte, the oxidation peak of the lead film did not appear in the non-aqueous electrolyte. Therefore, it was desirable to investigate that the formed lead film was not oxidized/cleaned during the scan/pretreatment, which ended up lowering the sensitivity of the GCE surface.

Despite the observed improvement in the overall current signal after the removal of the lead film, as depicted in Figure 30, it was evident that the peak current signal did not exhibit complete proportionality to the analyte concentration. Furthermore, the peak current signal showed a decrease

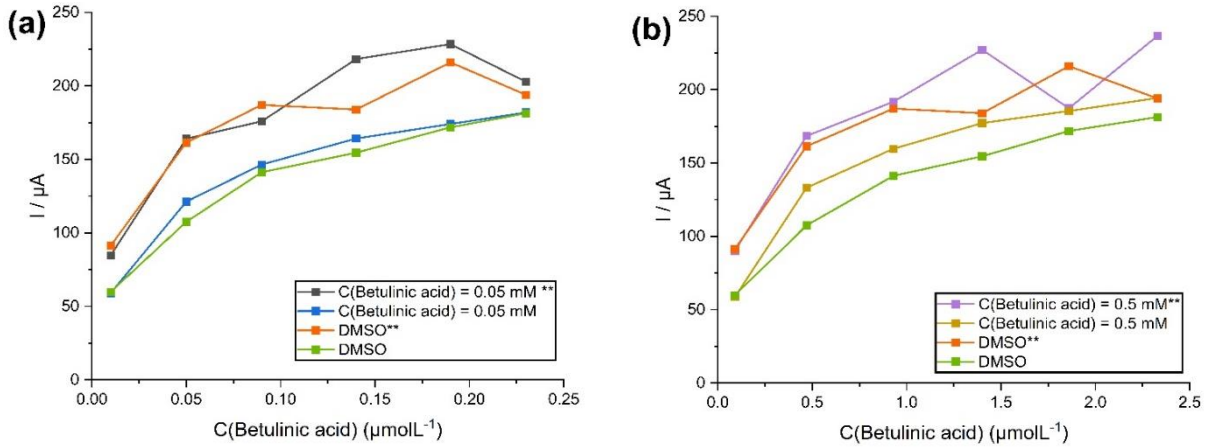

Figure 30. Calibration curve comparison of the peak current signals with a polished GCE (mark in the legend) before each addition, and the peak current signals without a polishing step before every addition.**

even with the addition of the analyte, which could be attributed to irregularities caused by manual polishing and partial loss of analytes attached to the GCE surface. Consequently, considering the experimental findings and the impracticality associated with polishing during measurements, it was decided not to perform electrode polishing between measurements for subsequent experiments.

5.2.3. DPV measurements of the real samples

Betula

Differential pulse voltammetric measurements were performed to observe the electrochemical behavior of the real samples. According to the results from gas chromatography analysis, Betula 3 and Betula 5 contains 79.86 mg and 59.56 mg Betulin per 1kg sample, respectively.

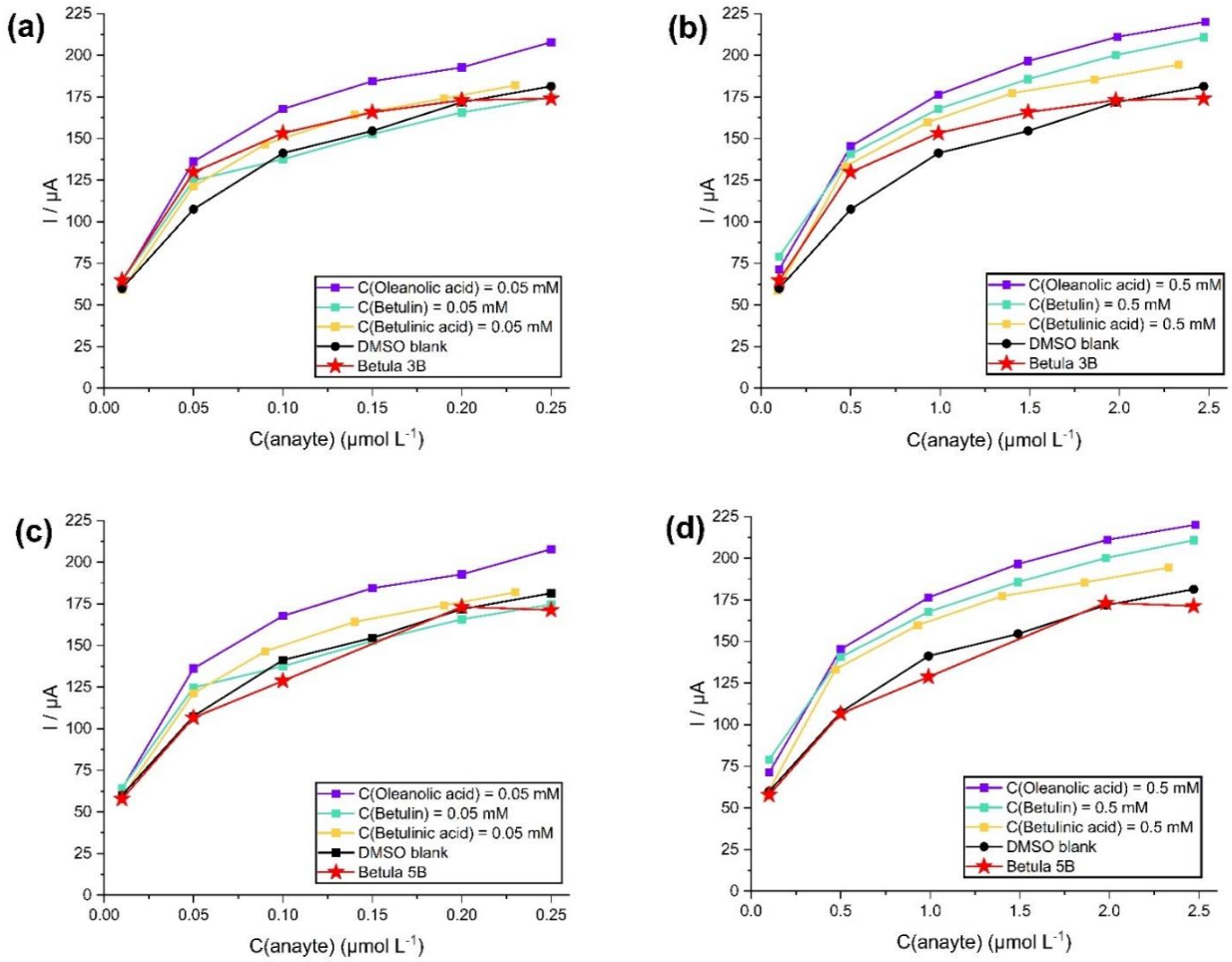

Figure 31. Comparison of the peak current responses to the addition of (a) 0.05 mM Betula 3 (b) 0.5 mM Betula 3, (c) 0.05 mM Betula 5, and (d) 0.5 mM Betula 5 sample solution

As shown in the calibration curve in Figure 31a, Betula 3 showed more or less equivalent signals to the signals from betulin 0.05mM addition. The peak current signals of Betula 3 were lower than the addition of the 0.5mM working solution. Supposedly, betulin content in Betula 3 extract solution is 0.018mM with reference to the results from gas chromatography analysis if it was extracted perfectly. However, the separation of the components in the samples was not carried out, accordingly, the oxidized molecules might not be attributed to betulin certainly. On the other hand, Betula 5 exhibited comparable current signals to the DMSO blank (Figure 31c and d), which is reasonable due to its lower concentration than Betula 3. If betulin was extracted completely, the concentration of the Betula 5 sample solution would be 0.014 mM, which is not detectable above the DMSO blank.

Conifer

Conifer 2 and conifer 4 pulp contain triterpenoids 0.43 mg and 0.96 mg teriterpenoids per 1kg sample, respectively, consequently they should not show the same electrochemical performance as Betula samples.

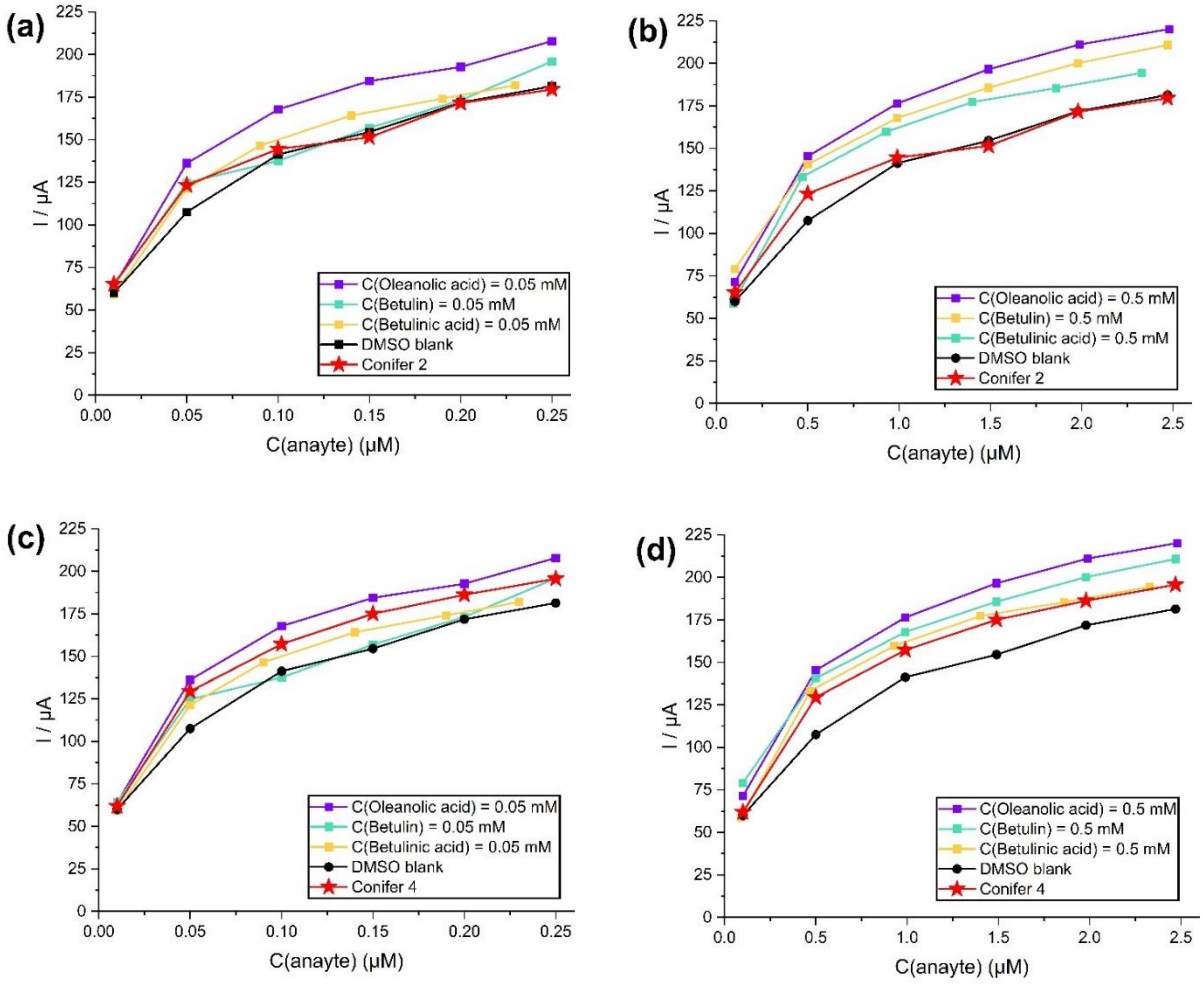

Figure 32. Comparison of the peak current responses to the addition of (a) 0.05 mM Conifer 2 (b) 0.5 mM Conifer 2, (c) 0.05 mM Conifer 4, and (d) 0.5 mM Conifer 4 sample solution

As presented in the calibration curves of Conifer 2 (Figure 32 a and b), the peak currents signals were comparable to the calibration curve of blank DMSO. However, the calibration curve of Conifer 4 showed higher current signals than blank DMSO (Figure 32 c and d). The peak currents of Conifer 4 were not higher than oleanolic acid, so it can be interpreted that the sample contains betulin, betulinic acid, and other components under the condition that the separation technique was applied. The experimental result of Conifer 4 can suggest that employing separation techniques before measurements is indispensable for more accurate measurement. As stated in articles [19, 22], the lead-

film electrodes have a poor resolution in selectivity for pentacyclic triterpenes, thus separation of the analyte of interest should precede the measurements.

5.2.4. Summary table of the investigated voltammetric methods and the electrochemical set-ups for further studies

Not all of the voltammograms that were investigated are included in this thesis. However, the obtained results from different voltammetric methods, along with their corresponding experimental parameters, have been organized in Table 11 (Appendix G). In the case of standard addition using 0.2 M NaOH as a supporting electrolyte, a working solution of 0.1 mg/L (equivalent to 0.0002 mM) was employed to match the concentrations used in the cited articles [19, 22], except for the standard solution prepared using DMSO. As presented in both Table 11 and Figure D-3 (Appendix D), irrespective of the concentration of the stock solution, the solvents had a significant impact on the peak current signals around 1.35 V. However, for the standard addition in Tris-HCl buffer (pH 7.4) and in 0.1 M $TBAPF_6$ in acetonitrile, a 5 mM stock solution was added to investigate the electrochemical behavior using cyclic voltammetric methods, based on the article [9] and the higher solubility of pentacyclic triterpenes in DMSO.

In future investigations, the electrochemical configurations can be differential pulse voltammetry in 0.1 M $TBAPF_6$ (ACN) solution, incorporating lead-film deposition and analyte accumulation. Additionally, square wave voltammetric measurements in combination with a lead-film deposition and the analyte preconcentration can be performed in Tris-HCl (pH 7.4) solution for pentacyclic triterpenes with a higher concentration. For non-aqueous solvents, possessing a broader electrochemical range and organic molecule compatibility offers benefits. However, drawbacks arise from the lead film deposition process in non-aqueous media, primarily because $Pb(OH)_4^{2-}$ can undergo redox reactions in aqueous solvents. Additionally, the substantial impact of blank DMSO on peak current intensity further contributes to the limitations. Similarly, in the case of aqueous electrolytes, significant limitations stem from a narrow electrochemical window and low compatibility with organic molecules. In contrast, the lead film exhibits redox reactions in Tris-HCl (pH 7.4) solution, and the solvent itself is non-toxic. Moreover, the presence of blank DMSO does not exert a notable influence on the current signals at the same redox potential as the analytes. Despite the achievable calibration range not being optimal for the analysis of wood extractives, further investigations can be proceeded by performing SWV measurements in Tris-HCl (pH 7.4) for relatively higher concentration and conducting DPV

measurements in 0.1 M $TBAPF_6$ (ACN) with comparatively lower concentration, using DMSO as the solvent.

6. Conclusions

This thesis presents the establishment of two electrochemical analysis approaches: potentiometric sensors as a qualitative method and voltammetric sensors as a quantitative method. One potential application of these approaches is that betulin is qualitatively analyzed using potentiometric sensors, followed by quantitative determination using the voltammetric method.

The experimental results obtained from a batch of potentiometric sensors, combined with chemometric data treatment, demonstrated a distinct separation in data variance between solutions containing betulin and those without betulin. The data analysis using first two principal components accounted for 81.17 % of the variance when considering all 12 ion-selective electrodes (ISEs). Additionally, by excluding the data from the neutral ISEs, which exhibited inconsistent responses to betulin addition, the first two principal components accounted for 95.89 % of the variance. This result implies that for quantitative analysis of betulin, a set of 12 ion-selective electrodes (ISEs) can be employed, while a more precise classification can be conducted using 8(4 cationic and 4 anionic) ISEs. In contrast, the utilization of potentiometric sensors for stearic acid analysis was hindered due to the precipitation of stearic acid, which adhered to ion-selective membranes. As presented in the results, the slopes of anionic ISEs were significantly affected by the adhesion of stearic acid to the membrane surface. For investigating this effect, optical microscopy and structural analysis techniques such as dark-field microscopy and infrared spectroscopy [36] can be used.

The selection of appropriate voltammetric techniques, such as square wave voltammetry and differential pulse voltammetry, was based on the attainable detection limit and the shapes of the voltammograms according to the observed experimental results. The hydrophobicity of the target analytes was considered when preparing standard solutions. Based on earlier works, ethanol was initially used as the solvent [19, 22]. However, based on the square wave voltammograms, the peak currents observed at 1.35 V were attributed to the solvent itself rather than the pentacyclic triterpenes. Regardless of the type of solvents (ethanol, methanol, acetone, DMF, and DMSO) used in the standard solution, the peak current signals corresponding to the solvent appeared around 1.35 V. In neutral aqueous media (Tris-HCl buffer pH 7.4), DMSO was utilized as the solvent, where the solvent itself underwent oxidation at 1.2 V and 1.3 V, while the pentacyclic triterpenes exhibited their oxidation reaction at approximately 1.6 V. Considering the analysis results from UPM NERC, which indicates a betulin content of 0.05 mg/g, which is 0.01mM if it is prepared in 10 mL DMSO by soaking 1g of sample, the detection limit should be lower than the concentration found in the sample. However, the redox behavior of the analyte was not detectable when a 0.5 mM standard solution was added to the

aqueous neutral media. Despite employing three-electrode setups and the earlier works that recorded voltammograms within the range from −1.0 V to 1.7 V, it was suspected that a wide potential range could have an unfavorable effect on the GC electrode and potentially lead to water electrolysis.

Subsequently, differential pulse voltammograms were acquired in a non-aqueous electrolyte, leveraging the benefits of a broader electrochemical window and the compatibility between DMSO and acetonitrile. The glassy carbon electrode with an in situ plated lead film was also investigated using a 0.1 M TBAPF6 solution in acetonitrile as the electrolyte and DMSO as the solvent for the standard solution. The results indicated that the influence of DMSO was relatively significant compared to aqueous media due to overlapping oxidation potentials. However, through a preconcentration step, the oxidation peak signals exceeded those of the blank DMSO solution. Although there was an issue of incompletely proportional current signals with respect to the analyte concentration, it was still meaningful to observe the correlation between the current peak signals by the addition of the two lower concentrations: 0.5 mM and 0.05 mM working solutions. If abundant reproducible results can be obtained in non-aqueous media by adding the 0.05 mM and 0.5 mM working solutions, chemometric data treatment can be also applied to those experimental results, allowing for the determination of the concentration range for the sample. On top of that, considering the literature references [19, 22], it is crucial to address the insufficient selectivity of the in situ plated lead film electrode, thereby necessitating the prior separation of target molecules before conducting measurements for accurate analysis.

In contrast to aqueous electrolytes, the inclusion of a polishing step prior to measurements became necessary for non-aqueous electrolytes due to the absence of an observed oxidation peak for the lead film and the higher likelihood of surface absorption by the analyte, as indicated by the characteristics of differential pulse voltammetry. Hence, every time before recording the voltammograms, the GC electrode was polished. It is plausible that the process is predominantly attributed to the desorption step following adsorption during the preconcentration step. Consequently, it is reasonable to pursue further investigations to examine the deposition of the lead film in non-aqueous media and the subsequent reactions occurring during the scan, with the aim of clarifying the experimental results that demonstrate imperfect proportionality to the analyte concentration.

7. References

[1] C. A. Dehelean *et al.*, "Study of the betulin enriched birch bark extracts effects on human carcinoma cells and ear inflammation," *Chemistry Central Journal*, vol. 6, no. 1, p. 137, Dec. 2012, doi: 10.1186/1752-153X-6-137.

[2] B. Green, M. D. Bentley, B. Y. Chung, N. G. Lynch, and B. L. Jensen, "Isolation of Betulin and Rearrangement to Allobetulin. A Biomimetic Natural Product Synthesis," *J. Chem. Educ.*, vol. 84, no. 12, p. 1985, Dec. 2007, doi: 10.1021/ed084p1985.

[3] A. Gutiérrez, J. C. Del Río, J. Rencoret, D. Ibarra, and Á. T. Martínez, "Main lipophilic extractives in different paper pulp types can be removed using the laccase–mediator system," *Appl Microbiol Biotechnol*, vol. 72, no. 4, pp. 845–851, Oct. 2006, doi: 10.1007/s00253-006-0346-1.

[4] P. Valto, J. Knuutinen, and R. Alén, "OVERVIEW OF ANALYTICAL PROCEDURES FOR FATTY AND RESIN ACIDS IN THE PAPERMAKING PROCESS," *BioResources*, vol. 7, no. 4, pp. 6041–6076, Sep. 2012, doi: 10.15376/biores.7.4.6041-6076.

[5] E. Małachowska, D. Pawcenis, J. Dańczak, J. Paczkowska, and K. Przybysz, "Paper Ageing: The Effect of Paper Chemical Composition on Hydrolysis and Oxidation," *Polymers*, vol. 13, no. 7, p. 1029, Mar. 2021, doi: 10.3390/polym13071029.

[6] I. Jasicka-Misiak, J. Lipok, I. A. Świder, and P. Kafarski, "Possible Fungistatic Implications of Betulin Presence in Betulaceae Plants and their Hymenochaetaceae Parasitic Fungi," *Zeitschrift für Naturforschung C*, vol. 65, no. 3–4, pp. 201–206, Apr. 2010, doi: 10.1515/znc-2010-3-406.

[7] D. Kumar and K. K. Dubey, "Hybrid Approach for Transformation for Betulin (an Anti-HIV Molecule)," *New and Future Developments in Microbial Biotechnology and Bioengineering: Microbial Secondary Metabolites Biochemistry and Applications*, pp. 193–203, Jan. 2019, doi: 10.1016/B978-0-444-63504-4.00015-3.

[8] G. Zhao, W. Yan, and D. Cao, "Simultaneous determination of betulin and betulinic acid in white birch bark using RP-HPLC," *Journal of Pharmaceutical and Biomedical Analysis*, vol. 43, no. 3, pp. 959–962, Feb. 2007, doi: 10.1016/j.jpba.2006.09.026.

[9] P. Venmathy, J. Jeyasundari, P. Nandhakumar, V. S. Vasantha, and C. Author, "Investigated the Interaction between Terpenoids of Betulinic Acid and Ursolic Acid Binding with (Ct-(Ds) DNA) Was Studied By Spectroscopic, Electrochemical and Molecular Modeling Approach," *IOSR Journal of Pharmacy and Biological Sciences (IOSR-JPBS*, vol. 13, no. 2, pp. 45–54, doi: 10.9790/3008-1302034554.

[10] R. W. Cattrall, *Chemical Sensors*. in Oxford chemistry primers. Oxford University Press, 1997. [Online]. Available: https://books.google.fi/books?id=BnbxAAAAMAAJ

[11] K. N. Mikhelson, *Ion-Selective Electrodes*. in Lecture Notes in Chemistry. Springer Berlin Heidelberg, 2013. [Online]. Available: https://books.google.fi/books?id=JVZEAAAAQBAJ

[12] J. M. Zook, J. Langmaier, and E. Lindner, "Current-polarized ion-selective membranes: The influence of plasticizer and lipophilic background electrolyte on concentration profiles, resistance, and voltage transients," *Sensors and Actuators B: Chemical*, vol. 136, no. 2, pp. 410–418, Mar. 2009, doi: 10.1016/j.snb.2008.12.047.

[13] E. Bakker and E. Pretsch, "Lipophilicity of tetraphenylborate derivatives as anionic sites in neutral carrier-based solvent polymeric membranes and lifetime of corresponding ion-selective electrochemical and optical sensors," *Analytica Chimica Acta*, vol. 309, no. 1–3, pp. 7–17, Jun. 1995, doi: 10.1016/0003-2670(95)00077-D.

[14] J. Bobacka, A. Ivaska, and A. Lewenstam, "Potentiometric Ion Sensors," *Chem. Rev.*, vol. 108, no. 2, pp. 329–351, Feb. 2008, doi: 10.1021/cr068100w.

[15] J. A. C. Broekaert, "Daniel C. Harris: Quantitative chemical analysis, 9th ed.," *Analytical and Bioanalytical Chemistry*, vol. 407, no. 30, pp. 8943–8944, 2015, doi: 10.1007/s00216-015-9059-6.

[16] J. N. Miller and J. C. Miller, *Statistics and Chemometrics for Analytical Chemistry*. Prentice Hall/Pearson, 2010. [Online]. Available: https://books.google.fi/books?id=uxEiQwAACAAJ

[17] "Electrochemistry. Principles, methods and applications," *Electrochimica Acta*, vol. 39, no. 6, p. 853, Apr. 1994, doi: 10.1016/0013-4686(94)80035-9.
[18] Analytical Sciences Digital Library, "c) Anodic Stripping Voltammetry." https://chem.libretexts.org/Bookshelves/Analytical_Chemistry/Supplemental_Modules_(Analytical_Chemistry)/Analytical_Sciences_Digital_Library/Courseware/Analytical_Electrochemistry%3A_The_Basic_Concepts/04_Voltammetric_Methods/A._Basics_of_Voltammetry/02_Potential_Sweep_Methods/c)_Anodic_Stripping_Voltammetry (accessed May 06, 2023).
[19] K. Tyszczuk-Rotko, M. Wójciak-Kosior, and I. Sowa, "Voltammetric determination of betulinic acid at lead film electrode after chromatographic separation in plant material," *Analytical Biochemistry*, vol. 436, no. 2, pp. 121–126, May 2013, doi: 10.1016/j.ab.2013.02.002.
[20] K. Tyszczuk-Rotko and I. H. Tademir, "Application of an in situ plated lead film electrode to the determination of organic compounds in alkaline media," *Journal of Electroanalytical Chemistry*, vol. 670, pp. 11–15, Apr. 2012, doi: 10.1016/j.jelechem.2012.02.010.
[21] K. Tyszczuk, "Correlation between the plating regime of lead film deposition and electrode response after accumulation of organic compound. Microscopic study," *Sensors and Actuators B: Chemical*, vol. 156, no. 2, pp. 899–905, Aug. 2011, doi: 10.1016/j.snb.2011.03.003.
[22] K. Tyszczuk-Rotko, K. Domańska, I. Sadok, M. Wójciak-Kosior, and I. Sowa, "Voltammetric procedure for the determination of oleanolic and ursolic acids in plant extracts," *Analytical Methods*, vol. 7, no. 22, pp. 9435–9441, Nov. 2015, doi: 10.1039/c5ay01976a.
[23] J. Wang, *Stripping Analysis: Principles, Instrumentation, and Applications*. VCH, 1985. [Online]. Available: https://books.google.fi/books?id=GOLvAAAAMAAJ
[24] Á. Molina and J. González, *Pulse Voltammetry in Physical Electrochemistry and Electroanalysis*. Cham: Springer International Publishing, 2016. doi: 10.1007/978-3-319-21251-7.
[25] P. Westbroek, "Electrochemical methods," *Analytical Electrochemistry in Textiles*, pp. 37–69, Jan. 2005, doi: 10.1533/9781845690878.1.37.
[26] A. E. Rusheen *et al.*, "Evaluation of electrochemical methods for tonic dopamine detection in vivo," *TrAC Trends in Analytical Chemistry*, vol. 132, p. 116049, Nov. 2020, doi: 10.1016/J.TRAC.2020.116049.
[27] "Screen-printed Carbon Electrodes ref. C110, Metrohm DropSens, Oviedo, Spain." https://www.dropsens.com/en/screen_printed_electrodes_pag.html#unmodified_spes (accessed May 14, 2023).
[28] Q. Li, C. Batchelor-McAuley, N. S. Lawrence, R. S. Hartshorne, and R. G. Compton, "Anomalous solubility of oxygen in acetonitrile/water mixture containing tetra-n-butylammonium perchlorate supporting electrolyte; the solubility and diffusion coefficient of oxygen in anhydrous acetonitrile and aqueous mixtures," *Journal of Electroanalytical Chemistry*, vol. 688, pp. 328–335, Jan. 2013, doi: 10.1016/j.jelechem.2012.07.039.
[29] "FoodDB." https://foodb.ca/compounds/FDB015789 (accessed Jul. 25, 2023).
[30] A. W. Ralston and C. W. Hoerr, "THE SOLUBILITIES OF THE NORMAL SATURATED FATTY ACIDS," *J. Org. Chem.*, vol. 07, no. 6, pp. 546–555, Nov. 1942, doi: 10.1021/jo01200a013.
[31] D. Cao, G. Zhao, and W. Yan, "Solubilities of betulin in fourteen organic solvents at different temperatures," *Journal of Chemical and Engineering Data*, vol. 52, no. 4, pp. 1366–1368, Jul. 2007, doi: 10.1021/je700069g.
[32] "T3DB." http://www.t3db.ca/toxins/T3D4755 (accessed Jul. 25, 2023).
[33] T. Tsukatani and K. Toko, "Ethanol Sensor Using Two Chloride Ion-Selective Polymeric Membrane Electrodes.," *FSTR*, vol. 5, no. 2, pp. 223–226, 1999, doi: 10.3136/fstr.5.223.
[34] J. R. Loften, J. G. Linn, J. K. Drackley, T. C. Jenkins, C. G. Soderholm, and A. F. Kertz, "Invited review: Palmitic and stearic acid metabolism in lactating dairy cows," *Journal of Dairy Science*, vol. 97, no. 8, pp. 4661–4674, Aug. 2014, doi: 10.3168/jds.2014-7919.
[35] J. G. Speight, "Introduction Into the Environment," in *Environmental Organic Chemistry for Engineers*, Elsevier, 2017, pp. 263–303. doi: 10.1016/B978-0-12-804492-6.00006-X.

[36] V. Vodyanoy, S. Pathirana, and W. C. Neely, “Stearic Acid Assisted Complexation of K+ by Valinomycin in Monolayers,” *Langmuir*, vol. 10, no. 5, pp. 1354–1357, May 1994, doi: 10.1021/la00017a008.
[37] “Principal Component Ananlysis Calculator.” https://statskingdom.com/pca-calculator.html (accessed May 26, 2023).
[38] Y. Kawamata *et al.*, “Scalable, Electrochemical Oxidation of Unactivated C-H Bonds,” *Journal of the American Chemical Society*, vol. 139, no. 22, pp. 7448–7451, Jun. 2017, doi: 10.1021/jacs.7b03539.

8. Appendices

8.1. Appendix A

Supplementary data obtained with Figure 12, Potential responses of cationic and anionic ISEs to the increasing concentration of betulin stock solution

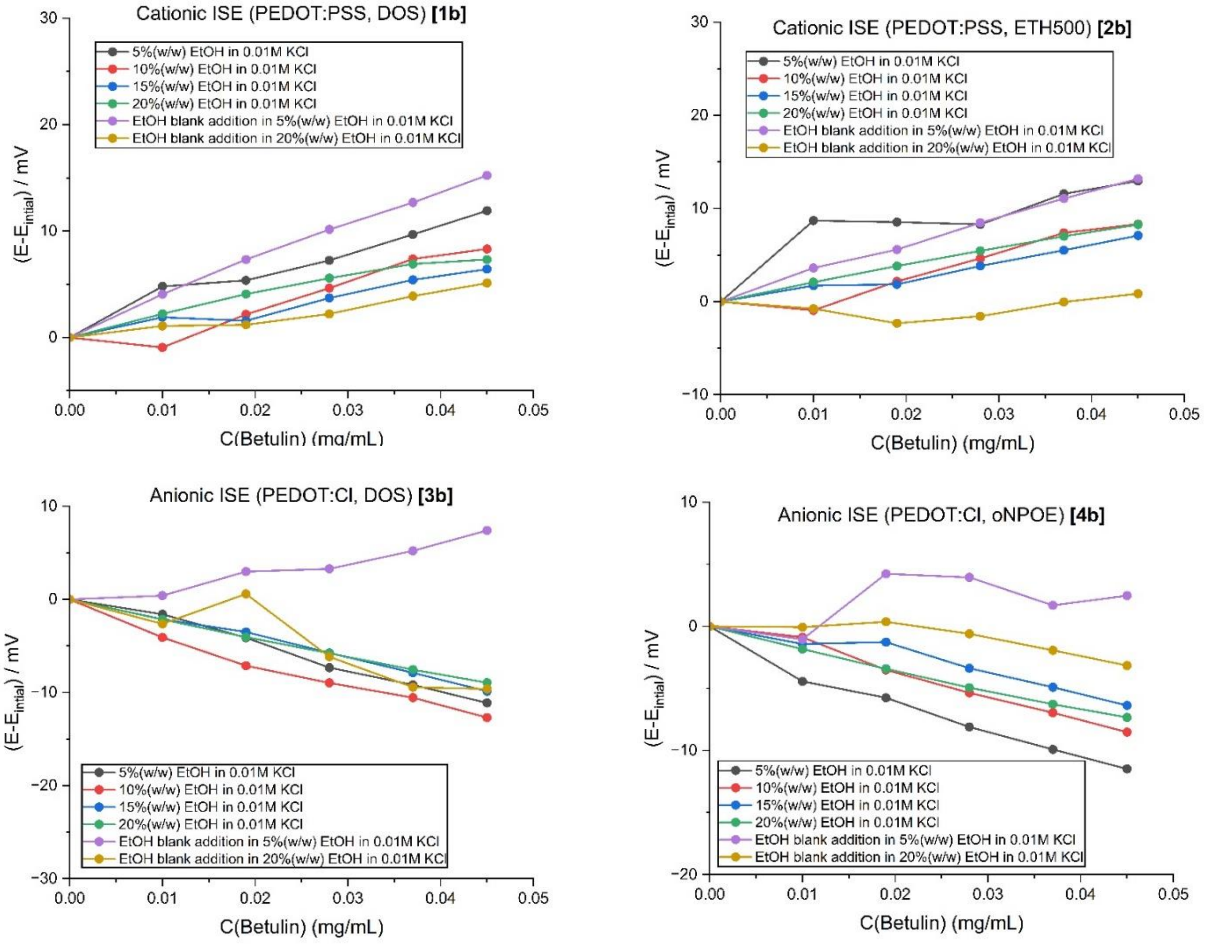

8.2. Appendix B

Supplementary data obtained with Figure 13, Potential responses of cationic and anionic ISEs to the increasing concentration of stearic acid stock solution

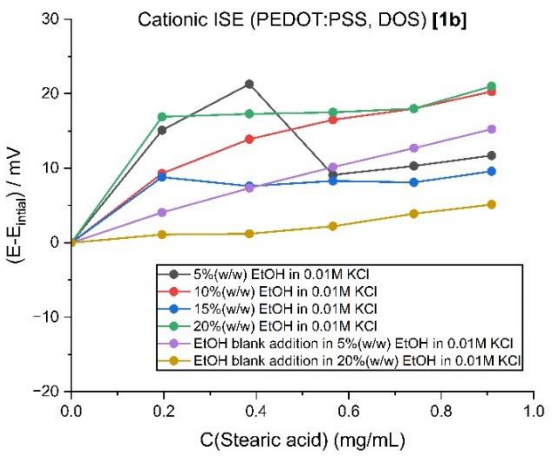

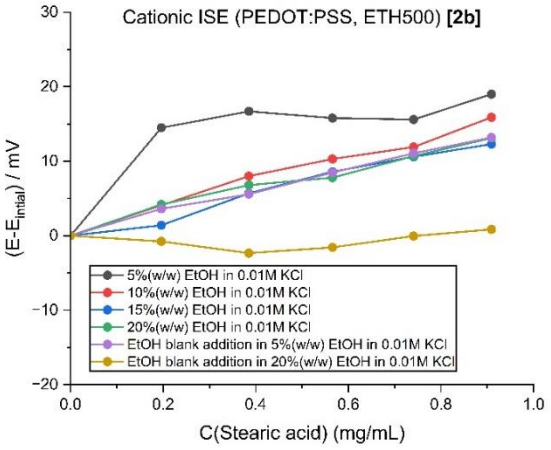

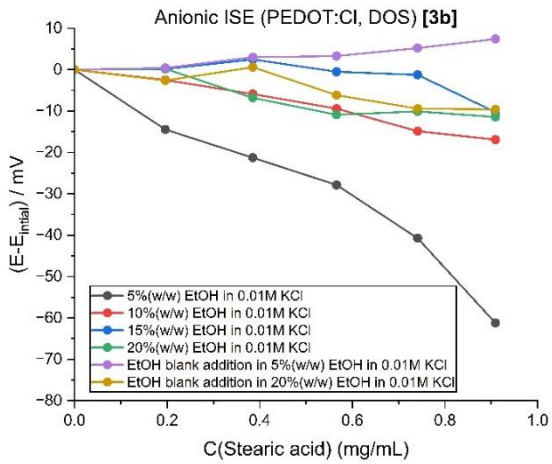

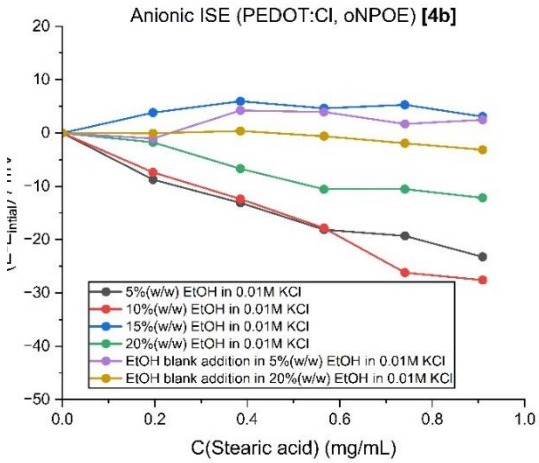

Table 9. Potentiometric calibration data for cationic ISEs

(a) before the stearic acid stock solution addition (b) after the stearic acid stock solution addition

(a)

	Cationic ISE (PEDOT:PSS, DOS, ETH500) [1a]	Cationic ISE (PEDOT:PSS, DOS) [1b]	Cationic ISE (PEDOT:PSS, oNPOE, ETH500) [2a]	Cationic ISE (PEDOT:PSS, oNPOE) [2b]
Slope	45.81	46.74	47.31	47.58
Intercept	229.94	270.44	211.67	242.33
R^2	0.988	0.992	0.992	0.994

(b)

	Cationic ISE (PEDOT:PSS, DOS, ETH500) [1a]	Cationic ISE (PEDOT:PSS, DOS) [1b]	Cationic ISE (PEDOT:PSS, oNPOE, ETH500) [2a]	Cationic ISE (PEDOT:PSS, oNPOE) [2b]
Slope	43.27	43.61	43.82	43.92
Intercept	222.85	278.32	204.93	235.76
R^2	1.00	1.00	1.00	1.00

Table 10. Potentiometric calibration data for neutral ISEs

(a) before the stearic acid stock solution addition (b) after the stearic acid stock solution addition

(a)

	Neutral ISE (PEDOT:Cl, DOS, ETH 500) [5a]	Neutral ISE (PEDOT:PSS , oNPOE, ETH500) [5b]
Slope	6.83	7.92
Intercept	236.74	202.76
R^2	0.33	0.63

(b)

	Neutral ISE (PEDOT:Cl, DOS, ETH 500) [5a]	Neutral ISE (PEDOT:PSS , oNPOE, ETH500) [5b]
Slope	-6.37	-6.70
Intercept	284.98	220.63
R^2	0.61	0.99

8.3. Appendix C

Figure C-1. Three-dimensional PCA charts of 12 ISEs (a) Three classes without samples, (b) Three classes with the corresponding samples

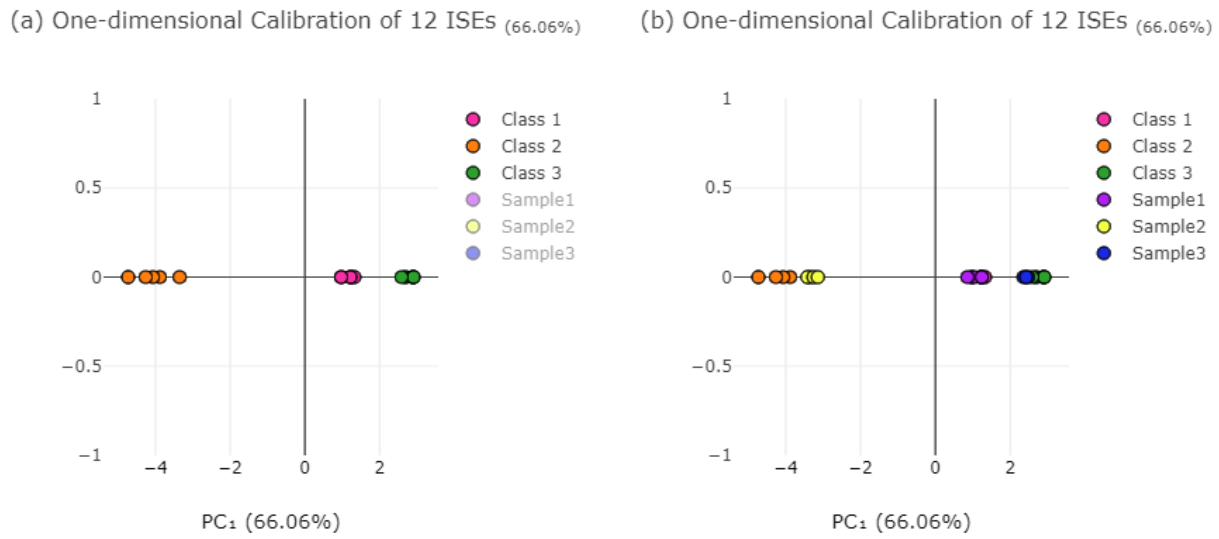

Figure C-2. One-dimensional PCA charts of 12 ISEs (a) Three classes without samples, (b) Three classes with the corresponding samples

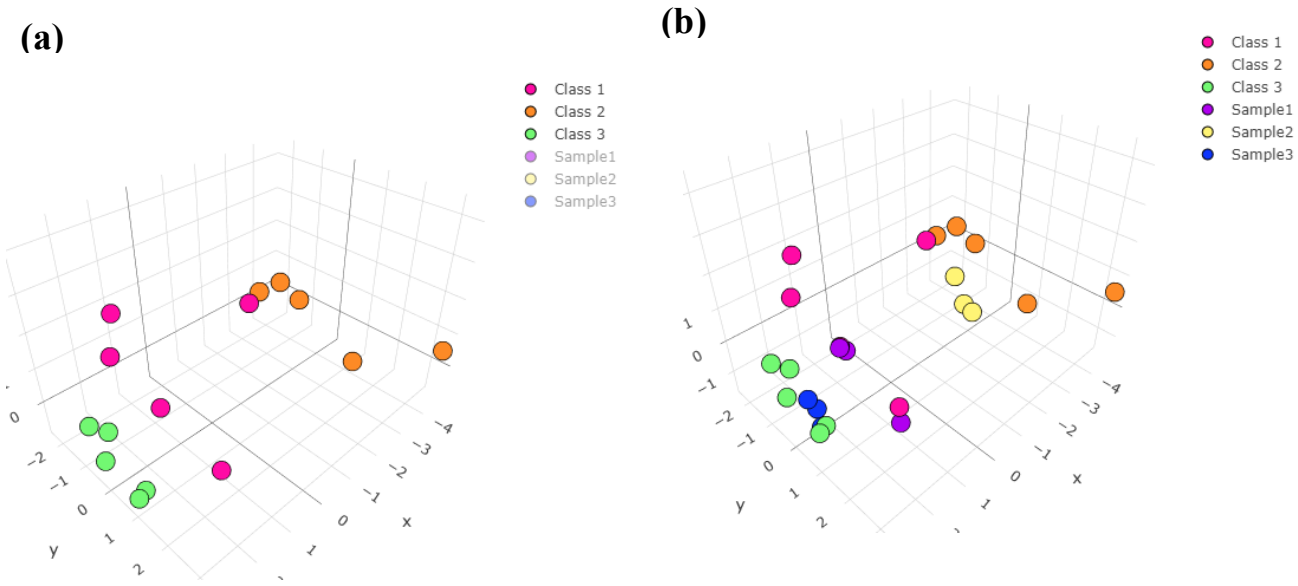

Figure C-3. One-dimensional PCA charts of 8 ISEs except neutral ISEs (a) Three classes without samples, (b) Three classes with the corresponding samples

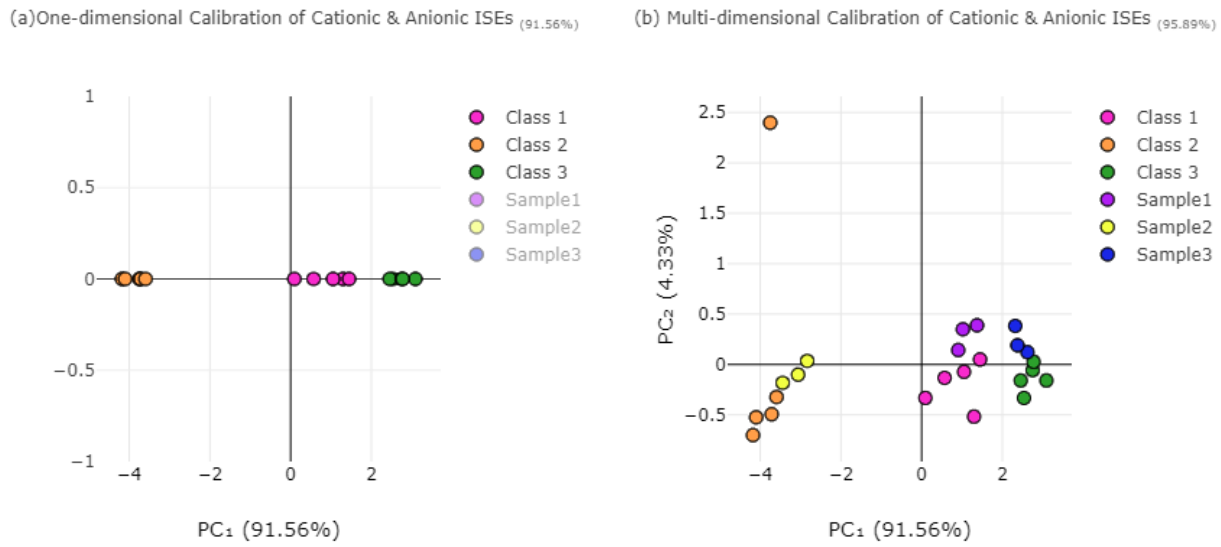

Figure C-4. Three-dimensional PCA charts of 8 ISEs except neutral ISEs (a) Three classes without samples, (b) Three classes with the corresponding samples

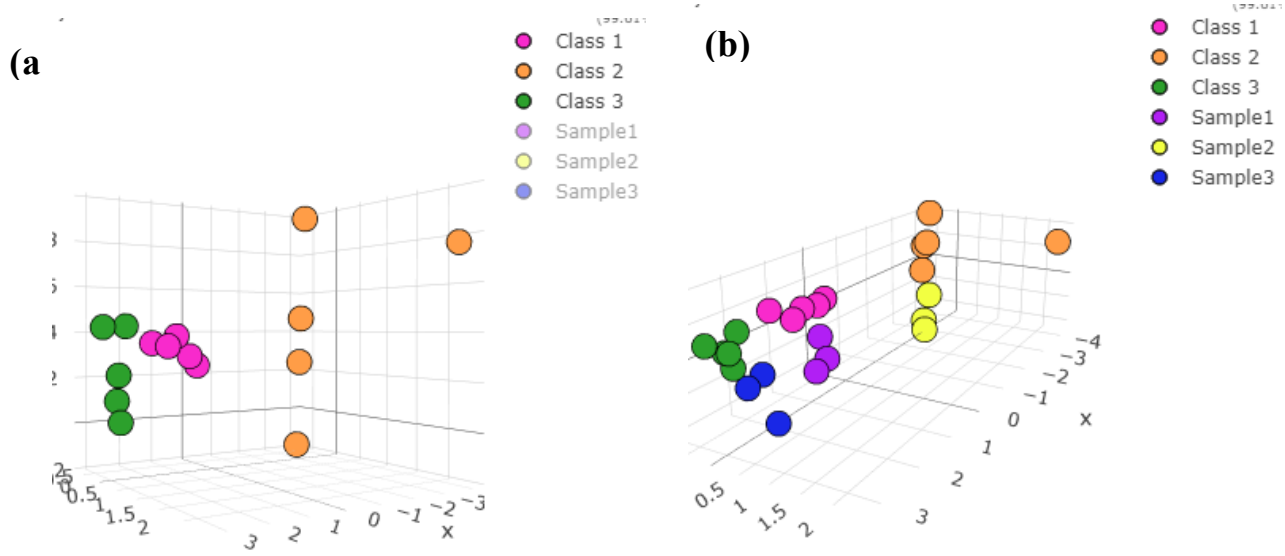

8.4. Appendix D

Figure D-1. Square wave voltammograms (SWV) obtained at the lead film electrode in 0.2 M NaOH solution, (a) without deaeration for betulin addition (b) with deaeration for betulin addition, (c) without deaeration for BA addition, and (d) with deaeration for BA addition

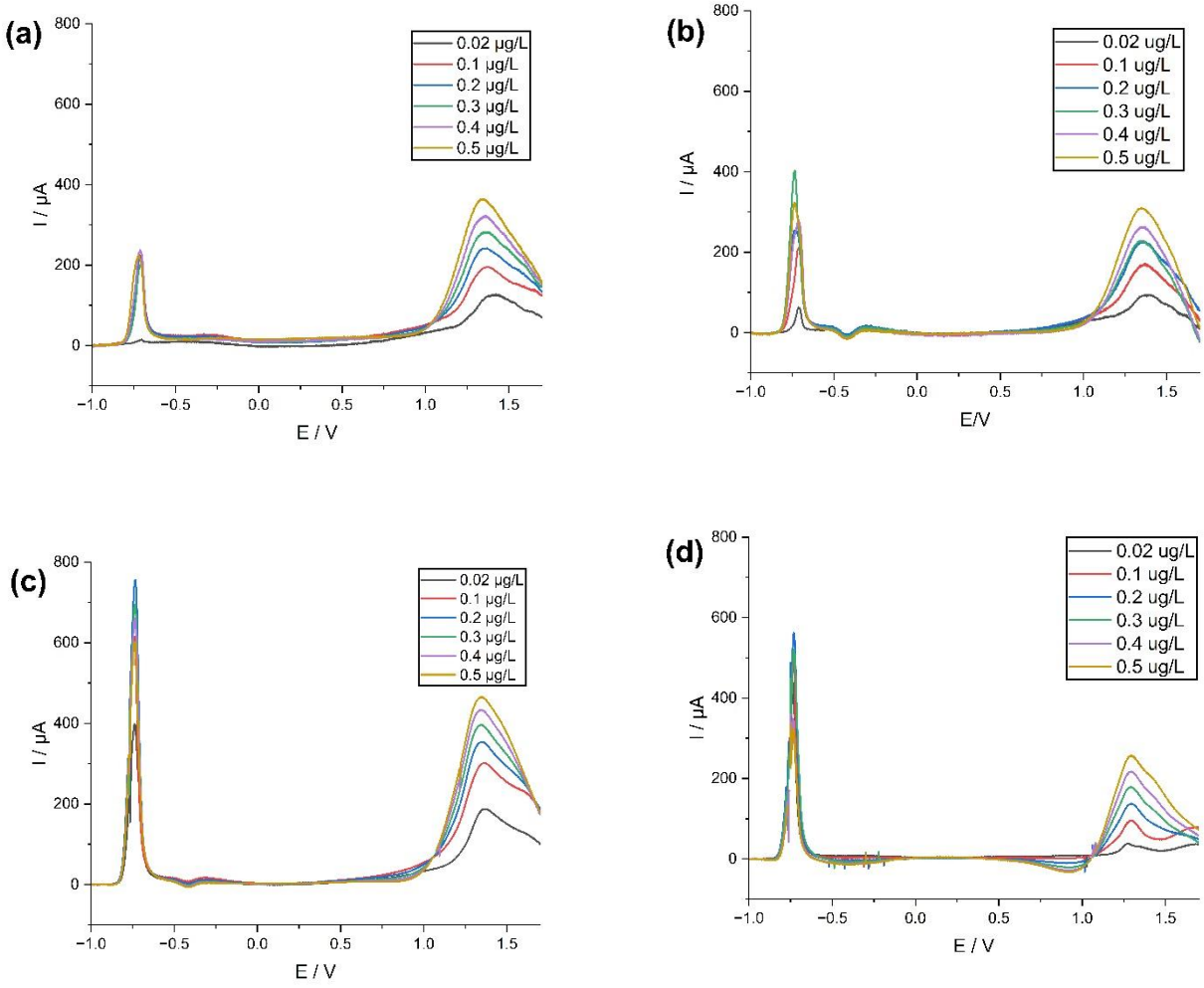

Figure D-2. Square wave voltammograms (SWV) obtained at the lead film electrode in 0.2 M NaOH solution, (a) without deaeration for ethanol blank addition (b) with deaeration for ethanol blank addition, (c) calibration curve by BA and betulin addition, (d) ethanol blank addition

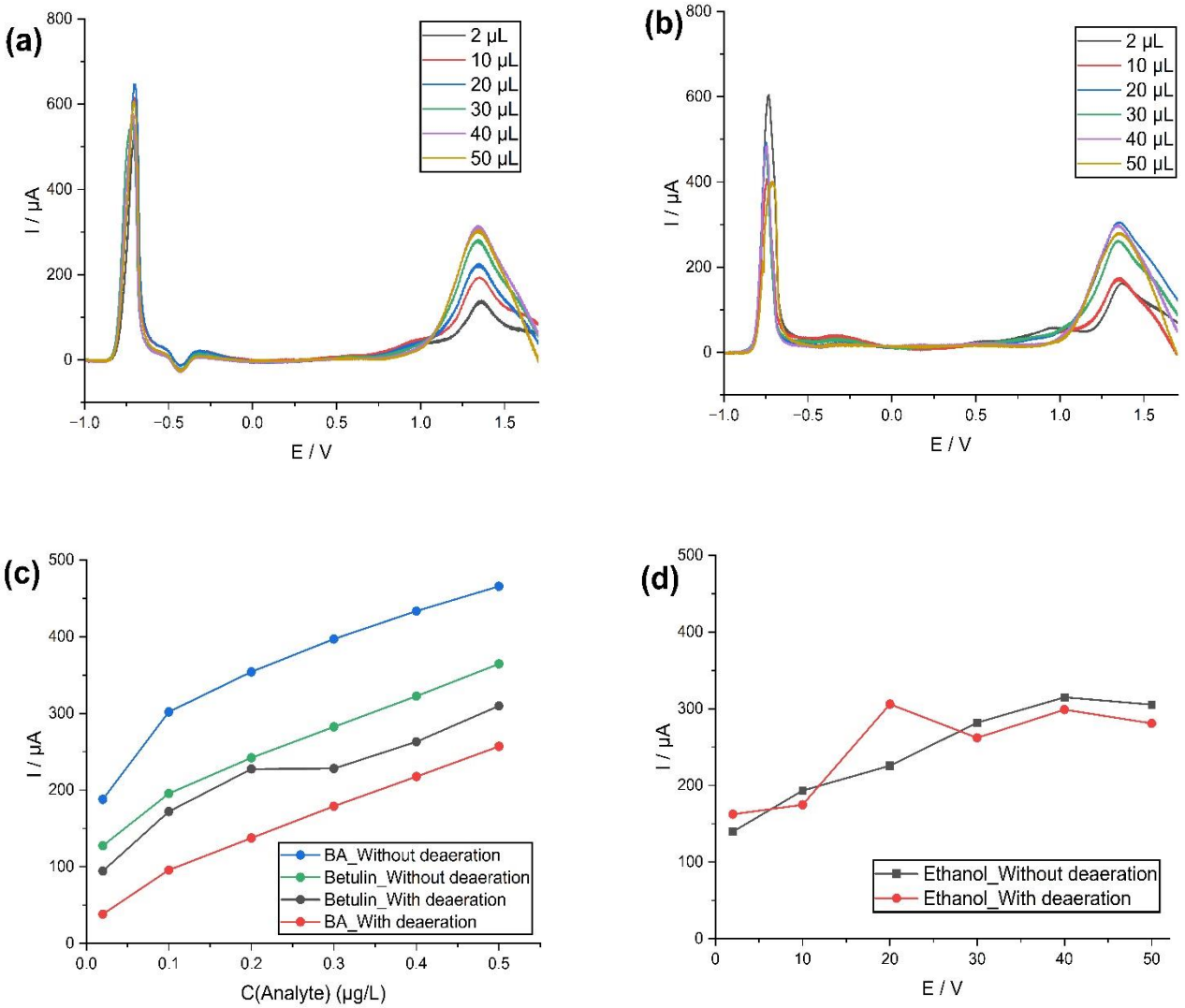

Figure D-3. Square wave voltammograms (SWV) obtained at the lead film electrode in 0.2 M NaOH solution with the blank solvent addition, (a) Methanol, (b)Acetone, (c) DMF, (d) DMSO, and (e) Betulin 5mM (DMSO) addition.

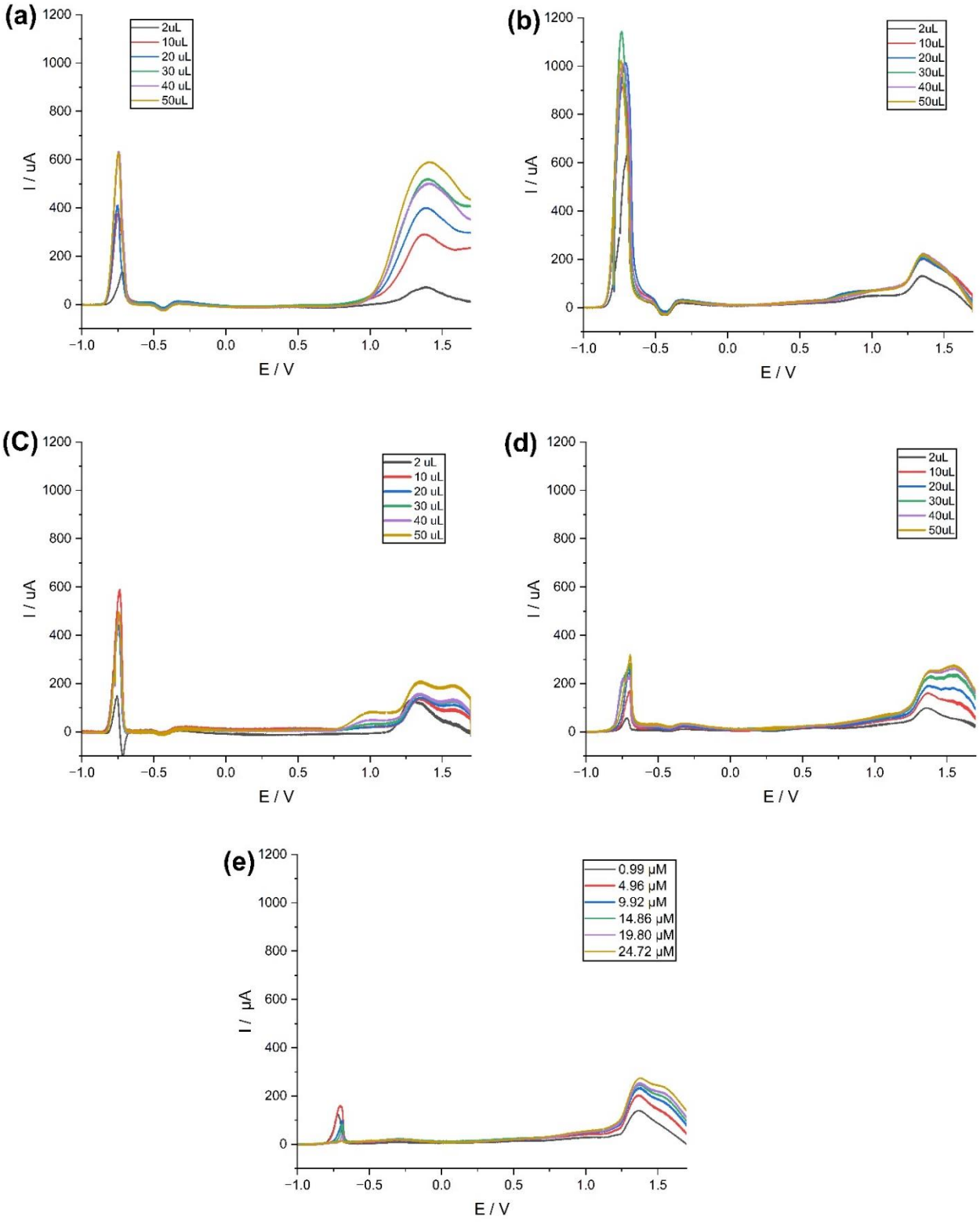

8.5. Appendix E

Differential pulse voltammograms (DPV) obtained at the lead film electrode with (a) corresponding volume of DMSO addition to the standard, (b) 0.5 mM Betulin addition, (c) 0.5 mM Betulinic acid, and (d) 0.5 mM Oleanolic acid

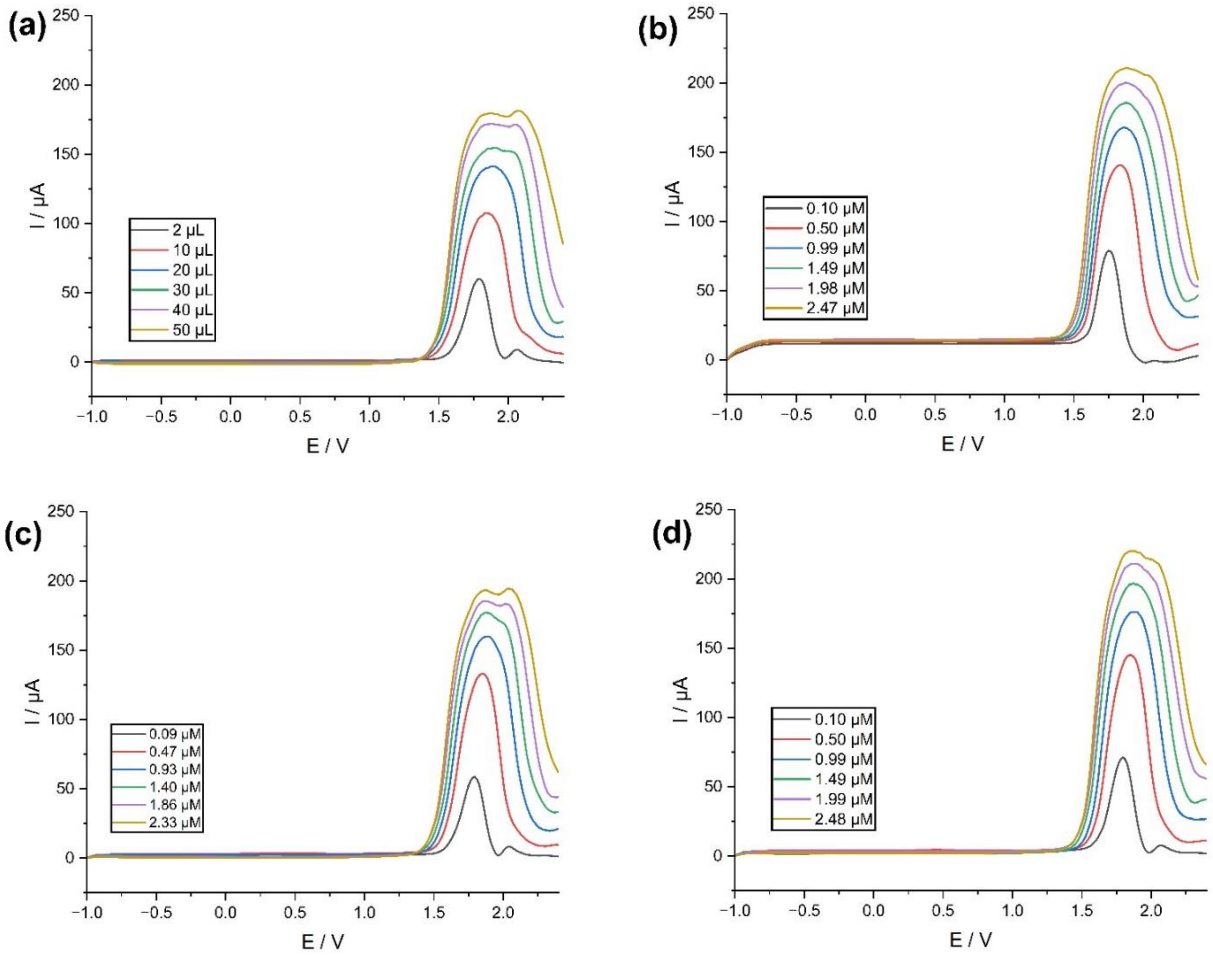

8.6. Appendix F

Figure F-1. Differential normal pulse voltammograms (DNPV) obtained at the lead film electrode in Tris-HCl buffer pH 7.4 with (a) corresponding volume of DMSO addition to the stock solution, (b) 5 mM Betulin addition, (c) 5 mM Betulinic acid, and (d) 5 mM Oleanolic acid

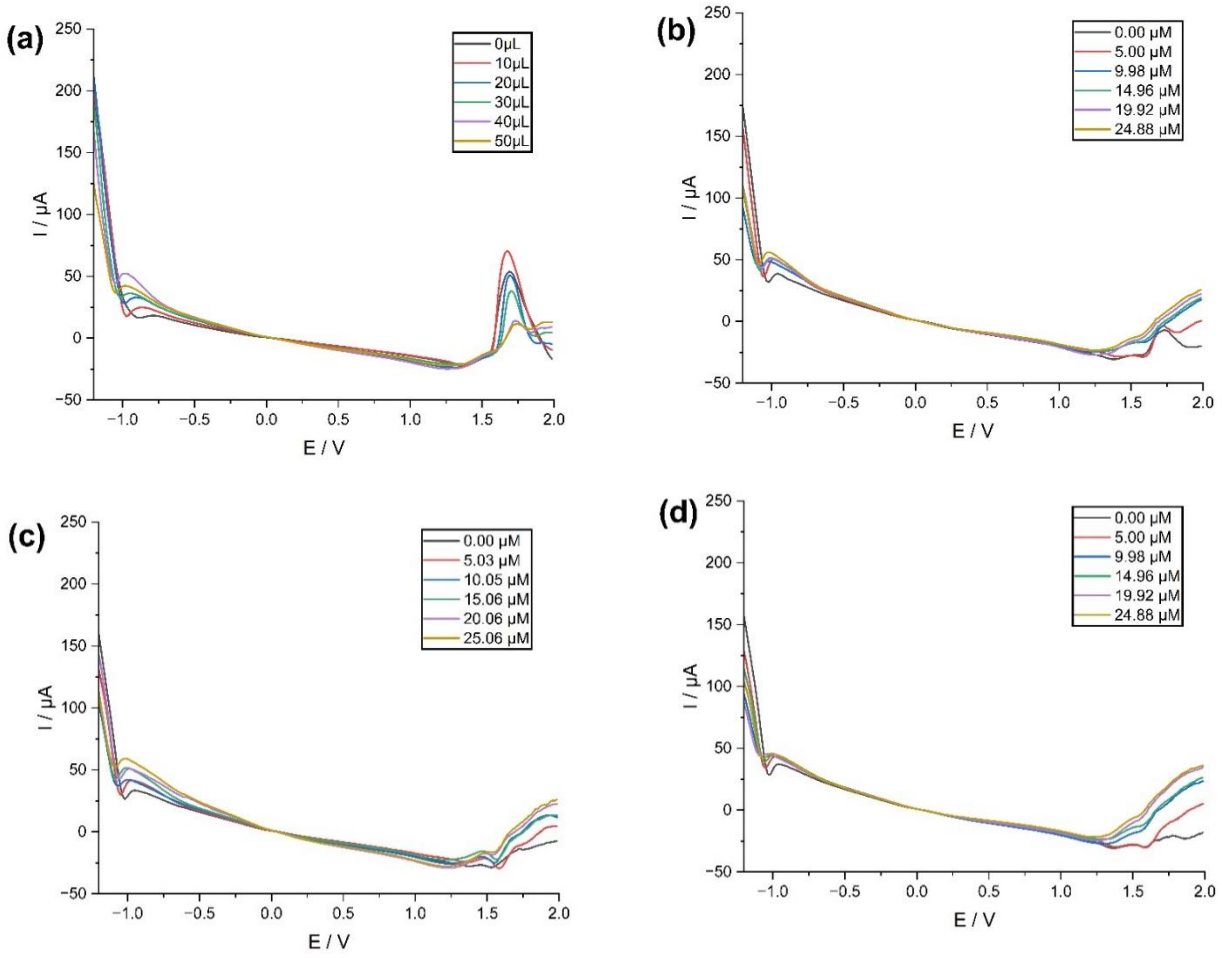

Figure F-2. Differential normal pulse voltammograms (DNPV) obtained at the lead film electrode in $TBAPF_6$ in acetonitrile with (a) corresponding volume of DMSO addition to the stock solution, (b) 5 mM Betulinic acid stock solution, and (c) 5 mM Oleanolic acid stock solution

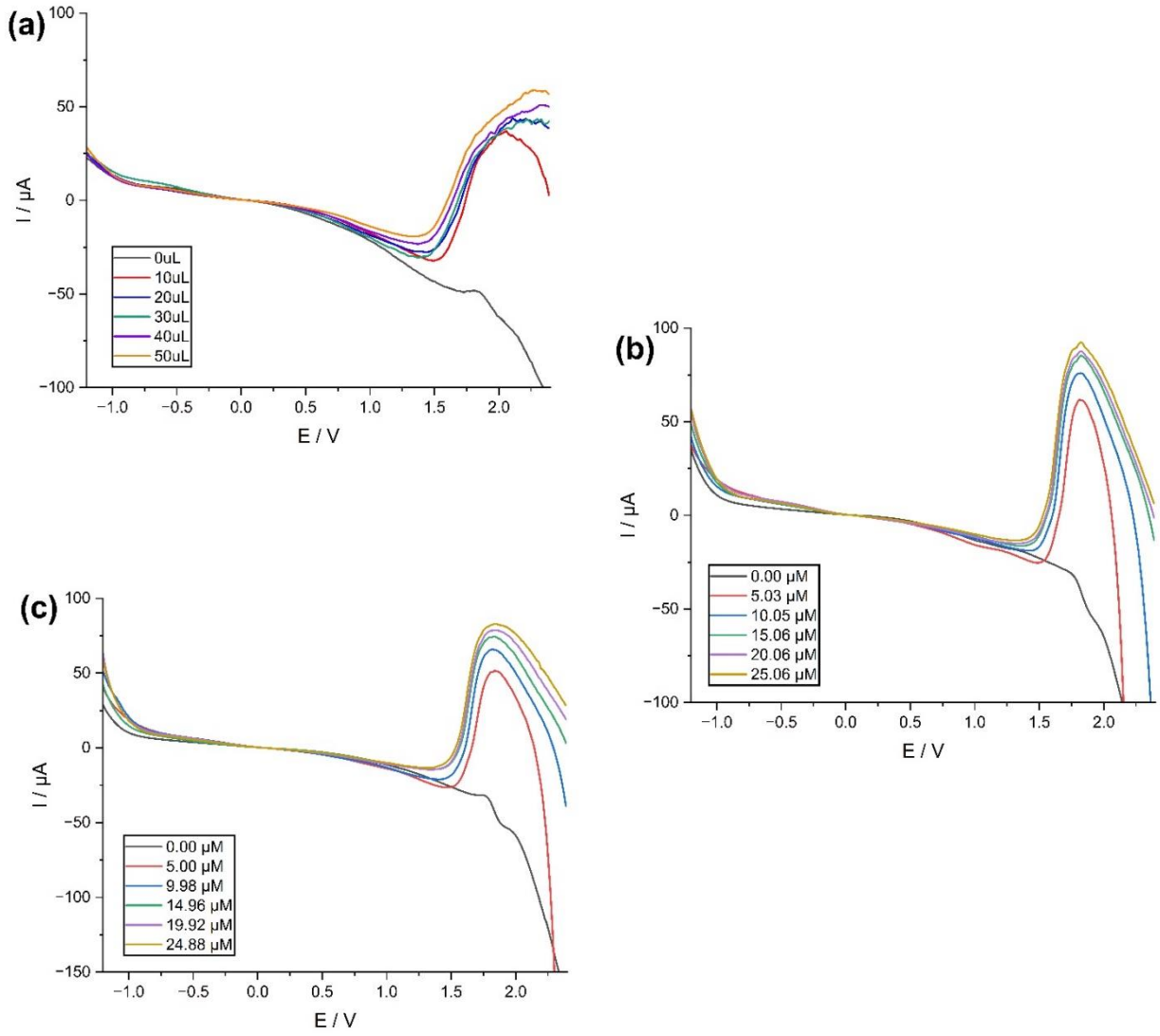

8.7. Appendix G

I. Data treatment: Background subtraction and current starting point adjustment to 0 µA (This was applied depending on the stability of current signal in the middle range of the scan, aiming to overlap in the middle range in which it does not show any peaks.)

II. *DMSO: Old DMSO (yellowish colour probably due to oxidation)

III. DMSO: Newly ordered DMSO (colorless)

IV. N/A: not available, not studied

V. Bold font: The corresponding voltammograms are presented as Figures in section 5 or Appendices

VI. Lead film: O (As a part of the pre-treatment step, the lead film was in situ deposited) vs X (The pre-treatment step was not applied)

Table 11. Summary table of the investigated voltammetric methods

Scan range	Background electrolyte	Method	Solvent	Analyte	Lead film	Result
−1.0 V ~ 1.7 V	**0.2 M NaOH**	**SWV**	**Ethanol**	**BA**	**O**	**Positive peaks due to the solvent at ca 1.35 V**
−1.0 V ~ 1.7 V	**0.2 M NaOH**	**SWV**	**Ethanol**	**Betulin**	**O**	**Positive peaks due to the solvent at ca 1.35 V**
−1.0 V ~ 1.7 V	**0.2 M NaOH**	**SWV**	**Ethanol**	**Ethanol blank**	**O**	**Positive peaks due to the solvent at ca 1.35 V**
−1.0 V ~ 1.7 V	**0.2 M NaOH**	**SWV**	**Ethanol**	**Methanol blank**	**O**	**Positive peaks due to the solvent at ca 1.35 V**
−1.0 V ~ 1.7 V	**0.2 M NaOH**	**SWV**	**Acetone**	**Acetone blank**	**O**	**Positive peaks due to the solvent at 1.35 V**
−1.0 V ~ 1.7 V	**0.2 M NaOH**	**SWV**	**Acetone**	**BA**	**O**	**Positive peaks, but lower than those of the blank acetone at ca 1.35 V**
−1.0 V ~ 1.7 V	**0.2 M NaOH**	**SWV**	**DMF**	**DMF blank**	**O**	**- Positive peaks due to the solvent at ca 1.35 V, not proportional to the added solvent**

						- DMF was not considered afterwards due to its toxicity
−1.0 V ~ 1.7 V	**0.2 M NaOH**	**SWV**	**DMSO**	**DMSO blank**	**O**	**Positive peaks due to the solvent at ca 1.35 V**
−1.0 V ~ 1.7 V	**0.2 M NaOH**	**SWV**	**DMSO**	**Betulin**	**O**	**Comparable current signals to the DMSO blank at ca 1.35 V**
−1.0 V ~ 1.7 V	0.2 M NaOH	SWV	DMSO	BA	O	N/A
−1.0 V ~ 1.7 V	0.2 M NaOH	SWV	DMSO	OA	O	N/A
−1.2 V ~ 1.2 V	Tris-HCl buffer (pH 7.4)	CV	*DMSO	*DMSO blank	X	No current peak signal change depending on the addition
−1.2 V ~ 1.2 V	Tris-HCl buffer (pH 7.4)	CV	*DMSO	OA	X	No current peak signal changes depending on the addition
−1.2 V ~ 1.5 V	Tris-HCl buffer (pH 7.4)	DPV	*DMSO	*DMSO blank	X	Negative current peaks after the data treatment
−1.2V ~ 1.5V	Tris-HCl buffer (pH 7.4)	DPV	*DMSO	OA	X	No current peak signal change by the addition
−1.2 V ~ 2.0 V	Tris-HCl buffer (pH 7.4)	DPV	*DMSO	*DMSO blank	O	Positive peaks after data treatment
−1.2 V ~ 2.0 V	Tris-HCl buffer (pH 7.4)	DPV	*DMSO	OA	O	Positive peaks after the data treatment (Clearly higher than the blank addition)
−1.2 V ~ 2.0 V	Tris-HCl buffer (pH 7.4)	DPV	*DMSO	BA	O	Comparable current signals to those of DMSO blank addition

−1.2 V ~ 2.0 V	Tris-HCl buffer (pH 7.4)	DPV	*DMSO	Betulin	O	Positive peaks to the similar extent to the blank addition after data treatment
−1.2 V ~ 2.0 V	Tris-HCl buffer (pH 7.4)	DNPV	*DMSO	*DMSO blank	O	Positive peaks after the data treatment
−1.2 V ~ 2.0 V	**Tris-HCl buffer (pH 7.4)**	**DNPV**	***DMSO**	**OA**	**O**	**Positive peaks after the data treatment, lower than those of the DMSO blank**
−1.2 V ~ 2.0 V	**Tris-HCl buffer (pH 7.4)**	**DNPV**	***DMSO**	**BA**	**O**	**Positive peaks after the data treatment, lower than those of the DMSO blank**
−1.2 V ~ 2.0 V	**Tris-HCl buffer (pH 7.4)**	**DNPV**	***DMSO**	**Betulin**	**O**	**Positive peaks after data treatment, lower than those of the DMSO blank**
−1.0 V ~ 1.7 V	**Tris-HCl buffer (pH 7.4)**	**SWV**	**DMSO**	**DMSO blank**	**O**	**No current peak signal change depending on the addition at ca 1.6 V**
−1.0 V ~ 1.7 V	**Tris-HCl buffer (pH 7.4)**	**SWV**	**DMSO**	**OA**	**O**	**Positive peaks after data treatment at ca 1.6 V**
−1.0 V ~ 1.7 V	**Tris-HCl buffer (pH 7.4)**	**SWV**	**DMSO**	**BA**	**O**	**Positive peaks after data treatment at ca 1.6 V**
−1.0 V ~ 1.7 V	**Tris-HCl buffer (pH 7.4)**	**SWV**	**DMSO**	**Betulin**	**O**	**Positive peaks after data treatment at ca 1.6 V**
−1.2 V ~ 1.5 V	Tris-HCl buffer (pH 7.4)	DNPV	DMSO	DMSO blank	X	Negative peaks after data treatment
−1.2 V ~ 1.5 V	Tris-HCl buffer (pH 7.4)	DNPV	DMSO	OA	X	Negative peaks after data treatment

−1.0 V ~ 2.4 V	**0.1M $TBAPF_6$ (ACN)**	**DPV**	**DMSO**	**DMSO blank**	**X**	**Positive peaks after data treatment**
−1.0 V ~ 2.4 V	**0.1M $TBAPF_6$ (ACN)**	**DPV**	**DMSO**	**OA**	**X**	**Positive peaks after data treatment but lower than blank DMSO**
−1.0 V ~ 2.4 V	**0.1M $TBAPF_6$ (ACN)**	**DPV**	**DMSO**	**BA**	**X**	**Positive peaks after data treatment but lower than blank DMSO**
−1.0 V ~ 2.4 V	**0.1M $TBAPF_6$ (ACN)**	**DPV**	**DMSO**	**Betulin**	**X**	**Positive peaks after data treatment but lower than blank DMSO**
−1.2 V ~ 1.7 V	0.1M $TBAPF_6$ (ACN)	DNPV	*DMSO	*DMSO blank	X	-Small positive peaks - Positive peaks after data treatment - Expansion for the scan range might be required because there are peaks over 1.7 V
−1.0 V ~ 2.4 V	**0.1M $TBAPF_6$ (ACN)**	**DPV**	**DMSO**	**DMSO blank**	**O**	**Positive peaks after the data treatment**
−1.0 V ~ 2.4 V	**0.1M $TBAPF_6$ (ACN)**	**DPV**	**DMSO**	**OA**	**O**	**Slightly higher peaks after data treatment than the peaks of DMSO blank addition**
−1.0 V ~ 2.4 V	**0.1M $TBAPF_6$ (ACN)**	**DPV**	**DMSO**	**BA**	**O**	**Slightly higher peaks after the data treatment than those of the DMSO blank**
−1.0 V ~ 2.4 V	**0.1M $TBAPF_6$ (ACN)**	**DPV**	**DMSO**	**Betulin**	**O**	**Slightly higher peaks after data treatment than those of DMSO blank**
−1.2 V ~ 2.4 V	**0.1M $TBAPF_6$ (ACN)**	**DNPV**	**DMSO**	**DMSO blank**	**O**	**Positive peaks after data treatment**

−1.2 V ~ 2.4 V	**0.1M $TBAPF_6$ (ACN)**	**DNPV**	**DMSO**	**OA**	**O**	**Slightly higher peaks after the data treatment than those of the DMSO blank**
−1.2 V ~ 2.4 V	**0.1M $TBAPF_6$ (ACN)**	**DNPV**	**DMSO**	**BA**	**O**	**Slightly higher peaks after the data treatment than those of the DMSO blank**
−1.2 V ~ 2.4 V	0.1M $TBAPF_6$ (ACN)	DNPV	DMSO	Betulin	O	N/A
−1.2 V ~ 2.4 V	0.1M $TBAPF_6$ (ACN)	SWV	DMSO	DMSO blank	O	Positive peaks after the data treatment
−1.2 V ~ 2.4 V	0.1M $TBAPF_6$ (ACN)	SWV	DMSO	OA	O	Higher peaks after the data treatment than those of the DMSO blank
−1.2 V ~ 2.4 V	0.1M $TBAPF_6$ (ACN)	SWV	DMSO	BA	O	Higher peaks after the data treatment than those of the DMSO blank
−1.2 V ~ 2.4 V	0.1M $TBAPF_6$ (ACN)	SWV	DMSO	Betulin	O	N/A